

Final Report**Development, Evaluation and Testing of
Version 6 of the Carbon Bond
Chemical Mechanism (CB6)**

Work Order No. 582-7-84005-FY10-26

Prepared for

Texas Commission on Environmental Quality
12118 Park 35 Circle
Austin, Texas 78753

Prepared by

Greg Yarwood, Gary Z. Whitten and Jaegun Jung

ENVIRON International Corporation
773 San Marin Drive, Suite 2115
Novato, CA 94998

Gookyung Heo and David T. Allen

Center for Energy and Environmental Resources
The University of Texas at Austin
10100 Burnet Road, Bldg. 133, R7100
Austin, TX 78758, USA

September 22, 2010

TABLE OF CONTENTS

	Page
1. INTRODUCTION.....	1-1
2. MECHANISM DESIGN AND IMPLEMENTATION.....	2-1
2.1 Mechanism Design.....	2-1
2.2 Mechanism Implementation.....	2-12
2.3 Reaction Rate Changes From CB05	2-22
3. MECHANISM EVALUATION.....	3-1
3.1 Introduction.....	3-1
3.2 Data and Methods Used in Evaluating CB6	3-1
3.3 Chamber Simulation Results for CB6.....	3-9
3.4 Summary	3-55
4. CAMx MODELING	4-1
4.1 Data for Deposition Calculations.....	4-1
4.2 Emission Inventory Preparation.....	4-3
4.3 Los Angeles Modeling.....	4-4
4.4 Texas Modeling For the Eastern US	4-8
5. SUMMARY AND CONCLUSIONS	5-1
6. REFERENCES.....	6-1

APPENDICES

Appendix A: Chamber Experiments Used to Evaluate CB6

TABLES

Table 2-1.	Description of photolysis data for CB6	2-2
Table 2-2.	All potential peroxy radical reactions for CB6 and the reactions included.....	2-5
Table 2-3.	Summary of peroxy radical rate constants (k_{298} and temperature dependence) from IUPAC (2010).	2-6
Table 2-4.	CB6 rate constants (k_{298} and temperature dependence) for acylperoxy (RCO3) and peroxy (RO2) radical reactions	2-6
Table 2-5.	Mechanism for OH formation from NO_2^* with the rate constant for $\text{NO}_2\text{S} + \text{H}_2\text{O}$ reported by Li et al. (2008).	2-11
Table 2-6.	Rate constant expressions used in CB6	2-12
Table 2-7.	Listing of reactions and rate parameters for CB6	2-13
Table 2-8.	Model species names for CB6	2-21
Table 2-9.	Comparison of CB6 to CB05 rate constants for inorganic reactions.....	2-23
Table 2-10.	Comparison of CB6 and CB05 photolysis reaction rates	2-24
Table 3-1.	An overview of environmental chambers at UCR and TVA used for mechanism evaluation (Heo, 2009).....	3-3
Table 3-2.	Summary of 194 UCR and TVA chamber experiments of single test compounds and special mixtures used for evaluating CB6. ^a	3-5
Table 3-3.	145 non-blacklight surrogate mixture experiments used for evaluating CB6. ^a	3-6
Table 3-4.	Summary of model errors for CB6 and SAPRC-07 against 33 CO - NOx experiments	3-8
Table 3-5.	Summary of model errors for 33 CO - NOx experiments	3-10
Table 3-6.	Summary of model errors for 9 FORM - NOx experiments.....	3-12
Table 3-7.	Summary of model errors for 2 blacklight MEOH - other VOCs - NOx experiments	
Table 3-8a.	Summary of model errors for 11 non-blacklight ETH - NOx experiments	3-16
Table 3-8b.	Summary of model errors for 22 blacklight ETH - NOx experiments.....	3-18
Table 3-9.	Summary of model errors for 8 ALD2-NOx experiments.....	3-20
Table 3-10.	Summary of model errors for 3 blacklight ETOH -other VOCs - NOx experiments	3-22
Table 3-11.	Summary of model errors for 4 ACET - NOx experiments.....	3-24
Table 3-12.	Summary of model errors for 2 Methyl Ethyl Ketone - NOx experiments	3-26
Table 3-13.	Summary of model errors for 2 blacklight ETHA - other VOCs - NOx experiments	3-28
Table 3-14a.	Summary of model errors for 5 PAR - NOx experiments	3-30
Table 3-14b.	Summary of model errors only for 3 n-Butane - NOx experiments	3-30
Table 3-14c.	Summary of model errors only for 2 n-Butane/2,3-Dimethyl Butane/NOx experiments.....	3-30
Table 3-15.	Summary of model errors for 48 OLE - NOx experiments.	3-32
Table 3-16.	Summary of model errors for 3 IOLE-NOx experiments.....	3-34
Table 3-17.	Summary of model errors for 20 TOL-NOx experiments	3-36
Table 3-18.	Summary of model errors for 27 XYL-NOx experiments.....	3-38
Table 3-19.	Summary of model errors for 6 isoprene - NOx experiments	3-40

Table 3-20a.	Summary of model errors for 2 non-blacklight terpene-NOx experiments.....	3-20
Table 3-20b.	Summary of model errors for 14 blacklight terpene-NOx experiments.....	3-20
Table 3-21.	Summary of model errors for 2 blacklight PRPA - other VOCs - NOx experiments.....	3-44
Table 3-22.	Summary of model errors for 2 BENZ - NOx experiments.....	3-46
Table 3-23.	Summary of model errors for 2 ETHY - NOx experiments.....	3-48
Table 3-24.	Summary of model errors for 2 Surg-NA type VOC mixture - NOx experiments.....	3-50
Table 3-25.	Summary of model errors for 57 incomplete surrogate VOC mixture - NOx experiments.....	3-52
Table 3-26.	Summary of model errors for 81 full surrogate VOCs - NOx experiments.....	3-54
Table 3-27.	Numerical summary of average model errors of Max(O ₃), Max(D(O ₃ -NO)) and the NOx crossover time.....	3-59
Table 4-1.	Data for use in deposition calculations.....	4-1
Table 4-2.	Comparison of CB05 and CB6 incremental reactivity factors (mole O ₃ /mole VOC).....	4-6

FIGURES

Figure 3-1.	Schematic diagram showing a hierarchical approach to evaluating CB6. Note: Key CB species and backbone chemistry parts are displayed in bold.	3-2
Figure 3-2.	Mechanism performance comparison between CB6 and SAPRC-07 against 33 CO - NOx experiments: (a) Max(O ₃), (b) Max(D(O ₃ -NO)), (c) NOx crossover time.	3-8
Figure 3-3.	Mechanism performance against 33 CO - NOx experiments: (a) Max(O ₃), (b) Max(D(O ₃ -NO)), (c) NOx crossover time.....	3-10
Figure 3-4.	Mechanism performance against 9 FORM - NOx experiments: (a) Max(O ₃), (b) Max(D(O ₃ -NO)), (c) NOx crossover time.....	3-12
Figure 3-5.	Mechanism performance against 2 blacklight MEOH - other VOCs - NOx experiments: (a) Max(O ₃), (b) Max(D(O ₃ -NO)), (c) NOx crossover time.....	3-14
Figure 3-6a.	Mechanism performance against 11 non-blacklight ETH - NOx experiments: (a) Max(O ₃), (b) Max(D(O ₃ -NO)), (c) NOx crossover time.....	3-16
Figure 3-6b.	Mechanism performance against 22 blacklight ETH - NOx experiments: (a) Max(O ₃), (b) Max(D(O ₃ -NO)), (c) NOx crossover time.....	3-18
Figure 3-7.	Mechanism performance against 8 ALD2 - NOx experiments: (a) Max(O ₃), (b) Max(D(O ₃ -NO)), (c) NOx crossover time.....	3-20
Figure 3-8.	Mechanism performance against 3 blacklight ETOH - other VOCs - NOx experiments: (a) Max(O ₃), (b) Max(D(O ₃ -NO)), (c) NOx crossover time.....	3-22

Figure 3-9.	Mechanism performance against 4 ACET - NOx experiments: (a) Max(O ₃), (b) Max(D(O ₃ -NO)), (c) NOx crossover time	3-24
Figure 3-10.	Mechanism performance against 2 Methyl Ethyl Ketone (MEK) - NOx experiments: (a) Max(O ₃), (b) Max(D(O ₃ -NO)), (c) NOx crossover time	3-26
Figure 3-11.	Mechanism performance against 2 blacklight ETHA - other VOCs - NOx experiments: (a) Max(O ₃), (b) Max(D(O ₃ -NO)), (c) NOx crossover time	3-28
Figure 3-12.	Mechanism performance against 5 PAR - NOx experiments: (a) Max(O ₃), (b) Max(D(O ₃ -NO)), (c) NOx crossover time	3-30
Figure 3-13.	Mechanism performance against 48 OLE - NOx experiments: (a) Max(O ₃), (b) Max(D(O ₃ -NO)), (c) NOx crossover time	3-32
Figure 3-14.	Mechanism performance against 3 IOLE - NOx experiments: (a) Max(O ₃), (b) Max(D(O ₃ -NO)), (c) NOx crossover time	3-34
Figure 3-15.	Mechanism performance against 20 TOL - NOx experiments: (a) Max(O ₃), (b) Max(D(O ₃ -NO)), (c) NOx crossover time	3-36
Figure 3-16.	Mechanism performance against 27 XYL - NOx experiments: (a) Max(O ₃), (b) Max(D(O ₃ -NO)), (c) NOx crossover time	3-38
Figure 3-17.	Mechanism performance against 6 ISOP - NOx experiments: (a) Max(O ₃), (b) Max(D(O ₃ -NO)), (c) NOx crossover time	3-40
Figure 3-18.	Mechanism performance against 2 non-blacklight and 14 blacklight terpene (TERP) - NOx experiments: (a) Max(O ₃), (b) Max(D(O ₃ -NO)), (c) NOx crossover time	3-42
Figure 3-19.	Mechanism performance against 2 blacklight PRPA - other VOCs - NOx experiments: (a) Max(O ₃), (b) Max(D(O ₃ -NO)), (c) NOx crossover time	3-44
Figure 3-20.	Mechanism performance against 2 BENZ - NOx experiments: (a) Max(O ₃), (b) Max(D(O ₃ -NO)), (c) NOx crossover time	3-46
Figure 3-21.	Mechanism performance against 2 ETHY - NOx experiments: (a) Max(O ₃), (b) Max(D(O ₃ -NO)), (c) NOx crossover time	3-48
Figure 3-22.	Mechanism performance against 2 Surg-NA type VOC mixture - NOx experiments: (a) Max(O ₃), (b) Max(D(O ₃ -NO)), (c) NOx crossover time	3-50
Figure 3-23.	Mechanism performance against 57 incomplete surrogate VOC mixture - NOx experiments: (a) Max(O ₃), (b) Max(D(O ₃ -NO)), (c) NOx crossover time	3-52
Figure 3-24.	Mechanism performance against 81 full surrogate VOC mixture - NOx experiments: (a) Max(O ₃), (b) Max(D(O ₃ -NO)), (c) NOx crossover time	3-54
Figure 3-25.	Graphical summary of mechanism performance in simulating Max(O ₃) against 194 single test compound (or special VOC mixture) - NOx experiments and 145 surrogate VOC mixture - NOx experiments	3-56
Figure 3-26.	Graphical summary of mechanism performance in simulating Max(D(O ₃ -NO)) against 194 single test compound (or special VOC mixture) - NOx experiments and 145 surrogate VOC mixture - NOx experiments	3-57

Figure 3-27.	Graphical summary of mechanism performance in simulating NO _x crossover times against 194 single test compound (or special VOC mixture) - NO _x experiments and 145 surrogate VOC mixture - NO _x experiments.	3-58
Figure 4-1.	Modeling domain for the Los Angeles modeling scenario used to test Chemical Process Analysis	4-4
Figure 4-2.	Daily maximum 8-hour ozone (ppb) for the Los Angeles domain on August 5, 1997.....	4-5
Figure 4-3.	CB6 ozone sensitivities to VOC emissions (dO ₃ /dVOC) compared to dO ₃ /dETHA for Los Angeles	4-7
Figure 4-4.	Modeling domain for HGB with 36-km (Eastern US), 12-km (East Texas) and 4-km (HGB/BPA) resolution nested grids	4-8
Figure 4-5.	Average daily maximum 8-hr O ₃ (ppb) for June 3-15, 2006, with CB6 and CB05	4-9
Figure 4-6.	Difference (CB6 – CB05) in average daily maximum 8-hr O ₃ (ppb) for June 3-15, 2006, for the 12-km and 4-km grids	4-9
Figure 4-7.	Average OH (ppb) at 13:00-14:00 CST for June 3-15, 2006, with CB6 and CB05.....	4-10
Figure 4-8.	Average daily maximum 8-hr isoprene (ISOP; ppb) for June 3-15, 2006, with CB6 and CB05	4-11
Figure 4-9.	Average daily maximum 8-hr isoprene product (ISPD; ppb) for June 3-15, 2006, with CB6 and CB05	4-11
Figure 4-10.	Average daily maximum 8-hr formaldehyde (FORM; ppb) for June 3-15, 2006, with CB6 and CB05.....	4-11
Figure 4-11.	Average daily maximum 8-hr H ₂ O ₂ (ppb) for June 3-15, 2006, with CB6 and CB05.....	4-12
Figure 4-12.	Average daily maximum 8-hr HNO ₃ (ppb) for June 3-15, 2006, with CB6 and CB05.....	4-12

1. INTRODUCTION

ENVIRON performed this project for the Texas Commission on Environmental Quality (TCEQ) to update the Carbon Bond (CB) chemical mechanism used by the TCEQ for photochemical modeling.

The TCEQ is responsible for developing the Texas State Implementation Plan (SIP) for ozone. Ozone SIP development relies upon modeling using the Comprehensive Air Quality Model with Extensions (CAMx) photochemical model and the CB05 chemical mechanism. The chemical mechanism is a critical component in ozone SIP development because it forms the linkage between emissions of ozone precursors, namely Nitrogen Oxides (NO_x) and Volatile Organic Compounds (VOCs), and ozone concentrations in the photochemical model. Research in atmospheric chemistry continually provides new information that should be evaluated and potentially incorporated into chemical mechanisms to maintain their accuracy and thereby provide the best possible strategies for improving ozone air quality.

Chemical mechanisms used in models such as CAMx are called condensed mechanisms because they represent tens of thousands of chemical reactions that occur in the atmosphere by hundreds of representative reactions that can be accommodated in an efficient computer model. CB is one approach to condensing atmospheric chemistry for organic compounds which focuses on the dominant role of chemical structure (e.g., the presence of an alkene bond) in determining the rates and products of atmospheric chemical reactions.

The updated mechanism will be the sixth version of the Carbon Bond mechanism and is named CB6. The TCEQ currently uses the version of CB developed in 2005 which is called CB05 (Yarwood et al., 2005). Completing development of CB6 required identifying which mechanism updates are needed (mechanism design), implementing mechanism updates, and testing the complete CB6 mechanism by comparing mechanism predictions to laboratory (i.e., environmental chamber) experiments. This report documents the design, implementation and evaluation of the CB6 mechanism. Finally, CB6 was tested in CAMx using modeling databases for Texas and Los Angeles and model results for CB6 and CB05 were compared.

2. MECHANISM DESIGN AND IMPLEMENTATION

2.1 MECHANISM DESIGN

CB6 was developed as an update to CB05 and to provide a condensed chemical mechanism for tropospheric oxidants that is suitable for use in atmospheric models such as photochemical grid models. Intended applications are modeling ozone, particulate matter (PM), acid deposition and air toxics.

As tighter ozone standards are adopted (EPA, 2010) ozone modeling will be required to focus on lower ozone concentrations and longer time periods. Two aspects of the CB6 design address these needs: (1) several organic compounds that are long-lived and relatively abundant, namely propane, acetone, benzene and ethyne (acetylene), are added explicitly in CB6 so as to improve oxidant formation from these compounds as they are slowly oxidized. (2) Attention is given to the fate of organic nitrates and the extent to which their degradation produces nitrogen oxides (NO_x) that may then actively participate in oxidant formation.

Gas-phase chemistry influences PM formation by producing aerosol precursors including sulfuric acid, nitric acid and semi-volatile organic compounds. Sulfur dioxide (SO₂) can be oxidized to sulfuric acid by hydrogen peroxide and organic hydroperoxides. CB6 includes several updates to peroxy radical chemistry that will improve formation of peroxides and therefore sulfate aerosol. Updates to reactions of dinitrogen pentoxide (N₂O₅) with water vapor will affect nighttime formation of nitric acid although heterogeneous reactions on aerosol (and other) surfaces may dominate nitric acid formation at night. Secondary organic aerosol (SOA) is very complex and uncertain and a wide variety of modeling approaches have been implemented for SOA. In general, formation SOA precursors is excluded from CB6 and modelers can add SOA formation to the mechanism according to their preferred methodology (e.g., using the volatility basis set; Robinson et al., 2007). An exception is formation of alpha-dicarbonyl compounds (glyoxal and analogues) which can form from SOA via aqueous-phase reactions (Carlton et al., 2007). Glyoxal and glycolaldehyde are added in CB6 (in addition to methylglyoxal) to support modeling of aqueous-phase SOA formation. Precursors to alpha-dicarbonyls included in CB6 are aromatics, alkenes and ethyne.

The main constraint in developing CB6 was maintaining backwards compatibility with previous CB mechanisms so that existing modeling databases can be used with CB6. CB6 can be used with emissions developed for the CB05 (and even CB4) mechanisms although doing so forgoes the benefit of some CB6 mechanism improvements.

2.1.1 Inorganic Reactions

Rate constants change periodically in response to newly published studies. The rate constants for inorganic reactions in CB6 were updated to the latest IUPAC data evaluation (Atkinson et al., 2010) from January 3, 2010.

The inorganic reactions included in CB6 are unchanged from CB05 except that the reaction between O(³P) atoms and O₃ was added to deal with instances where tropospheric models extend into the lower stratosphere, although CB6 is not intended for modeling the stratosphere.

Homogeneous (gas-phase) reaction between N_2O_5 and H_2O was included in CB05 and is retained in CB6. However, Brown et al. (2006) suggest that the homogeneous reaction is extremely slow and that in the atmosphere reaction between N_2O_5 and H_2O is dominated by heterogeneous pathways. In January 2010, the IUPAC panel revised downward their recommended rate constant for the homogeneous reaction between N_2O_5 and H_2O and this recommendation is followed in CB6. When CB6 is used for tropospheric modeling studies heterogeneous reaction between N_2O_5 and H_2O should be accounted for in addition to the gas-phase reaction included in CB6.

2.1.2 Photolysis Reactions

Absorption cross-sections (σ) and quantum yields (Φ) are required to calculate photolysis reaction rates (J). Cross-section and quantum yield data change periodically in response to newly published studies. Several new photolysis reactions were added in CB6 compared to CB05. The primary source of photolysis for CB6 is the IUPAC data evaluation (Atkinson et al., 2010). Additional data are from the 2006 NASA/JPL data evaluation (Sander et al., 2006) and other sources as listed in Table 2-1. The same data sources should be used when CB6 is implemented in models to provide consistency with the mechanism development and evaluation.

Table 2-1. Description of photolysis data for CB6.

Number	Reactants and products	Data source and comments
1	$\text{NO}_2 = \text{NO} + \text{O}$	IUPAC: Atkinson et al. (2010)
8	$\text{O}_3 = \text{O}$	IUPAC: Atkinson et al. (2010)
9	$\text{O}_3 = \text{O}1\text{D}$	IUPAC: Atkinson et al. (2010)
21	$\text{H}_2\text{O}_2 = 2 \text{OH}$	IUPAC: Atkinson et al. (2010)
27	$\text{NO}_3 = \text{NO}_2 + \text{O}$	JPL: Sander et al. (2006)
28	$\text{NO}_3 = \text{NO}$	JPL: Sander et al. (2006)
38	$\text{N}_2\text{O}_5 = \text{NO}_2 + \text{NO}_3$	IUPAC: Atkinson et al. (2010)
43	$\text{HONO} = \text{NO} + \text{OH}$	IUPAC: Atkinson et al. (2010)
47	$\text{HNO}_3 = \text{OH} + \text{NO}_2$	IUPAC: Atkinson et al. (2010)
50	$\text{PNA} = 0.59 \text{HO}_2 + 0.59 \text{NO}_2 + 0.41 \text{OH} + 0.41 \text{NO}_3$	IUPAC: Atkinson et al. (2010)
56	$\text{PAN} = 0.6 \text{NO}_2 + 0.6 \text{C}_2\text{O}_3 + 0.4 \text{NO}_3 + 0.4 \text{MEO}_2 + 0.4 \text{RO}_2$	IUPAC: Atkinson et al. (2010)
64	$\text{PANX} = 0.6 \text{NO}_2 + 0.6 \text{CXO}_3 + 0.4 \text{NO}_3 + 0.4 \text{ALD}_2 + 0.4 \text{XO}_2\text{H} + 0.4 \text{RO}_2$	IUPAC: Atkinson et al. (2010); Data for PAN
88	$\text{MEPX} = \text{MEO}_2 + \text{RO}_2 + \text{OH}$	IUPAC: Atkinson et al. (2010)
90	$\text{ROOH} = \text{HO}_2 + \text{OH}$	IUPAC: Atkinson et al. (2010) ; Data for CH_3OOH
92	$\text{NTR} = \text{NO}_2 + \text{XO}_2\text{H} + \text{RO}_2$	IUPAC: Atkinson et al. (2010) ; Data for $\text{i-C}_3\text{H}_7\text{ONO}_2$
97	$\text{FORM} = 2 \text{HO}_2 + \text{CO}$	IUPAC: Atkinson et al. (2010)
98	$\text{FORM} = \text{CO} + \text{H}_2$	IUPAC: Atkinson et al. (2010)
108	$\text{ALD}_2 = \text{MEO}_2 + \text{RO}_2 + \text{CO} + \text{HO}_2$	IUPAC: Atkinson et al. (2010)
112	$\text{ALDX} = \text{MEO}_2 + \text{RO}_2 + \text{CO} + \text{HO}_2$	SAPRC99: Carter (2000) ; Data for $\text{C}_2\text{H}_5\text{CHO}$
114	$\text{GLYD} = 0.74 \text{FORM} + 0.89 \text{CO} + 1.4 \text{HO}_2 + 0.15 \text{MEOH} + 0.19 \text{OH} + 0.11 \text{GLY} + 0.11 \text{XO}_2\text{H} + 0.11 \text{RO}_2$	IUPAC (Atkinson et al., 2010) cross sections for CH_2OHCHO with same total quantum yield as for ALDX . Product branching ratios from JPL (Sander et al., 2006): 0.70 for $\text{CH}_2\text{OH} + \text{HCO}$; 0.15 for $\text{CH}_3\text{OH} + \text{CO}$; 0.15 for $\text{OH} + \text{CH}_2\text{CHO}$

Number	Reactants and products	Data source and comments
117	GLY = 2 HO ₂ + 2 CO	Cross sections from IUPAC (Atkinson et al., 2010) and quantum yields from Feierabend et al. (2009)
119	MGLY = C ₂ O ₃ + HO ₂ + CO	IUPAC: Atkinson et al. (2010)
128	KET = 0.5 ALD ₂ + 0.5 C ₂ O ₃ + 0.5 XO ₂ H + 0.5 CXO ₃ + 0.5 MEO ₂ + RO ₂ - 2.5 PAR	Cross sections for methyl ethyl ketone with quantum yields for acetone from IUPAC (Atkinson et al., 2010)
129	ACET = 0.38 CO + 1.38 MEO ₂ + 1.38 RO ₂ + 0.62 C ₂ O ₃	IUPAC: Atkinson et al. (2010)
160	ISPD = 0.333 CO + 0.067 ALD ₂ + 0.9 FORM + 0.832 PAR + 0.333 HO ₂ + 0.7 XO ₂ H + 0.7 RO ₂ + 0.967 C ₂ O ₃	CB05: Yarwood et al., (2005); Cross-sections for acrolein from SAPRC99 with wavelength independent quantum yield of 0.0036
197	CRPX = CRNO + OH	IUPAC: Atkinson et al. (2010); Data for CH ₃ OOH
199	XOPN = CAO ₂ + 0.7 HO ₂ + 0.7 CO + 0.3 C ₂ O ₃ + RO ₂	J = 0.05 * J _{NO₂} . Unsaturated ketone based on Whitten et al. (2010) and Calvert et al. (2000).
203	OPEN = OPO ₃ + HO ₂ + CO	J = 0.028 * J _{NO₂} . Unsaturated aldehyde based on Whitten et al. (2010) and Calvert et al. (2000).

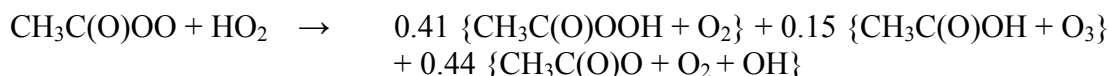
2.1.3 Organic Peroxy Radical Reactions

Organic peroxy radicals are generally referred to as RO₂ radicals because they have the structure R-OO· where R represents an organic group. Peroxyacyl radicals (RCO₃) have the structure R-C(O)OO· and are a sub-class of RO₂ radicals. CB6 includes RO₂ radical reactions with NO, NO₂, HO₂ and RO₂ radicals.

Several updates were implemented for RO₂ radical reactions in CB6.

OH yields from RCO₃ + HO₂ reactions

Recent studies show that reactions of RCO₃ radicals with HO₂ can form OH in addition to carboxylic acids (RCO₂H) and per-acids (RCO₃H):



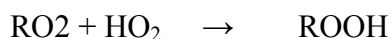
This OH production may be important under low-NO_x conditions. The primary data source for this update in CB6 is the IUPAC data evaluation (Atkinson et al., 2010).

Production of HO₂ following RO₂ reactions with NO

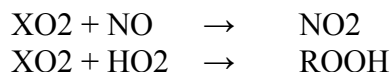
When many RO₂ radicals react with NO they form an alkoxy radical (RO) that promptly reacts with O₂ to form HO₂ plus organic products:



However, if the RO₂ radical reacts with HO₂ a hydroperoxide (ROOH) is formed and prompt HO₂ production is prevented:

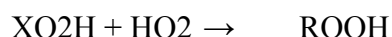


CB05 (and CB4) use the operator XO2 to represent NO to NO₂ conversion and hydroperoxide formation by RO₂ radicals:



But this approach is unable to represent the reduction in HO₂ production that accompanies hydroperoxide formation.

CB6 introduces a new operator (XO2H) that forms HO₂ upon reaction with NO but not upon reaction with HO₂:

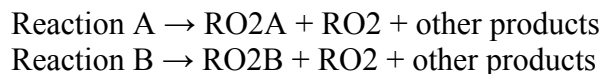


All of the organic reactions in CB6 were reviewed to determine whether the RO₂ radicals produced should be represented by XO₂ or XO₂H.

Representing peroxy radical reactions

Many different RO₂ radicals are formed from organic compounds leading to numerous possible reactions among RO₂ radicals (RO₂-RO₂ reactions). However, the fate of RO₂ radicals generally is dominated by reactions with NO or HO₂ rather than reaction with RO₂ radicals. It is inefficient to include all possible RO₂-RO₂ reactions in a condensed mechanism such as CB6 and in many cases the rate constants and products of RO₂-RO₂ reactions are unknown. Nevertheless, robust mechanism design requires that some RO₂-RO₂ reactions be included to preclude RO₂ radical concentrations from growing unreasonably large if NO and HO₂ are scarce.

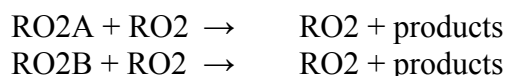
An efficient scheme for RO₂-RO₂ reactions was needed for CB6. A new operator (RO2) is introduced to represent the sum of all RO₂ radicals (excluding RCO₃ radicals). Suppose reactions A and B form RO₂ radicals RO₂A and RO₂B, respectively. The new CB6 operator RO2 is added as a product in both reactions to measure the total production of RO₂ radicals:



Then, RO₂ is removed by its self-reaction:



There are no products in the self-reaction of RO₂ because the only purpose is to establish the concentration of RO₂. Radicals RO₂A and RO₂B are removed by reaction with RO₂ (which represents the total RO₂ concentration, in this case RO₂A + RO₂B):



RO₂ is included on the product side of these reactions to avoid double counting the removal of RO₂ (already accounted for by the RO₂ + RO₂ reaction). This method is applied to all RO₂ radicals in the CB6 mechanism. Note that all RO₂-RO₂ reactions should be assigned the same rate constant for the concentration of RO₂ to most closely match the sum of individual RO₂ radical concentrations ($RO_2 \approx RO_{2A} + RO_{2B}$).

There is no efficiency gain in applying this approach with only two types of RO₂ radicals, as illustrated above. However, with many types of RO₂ radicals this approach greatly reduces the number of reactions (80% reduction with 10 RO₂ radicals¹) at the expense of adding one extra species (RO₂). Table 2-2 shows all potential peroxy radical reactions for CB6 and identifies which reactions are included.

Table 2-2. All potential peroxy radical reactions for CB6 and the reactions included.

	HO ₂	RCO ₃ Radicals			RO ₂ Radicals										
		C ₂ O ₃	CXO ₃	OPO ₃	RO ₂	MEO ₂	XO ₂	XO ₂ H	XO ₂ N	BZO ₂	TO ₂	XLO ₂	CAO ₂	ISO ₂	EPX ₂
NO	•	•	•	•	•	•	•	•	•	•	•	•	•	•	•
NO ₂	•	•	•	•											
HO ₂	•	•	•	•	•	•	•	•	•	•	•	•	•	•	•
C ₂ O ₃		•	•		•										
CXO ₃			•		•										
OPO ₃					•										
RO₂					•	•	•	•	•	•	•	•	•	•	•
MEO ₂															
XO ₂															
XO ₂ H															
XO ₂ N															
BZO ₂															
TO ₂															
XLO ₂															
CAO ₂															
ISO ₂															
EPX ₂															

Note: The operator RO₂ represents the sum of all RO₂ radicals excluding RCO₃ radicals

Rate constants for peroxy radical reactions in CB6 are based on data from IUPAC (Atkinson, 2010). Table 2-3 summarizes the rate constants that are available from IUPAC and also shows the limited coverage of available data. Table 2-4 lists the rate constants selected for the main RCO₃ radicals (C₂O₃ and CXO₃) and the operator for total RO₂ radicals (RO₂) in CB6. Rate constants for reactions of RO₂ were selected to fall near the middle of the range or reported rate constants bearing in mind that methylperoxy radical is generally expected to be the most abundant RO₂ radical in the atmosphere.

¹ With N RO₂ radicals, the condensation scheme reduces the number of reactions required by $(N+1) / ((N \times N/2) + N/2)$

Table 2-3. Summary of peroxy radical rate constants (k_{298} and temperature dependence) from IUPAC (2010).

	RCO ₃ radicals		RO ₂ radicals					
	ACO3	PRO3	MEO2	ETO2	HOETO2	n-PRO2	i-PRO2	TOLO2
NO	2.0(-11) -290	2.1(-11) -340	7.7(-12) -360	9.1(-12) -380	9(-12)	9.4(-12) -350	9(-12) -360	
HO2	1.4(-11) -980		5.2(-12) -780	8(-12) -870	1.2(-11)			1.2(-11) -1310
ACO3	1.6(-11) -500		1.1(-11) -500	1.6(-11) -1070				
PRO3		1.7(-11)		1.2(-11)				
MEO2			3.5(-13) -365					
ETO2				6.4(-14) 0				
HOETO2					2.2(-12) -1000			
n-PRO2						3(-13)		
i-PRO2							1(-15) 2200	
TOLO2								5.5(-12) -1620

Notes:

- (1) ACO3 = CH₃C(O)OO; PRO3 = CH₃CH₂C(O)OO; MEO2 = CH₃OO; ETO2 = CH₃CH₂OO; HOETO2 = HOCH₂CH₂OO; n-PR = n-propyl; i-PR = i-propyl; TOLO2 = C₆H₅CH₂OO.
 (2) 2.0(-11) -290 denotes $k_{298} = 2.0 \times 10^{-11}$ with temperature dependence (E/R) of -290 K.

Table 2-4. CB6 rate constants (k_{298} and temperature dependence) for acylperoxy (RCO3) and peroxy (RO2) radical reactions.

	C2O3	CXO3	RO2
NO	2.0(-11) -290	2.1(-11) -340	8.0(-12) -360
HO2	1.4(-11) -980	1.4(-11) -980	7.0(-12) -800
C2O3	1.55(-11) -500	1.55(-11) -500	1.3(-11) -800
CXO3		1.7(-11) -500	1.0(-11) -800
RO2			3.5(-13) -500

Notes:

- (1) C2O3 is CH₃C(O)OO; CXO3 represents higher RCO3 radicals; RO2 represents the sum of RO2 radicals except for RCO3 radicals
 (2) 2.0(-11) -290 denotes $k_{298} = 2.0 \times 10^{-11}$ with temperature dependence (E/R) of -290 K.

2.1.4 Oxygenates

Add Ketone Species

Ketones are represented in CB05 and CB4 by the surrogate species PAR (e.g., acetone is 3 PAR). Two ketone species, acetone and a higher ketone, are added to CB6 because ketones photolyze and thereby provide sources of radicals. Having explicit acetone also may be useful for comparisons with ambient data.

In CB6, acetone (ACET) is an explicit 3-carbon species whereas the higher ketone (KET) is a 1-carbon species representing the carbonyl group. Methyl ethyl ketone (MEK) is represented as 3 PAR + KET in CB6 as compared to 4 PAR in CB05/CB4. The gas-phase reactions for ACET and KET are added in CB6 based on data from IUPAC (Atkinson et al., 2010).

Add Glyoxal and Glycolaldehyde

Glyoxal and glycolaldehyde are SOA precursors via aqueous-phase reactions (Lim et al., 2005, Carlton et al., 2004). They are formed in the oxidation of unsaturated hydrocarbons including alkenes, aromatics and alkynes. The gas-phase reactions of glyoxal (GLY) and glycolaldehyde (GLYD) are added in CB6 based on data from IUPAC (Atkinson et al., 2010) supplemented by other sources for their photolysis.

Eliminate Photolysis of Peroxyacetic Acid

Peroxyacetic acid ($\text{CH}_3\text{C}(\text{O})\text{OOH}$) is formed by reaction of peroxyacyl radical ($\text{CH}_3\text{C}(\text{O})\text{OO}\cdot$) with HO_2 . CB05 included photolysis of peroxyacetic acid but UV-absorption cross section data (Gigu et al., 1956) show that photolysis will be very slow and this reaction is deleted in CB6.

2.1.5 Alkanes

Explicit Propane

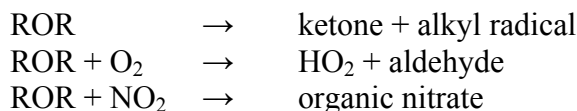
Propane reacts more slowly with OH than larger alkanes that are represented by PAR in CB mechanisms and propane is represented as 1.5 PAR + 1.5 NR in CB05. Propane has large emissions (e.g., associated with natural gas production) and is an important precursor to acetone. Propane is added as an explicit species in CB6 to improve mechanism performance at regional scales and in the remote troposphere. The OH-reaction of propane is based on kinetic data from IUPAC (Atkinson, 2010) with the bi-exponential rate expression simplified to an Arrhenius expression.

Ketone Formation

Two ketone species are added in CB6 and alkanes are important ketone precursors. The derivation of the CB chemistry for higher alkanes (PAR) included ketone formation (Gery et al., 1988) although ketones were eliminated from the CB4 (and CB05) mechanism by condensation. Ketone production from PAR is included in CB6 based on Gery et al. (1988).

Temperature Dependence of Alkoxy Radical (ROR) Reactions

Secondary alkoxy radicals ($R_1\text{-CH(O}\cdot\text{)-R}_2$) formed from higher alkanes (PAR) are represented by the species ROR in CB4 (and CB05). ROR can undergo unimolecular decomposition or react with O_2 or NO_2 :



The rate constants for these reactions have different temperature dependencies causing the products formed from ROR to vary with temperature. The rate constants for these 3 reactions were updated in CB6 using data for $CH_3CH(O\cdot)CH_2CH_3$ as reported by IUPAC (Atkinson et al., 2010).

2.1.6 Alkenes

Anthropogenic Alkenes

CB6 has three anthropogenic alkene species:

ETH – explicit ethene
OLE – terminal alkenes ($R_1\text{-CH=CH}_2$) based on propene
IOLE – internal alkenes ($R_1\text{-CH=CH-R}_2$) based on 2-butene

Each species has reactions with OH, O_3 , NO_3 and $O(^3P)$. Rate constants for OLE are for propene and rate constants for IOLE are for 2-butene assuming equal fractions of the cis and trans (Z and E) isomers. Rate constants were updated from IUPAC (Atkinson et al., 2010) where available.

Reaction of ethene with OH forms glycolaldehyde which is included explicitly in CB6 but was previously represented in CB05 by ALDX as a surrogate.

The products of OH reaction with OLE were derived assuming the following proportions of C3 to C8 terminal alkenes: 0.5, 0.12, 0.13, 0.14, 0.08 and 0.03 (Calvert et al., 2000) with product data of Kwok et al. (1996) and Shepson et al., (1985).

The decomposition products of Criegee di-radicals formed by ozonolysis of the anthropogenic alkenes were updated based on Atkinson et al. (2010) and Calvert et al. (2000).

Isoprene

The isoprene mechanism in CB05 is based on Carter and Atkinson (1996) and Carter (1996) and, for compactness, uses a single product (ISPD) to represent methacrolein and methylvinylketone other isoprene degradation C_4 products. As discussed below, substantial new research has emerged since this isoprene mechanism was developed.

Lelieveld et al. (2008) analyzed detailed atmospheric chemistry measurements made over pristine South American rain forest and concluded that isoprene oxidation causes much higher concentrations of OH than are predicted by current chemical mechanisms for low-NO_x environments (Butler et al., 2008; Archibald et al., 2010). However, Pugh et al. (2010) suggest that underestimating removal of isoprene degradation products by deposition may be an alternate explanation (or contributing factor) to the discrepancies presented by Lelieveld et al. (2008). Paulot et al. (2009 a,b) performed laboratory experiments on isoprene oxidation and proposed condensed reaction schemes for isoprene with OH for both high- and low-NO_x conditions. Peeters et al. (2009), Karl et al. (2009) and Archibald et al. (2010) have proposed isoprene oxidation mechanisms that may be able to account for the OH production at low-NO_x conditions reported by Lelieveld et al. (2008).

The CB6 isoprene mechanism was developed by condensation of the mechanism of Paulot et al. (2009a and b) using information from Horowitz et al. (2007) to constrain overall yields of organic nitrates and information from Perring et al. (2009) for nitrate radical reactions. Unsaturated organic nitrates formed from isoprene RO₂ radicals (ISO2) are represented by a species INTR which releases some NO_x upon reaction with OH. ISO2 radicals undergo unimolecular decomposition (as proposed by Peeters et al., 2009) at a rate of 1 s⁻¹ which is slower than the rate of 3 s⁻¹ proposed by Peeters et al. (2009) in order to improve agreement with chamber experiments. Methacrolein and methylvinylketone formed from ISO2 reaction with NO are condensed to a single species (ISPD) for compactness. Formation of a PAN-type compound from methacrolein is represented by formation of PANX in CB6. Glyoxal and glycolaldehyde are explicit products of isoprene degradation in CB6 because they are SOA precursors (Carlton et al., 2007).

2.1.7 Aromatics

Dicarbonyl Products

Several alpha-dicarbonyls (R₁-C(O)C(O)-R₂) are products of the OH-initiated oxidation of aromatic hydrocarbons (Calvert et al., 2002). Previous CB mechanisms included methylglyoxal (MGLY) and a higher alpha-dicarbonyl (OPEN) because alpha-dicarbonyls photolyze rapidly (Calvert et al., 2002) and therefore are important to oxidant formation from aromatics. Glyoxal was added to CB6 because it is an SOA precursor (Carlton et al., 2007). The aromatic hydrocarbon mechanisms in CB6 were updated to include production of glyoxal (GLY) and methylglyoxal as well as two higher alpha-dicarbonyls (OPEN and XOPN).

Add Explicit Benzene

Benzene is one of the most abundant aromatic compounds in the atmosphere because has many sources (e.g., fuel combustion and evaporation) and reacts slowly with OH and therefore tends to accumulate at regional scales. Previous CB mechanisms represented the oxidant formation potential of benzene using surrogate species. Benzene (BENZ) is added as an explicit species in CB6 because it is a precursor to glyoxal and therefore an SOA precursor. Having explicit benzene also may be useful for comparing model results with ambient data. The reaction mechanism for benzene was developed with the mechanisms for other aromatics, as discussed below.

Aromatic Mechanisms

CB6 has three aromatic hydrocarbons species:

BENZ – explicit species representing only benzene

TOL – based on toluene and representing mono-substituted aromatic hydrocarbons

XYL – based on xylene and representing poly-substituted aromatic hydrocarbons

The xylene mechanism was developed by combining kinetic and mechanistic data for o-, m- and p-xylene with weighting factors of 0.25, 0.5 and 0.25 based on gasoline composition (Hochhauser, 2009).

All aromatic mechanisms were based on the updated toluene mechanism for CB05 (CB05-TU) described by Whitten et al., (2009) with the following points noted:

- Rate constants for OH + aromatic reactions are from IUPAC (Atkinson et al., 2010)
- Branching ratios for H-abstraction from ring substituent groups vs. OH-addition to the aromatic ring are based on Bloss et al. (2005)
- Yields of alpha-dicarbonyl products are based on Arey et al. (2009)
- Glyoxal (GLY) and methylglyoxal (MGLY) are explicit products whereas biacetyl is represented as 1.5 MGLY
- In general, unsaturated aldehyde products are represented by OPEN and unsaturated ketone products are represented by XOPN, although the yields of OPEN and XOPN were adjusted to produce the reactivity trend XYL > TOL > BENZ
- The PAN compound formed from OPEN (OPAN) can condense to SOA (Hu et al., 2007) retarding its decomposition which was accounted for by slowing the rate constant for OPAN decomposition

Aromatic hydrocarbons are important precursors to SOA. BENZ, TOL and XYL each produce a unique RO₂ radical (BZO₂, TO₂ and XLO₂, respectively) following OH and O₂ addition to the aromatic ring in order to represent differences in products formed after reaction with NO (or RO₂ radicals) and ring opening. Reaction of these aromatic RO₂ Radicals with HO₂ forms low volatility hydroperoxides that condense to SOA and therefore are omitted from CB6. The reactions of BZO₂, TO₂ and XLO₂ with NO and HO₂ are a suitable points for modelers to integrate SOA formation into CB6 and account for the impact of NO_x on SOA formation from aromatics (Ng et al., 2007). For example, using the volatility basis set scheme of Robinson et al. (2007), the toluene aerosol products for high NO_x conditions (Lane et al., 2008a) could be added to the reaction between TO₂ and NO whereas the toluene aerosol products for low NO_x conditions (Lane et al., 2008b) could be added to the reaction between TO₂ and HO₂.

2.1.8 Arenes

Ethyne (acetylene) has large emissions (e.g., from combustion sources) and reacts slowly with OH and therefore tends to accumulate at regional scales. Previous CB mechanisms represented the oxidant formation potential of ethyne using surrogate species. Ethyne (ETHY) is added as an explicit species in CB6 because it is a precursor to glyoxal and therefore an SOA precursor. Having explicit ethyne also may be useful for comparing model results with ambient data. The OH reaction of ethyne is based in data from IUPAC (Atkinson et al., 2010).

2.1.9 Optional Mechanism Extensions

Electronically Excited NO₂*

Nitrogen dioxide (NO₂) absorbs solar radiation in the ultra-violet (UV) and visible regions of the spectrum. At wavelengths shorter than 420 nm NO₂ can photo-dissociate to nitric oxide (NO) and an oxygen atom (O(³P)) but otherwise electronically excited NO₂ (NO₂^{*}) is formed. Usually, NO₂^{*} is promptly quenched back to ground-state NO₂ by non-reactive collisions with air molecules (M). Li et al. (2008) reported that NO₂^{*} can react with a gaseous water molecule to form hydroxyl radical (OH) and nitrous acid (HONO) which could be an important source of OH in NO_x-rich environments (Wennberg and Dabdub, 2008). These reactions are shown in Table 2-5 with NO₂^{*} designated NO2S and the rate constant for NO2S + H₂O reported by Li et al. (2008).

Table 2-5. Mechanism for OH formation from NO₂^{*} with the rate constant for NO2S + H₂O reported by Li et al. (2008).

Reactants	Products	k ₂₉₈	Ea (K)
NO2	NO2S	Photolysis	
NO2S + M	NO2	2.94E-11	-102
NO2S + H ₂ O	OH + HONO	1.70E-13	0

The amount of OH production from NO₂^{*} depends upon the rate constant for reaction between NO₂^{*} and H₂O. Li et al. (2008) reported that 1% of collisions between NO₂^{*} and H₂O result in OH production. Crowley and Carl (1997) had previously concluded that the efficiency was much lower with less than 0.007% of collisions between NO₂^{*} and H₂O resulting in OH production. More recently, Carr et al., (2009) studied the reaction again and concluded that less than 0.006% of collisions between NO₂^{*} and H₂O result in OH production. In explanation of the apparent discrepancy between these three studies, Carr et al. (2009) suggested that the OH production reported by Li et al. (2008) could be an artifact of their laboratory experiment. Li et al. (2009) argued in response that their 2008 findings are real. Whether or not reaction between NO₂^{*} and H₂O is a source of OH under atmospheric conditions remains an unsettled question at this time. Ideally, the atmospheric chemistry review panels convened by IUPAC and NASA (IUPAC, 2010 and Sander et al., 2006) will resolve this question.

The NO₂^{*} reactions shown in Table 2-4 may be used with CB6 but were not included in the development and evaluation of the CB6 mechanism described here.

Nitryl Chloride (NO₂Cl)

During 2006 the TCEQ organized a major field study campaign for the Texas Gulf Coast region called the second Texas Air Quality Field Study (TexAQS2). The NOAA research vessel R/V Ronald H. Brown participated in TexAQS2 by making detailed measurements of atmospheric trace gases and aerosols in the Gulf of Mexico, Galveston Bay, Houston ship channel and the Atlantic Ocean. Using data collected from the Ron Brown, Osthoff et al. (2008) reported that dinitrogen pentoxide (N₂O₅) can interact with chloride-containing aerosols to produce nitryl chloride (NO₂Cl) gas. CB6 does not include NO₂Cl formation because reaction takes place on aerosol surfaces rather than in the gas phase.

Bertram and Thornton (2009) have proposed kinetic equations to describe reactions between N_2O_5 and H_2O or HCl to form nitric acid or NO_2Cl , respectively. The process of NO_2Cl formation is complex and has the following major ingredients: (1) reaction occurs on the surface of an aerosol that may be sea salt or another type of aerosol; (2) reaction requires HCl that may be supplied by the aerosol or by the gas phase; (3) reaction requires N_2O_5 that is supplied by the gas phase.

2.2 MECHANISM IMPLEMENTATION

Rate constants may depend upon temperature and pressure requiring several types of rate expressions, as shown in Table 2-6. The reactions and rate expressions for CB6 are listed in Table 2-7. CB6 model species names are explained in Table 2-8.

Table 2-6. Rate constant expressions used in CB6.

Rate constant type	Expression
Temperature dependent rate constant	$k = A \left(\frac{T}{T_R} \right)^B \exp \left[\frac{-E_a}{T} \right]$
Temperature and pressure dependent rate constant defined using Troe's formula	$k = \left[\frac{k^o[M]}{1 + k^o[M] / k^\infty} \right] F^G$ $k^o = A \left(\frac{T}{T_R} \right)^B \exp \left[\frac{-E_a}{T} \right]$ $k^\infty = A' \left(\frac{T}{T_R'} \right)^{B'} \exp \left[\frac{-E_a'}{T} \right]$ $G = \left[1 + \left(\frac{\log(k^o[M] / k^\infty)}{n} \right)^2 \right]^{-1}$
Previously defined rate constant (k_{ref}) multiplied by an equilibrium constant	$k = k_{ref} A \left(\frac{T}{T_R} \right)^B \exp \left[\frac{-E_a}{T} \right]$

Table notes:

- T is the temperature (K)
- T_R is a reference temperature of 300 K
- E_A is an Arrhenius activation energy (K)
- k_0 is the low pressure limit of the rate constant
- k_∞ is the high pressure limit of the rate constant
- [M] is the concentration of air

Table 2-7. Listing of reactions and rate parameters for CB6.

Number	Reactants and Products	k ₂₉₈	Rate Parameters			Notes
			A	E _a	B	
1	NO ₂ = NO + O	Photolysis				a
2	O + O ₂ + M = O ₃ + M	5.78E-34	5.68E-34	0.0	-2.60	a
3	O ₃ + NO = NO ₂	1.73E-14	1.40E-12	1310.0	0.00	a
4	O + NO + M = NO ₂ + M	1.01E-31	1.00E-31	0.0	-1.60	a
5	O + NO ₂ = NO	1.03E-11	5.50E-12	-188.0	0.00	a
6	O + NO ₂ = NO ₃	2.11E-12	Falloff, F=0.60, N=1.00			a
		k ₀	1.30E-31	0.0	-1.50	
		k _∞	2.30E-11	0.0	0.24	
7	O + O ₃ =	7.96E-15	8.00E-12	2060.0	0.00	a
8	O ₃ = O	Photolysis				a
9	O ₃ = O ₁ D	Photolysis				a
10	O ₁ D + M = O + M	3.28E-11	2.23E-11	-115.0	0.00	a
11	O ₁ D + H ₂ O = 2 OH	2.14E-10	2.14E-10			a
12	O ₃ + OH = HO ₂	7.25E-14	1.70E-12	940.0	0.00	a
13	O ₃ + HO ₂ = OH	2.01E-15	2.03E-16	-693.0	4.57	a
14	OH + O = HO ₂	3.47E-11	2.40E-11	-110.0	0.00	a
15	HO ₂ + O = OH	5.73E-11	2.70E-11	-224.0	0.00	a
16	OH + OH = O	1.48E-12	6.20E-14	-945.0	2.60	a
17	OH + OH = H ₂ O ₂	5.25E-12	Falloff, F=0.50, N=1.13			a
		k ₀	6.90E-31	0.0	-0.80	
		k _∞	2.60E-11	0.0	0.00	
18	OH + HO ₂ =	1.11E-10	4.80E-11	-250.0	0.00	a
19	HO ₂ + HO ₂ = H ₂ O ₂	2.90E-12	k = k ₁ + k ₂ [M]			a
		k ₁	2.20E-13	-600.0	0.00	
		k ₂	1.90E-33	-980.0	0.00	
20	HO ₂ + HO ₂ + H ₂ O = H ₂ O ₂	6.53E-30	k = k ₁ + k ₂ [M]			a
		k ₁	3.08E-34	-2800.0	0.00	
		k ₂	2.66E-54	-3180.0	0.00	
21	H ₂ O ₂ = 2 OH	Photolysis				a
22	H ₂ O ₂ + OH = HO ₂	1.70E-12	2.90E-12	160.0	0.00	a
23	H ₂ O ₂ + O = OH + HO ₂	1.70E-15	1.40E-12	2000.0	0.00	a
24	NO + NO + O ₂ = 2 NO ₂	1.95E-38	3.30E-39	-530.0	0.00	a
25	HO ₂ + NO = OH + NO ₂	8.54E-12	3.45E-12	-270.0	0.00	a
26	NO ₂ + O ₃ = NO ₃	3.52E-17	1.40E-13	2470.0	0.00	a
27	NO ₃ = NO ₂ + O	Photolysis				b
28	NO ₃ = NO	Photolysis				b
29	NO ₃ + NO = 2 NO ₂	2.60E-11	1.80E-11	-110.0	0.00	a
30	NO ₃ + NO ₂ = NO + NO ₂	6.56E-16	4.50E-14	1260.0	0.00	b
31	NO ₃ + O = NO ₂	1.70E-11	1.70E-11			a
32	NO ₃ + OH = HO ₂ + NO ₂	2.00E-11	2.00E-11			a
33	NO ₃ + HO ₂ = OH + NO ₂	4.00E-12	4.00E-12			a
34	NO ₃ + O ₃ = NO ₂	1.00E-17	1.00E-17			c,k
35	NO ₃ + NO ₃ = 2 NO ₂	2.28E-16	8.50E-13	2450.0	0.00	b
36	NO ₃ + NO ₂ = N ₂ O ₅	1.24E-12	Falloff, F=0.35, N=1.33			a
		k ₀	3.60E-30	0.0	-4.10	
		k _∞	1.90E-12	0.0	0.20	
37	N ₂ O ₅ = NO ₃ + NO ₂	4.46E-02	Falloff, F=0.35, N=1.33			a
		k ₀	1.30E-03	11000.0	-3.50	
		k _∞	9.70E+14	11080.0	0.10	

Number	Reactants and Products	k ₂₉₈	Rate Parameters			Notes
			A	E _a	B	
38	N ₂ O ₅ = NO ₂ + NO ₃	Photolysis				a
39	N ₂ O ₅ + H ₂ O = 2 HNO ₃	1.00E-22	1.00E-22			a
40	NO + OH = HONO	9.77E-12	Falloff, F=0.81 ,N=0.87			a
		k ₀	7.40E-31	0.0	-2.40	
		k _∞	3.30E-11	0.0	-0.30	
41	NO + NO ₂ + H ₂ O = 2 HONO	5.00E-40	5.00E-40			c,l
42	HONO + HONO = NO + NO ₂	1.00E-20	1.00E-20			c,m
43	HONO = NO + OH	Photolysis				a
44	HONO + OH = NO ₂	5.98E-12	2.50E-12	-260.0	0.00	a
45	NO ₂ + OH = HNO ₃	1.06E-11	Falloff, F=0.60 ,N=1.00			b
		k ₀	1.80E-30	0.0	-3.00	
		k _∞	2.80E-11	0.0	0.00	
46	HNO ₃ + OH = NO ₃	1.54E-13	k = k ₁ +k ₃ M/(1+k ₃ M/k ₂)			a
		k ₁	2.40E-14	-460.0	0.00	
		k ₂	2.70E-17	-2199.0	0.00	
		k ₃	6.50E-34	-1335.0	0.00	
47	HNO ₃ = OH + NO ₂	Photolysis				a
48	HO ₂ + NO ₂ = PNA	1.38E-12	Falloff, F=0.60 ,N=1.00			a
		k ₀	1.80E-31	0.0	-3.20	
		k _∞	4.70E-12	0.0	0.00	
49	PNA = HO ₂ + NO ₂	8.31E-02	Falloff, F=0.60 ,N=1.00			a
		k ₀	4.10E-05	10650.0	0.00	
		k _∞	4.80E+15	11170.0	0.00	
50	PNA = 0.59 HO ₂ + 0.59 NO ₂ + 0.41 OH + 0.41 NO ₃	Photolysis				a
51	PNA + OH = NO ₂	3.24E-12	3.20E-13	-690.0	0.00	a
52	SO ₂ + OH = SULF + HO ₂	8.12E-13	Falloff, F=0.53 ,N=1.10			a
		k ₀	4.50E-31	0.0	-3.90	
		k _∞	1.30E-12	0.0	-0.70	
53	C ₂ O ₃ + NO = NO ₂ + MEO ₂ + RO ₂	1.98E-11	7.50E-12	-290.0	0.00	a
54	C ₂ O ₃ + NO ₂ = PAN	1.05E-11	Falloff, F=0.30 ,N=1.00			a
		k ₀	2.70E-28	0.0	-7.10	
		k _∞	1.20E-11	0.0	-0.90	
55	PAN = NO ₂ + C ₂ O ₃	3.31E-04	Falloff, F=0.30 ,N=1.00			a
		k ₀	4.90E-03	12100.0	0.00	
		k _∞	5.40E+16	13830.0	0.00	
56	PAN = 0.6 NO ₂ + 0.6 C ₂ O ₃ + 0.4 NO ₃ + 0.4 MEO ₂ + 0.4 RO ₂	Photolysis				a
57	C ₂ O ₃ + HO ₂ = 0.41 PACD + 0.15 AACD + 0.15 O ₃ + 0.44 MEO ₂ + 0.44 RO ₂ + 0.44 OH	1.39E-11	5.20E-13	-980.0	0.00	a
58	C ₂ O ₃ + RO ₂ = C ₂ O ₃	1.30E-11	8.90E-13	-800.0	0.00	a
59	C ₂ O ₃ + C ₂ O ₃ = 2 MEO ₂ + 2 RO ₂	1.55E-11	2.90E-12	-500.0	0.00	a
60	C ₂ O ₃ + CXO ₃ = MEO ₂ + ALD ₂ + XO ₂ H + 2 RO ₂	1.55E-11	2.90E-12	-500.0	0.00	a
61	CXO ₃ + NO = NO ₂ + ALD ₂ + XO ₂ H + RO ₂	2.10E-11	6.70E-12	-340.0	0.00	a
62	CXO ₃ + NO ₂ = PANX	1.16E-11	Falloff, F=0.30 ,N=1.00			a
		k ₀	3.00E-28	0.0	-7.10	
		k _∞	1.33E-11	0.0	-0.90	
63	PANX = NO ₂ + CXO ₃	3.68E-04	Falloff, F=0.30 ,N=1.00			a
		k ₀	1.70E-03	11280.0	0.00	
		k _∞	8.30E+16	13940.0	0.00	

Number	Reactants and Products	k ₂₉₈	Rate Parameters			Notes
			A	E _a	B	
64	PANX = 0.6 NO ₂ + 0.6 CXO ₃ + 0.4 NO ₃ + 0.4 ALD ₂ + 0.4 XO ₂ H + 0.4 RO ₂	Photolysis				a
65	CXO ₃ + HO ₂ = 0.41 PACD + 0.15 AACD + 0.15 O ₃ + 0.44 ALD ₂ + 0.44 XO ₂ H + 0.44 RO ₂ + 0.44 OH	1.39E-11	5.20E-13	-980.0	0.00	a
66	CXO ₃ + RO ₂ = CXO ₃	1.30E-11	8.90E-13	-800.0	0.00	a
67	CXO ₃ + CXO ₃ = 2 ALD ₂ + 2 XO ₂ H + 2 RO ₂	1.71E-11	3.20E-12	-500.0	0.00	a
68	RO ₂ + NO = NO	8.03E-12	2.40E-12	-360.0	0.00	a
69	RO ₂ + HO ₂ = HO ₂	7.03E-12	4.80E-13	-800.0	0.00	a
70	RO ₂ + RO ₂ =	3.48E-13	6.50E-14	-500.0	0.00	a
71	MEO ₂ + NO = FORM + HO ₂ + NO ₂	7.70E-12	2.30E-12	-360.0	0.00	a
72	MEO ₂ + HO ₂ = 0.9 MEPX + 0.1 FORM	5.21E-12	3.80E-13	-780.0	0.00	a
73	MEO ₂ + C ₂ O ₃ = FORM + 0.9 HO ₂ + 0.9 MEO ₂ + 0.1 AACD + 0.9 RO ₂	1.07E-11	2.00E-12	-500.0	0.00	a
74	MEO ₂ + RO ₂ = 0.685 FORM + 0.315 MEOH + 0.37 HO ₂ + RO ₂	3.48E-13 k(ref) K	k = kref*K ref = 70 1.00E+00	0.0	0.00	a
75	XO ₂ H + NO = NO ₂ + HO ₂	9.04E-12	2.70E-12	-360.0	0.00	a
76	XO ₂ H + HO ₂ = ROOH	9.96E-12	6.80E-13	-800.0	0.00	a
77	XO ₂ H + C ₂ O ₃ = 0.8 HO ₂ + 0.8 MEO ₂ + 0.2 AACD + 0.8 RO ₂	1.30E-11 k(ref) K	k = kref*K ref = 58 1.00E+00	0.0	0.00	a
78	XO ₂ H + RO ₂ = 0.6 HO ₂ + RO ₂	3.48E-13 k(ref) K	k = kref*K ref = 70 1.00E+00	0.0	0.00	a
79	XO ₂ + NO = NO ₂	9.04E-12 k(ref) K	k = kref*K ref = 75 1.00E+00	0.0	0.00	a
80	XO ₂ + HO ₂ = ROOH	9.96E-12 k(ref) K	k = kref*K ref = 76 1.00E+00	0.0	0.00	a
81	XO ₂ + C ₂ O ₃ = 0.8 MEO ₂ + 0.2 AACD + 0.8 RO ₂	1.30E-11 k(ref) K	k = kref*K ref = 58 1.00E+00	0.0	0.00	a
82	XO ₂ + RO ₂ = 0.6 HO ₂ + RO ₂	3.48E-13 k(ref) K	k = kref*K ref = 70 1.00E+00	0.0	0.00	a
83	XO ₂ N + NO = NTR	9.04E-12 k(ref) K	k = kref*K ref = 75 1.00E+00	0.0	0.00	a
84	XO ₂ N + HO ₂ = ROOH	9.96E-12 k(ref) K	k = kref*K ref = 76 1.00E+00	0.0	0.00	a
85	XO ₂ N + C ₂ O ₃ = 0.8 HO ₂ + 0.8 MEO ₂ + 0.2 AACD + 0.8 RO ₂	1.30E-11 k(ref) K	k = kref*K ref = 58 1.00E+00	0.0	0.00	a
86	XO ₂ N + RO ₂ = 0.6 HO ₂ + RO ₂	3.48E-13 k(ref) K	k = kref*K ref = 70 1.00E+00	0.0	0.00	a

Number	Reactants and Products	k_{298}	Rate Parameters			Notes
			A	E_a	B	
87	MEPX + OH = 0.6 MEO2 + 0.6 RO2 + 0.4 FORM + 0.4 OH	1.00E-11	5.30E-12	-190.0	0.00	a
88	MEPX = MEO2 + RO2 + OH	Photolysis				a
89	ROOH + OH = 0.54 XO2H + 0.06 XO2N + 0.6 RO2 + 0.4 OH	6.05E-12	3.20E-12	-190.0	0.00	a
90	ROOH = HO2 + OH	Photolysis				a
91	NTR + OH = HNO3 + XO2H + RO2	8.10E-13	8.10E-13			a,c
92	NTR = NO2 + XO2H + RO2	Photolysis				a,c
93	FACD + OH = HO2	4.50E-13	4.50E-13			a
94	AACD + OH = MEO2 + RO2	6.93E-13	4.00E-14	-850.0	0.00	a
95	PACD + OH = C2O3	6.93E-13	4.00E-14	-850.0	0.00	a
96	FORM + OH = HO2 + CO	8.49E-12	5.40E-12	-135.0	0.00	a
97	FORM = 2 HO2 + CO	Photolysis				a
98	FORM = CO + H2	Photolysis				a
99	FORM + O = OH + HO2 + CO	1.58E-13	3.40E-11	1600.0	0.00	b
100	FORM + NO3 = HNO3 + HO2 + CO	5.50E-16	5.50E-16			a
101	FORM + HO2 = HCO3	7.90E-14	9.70E-15	-625.0	0.00	a
102	HCO3 = FORM + HO2	1.51E+02	2.40E+12	7000.0	0.00	a
103	HCO3 + NO = FACD + NO2 + HO2	5.60E-12	5.60E-12			a
104	HCO3 + HO2 = 0.5 MEPX + 0.5 FACD + 0.2 OH + 0.2 HO2	1.26E-11	5.60E-15	-2300.0	0.00	a
105	ALD2 + O = C2O3 + OH	4.49E-13	1.80E-11	1100.0	0.00	b
106	ALD2 + OH = C2O3	1.50E-11	4.70E-12	-345.0	0.00	a
107	ALD2 + NO3 = C2O3 + HNO3	2.73E-15	1.40E-12	1860.0	0.00	a
108	ALD2 = MEO2 + RO2 + CO + HO2	Photolysis				a
109	ALDX + O = CXO3 + OH	7.02E-13	1.30E-11	870.0	0.00	c,n
110	ALDX + OH = CXO3	1.91E-11	4.90E-12	-405.0	0.00	a
111	ALDX + NO3 = CXO3 + HNO3	6.30E-15	6.30E-15			a
112	ALDX = MEO2 + RO2 + CO + HO2	Photolysis				f
113	GLYD + OH = 0.2 GLY + 0.2 HO2 + 0.8 C2O3	8.00E-12	8.00E-12			a
114	GLYD = 0.74 FORM + 0.89 CO + 1.4 HO2 + 0.15 MEOH + 0.19 OH + 0.11 GLY + 0.11 XO2H + 0.11 RO2	Photolysis				a,b,f
115	GLYD + NO3 = HNO3 + C2O3	2.73E-15	1.40E-12	1860.0	0.00	a
116	GLY + OH = 1.7 CO + 0.3 XO2 + 0.3 RO2 + HO2	9.70E-12	3.10E-12	-340.0	0.00	a
117	GLY = 2 HO2 + 2 CO	Photolysis				a,q
118	GLY + NO3 = HNO3 + CO + HO2 + XO2 + RO2	2.73E-15	1.40E-12	1860.0	0.00	a
119	MGLY = C2O3 + HO2 + CO	Photolysis				a
120	MGLY + NO3 = HNO3 + C2O3 + XO2 + RO2	2.73E-15	1.40E-12	1860.0	0.00	a
121	MGLY + OH = C2O3 + CO	1.31E-11	1.90E-12	-575.0	0.00	a
122	H2 + OH = HO2	6.70E-15	7.70E-12	2100.0	0.00	a
123	CO + OH = HO2	2.28E-13	$k = k_1 + k_2[M]$			a
		k_1	1.44E-13	0.0	0.00	
		k_2	3.43E-33	0.0	0.00	
124	CH4 + OH = MEO2 + RO2	6.37E-15	1.85E-12	1690.0	0.00	a
125	ETHA + OH = 0.991 ALD2 + 0.991 XO2H + 0.009 XO2N + RO2	2.41E-13	6.90E-12	1000.0	0.00	a
126	MEOH + OH = FORM + HO2	8.95E-13	2.85E-12	345.0	0.00	a
127	ETOH + OH = 0.95 ALD2 + 0.9 HO2 + 0.1 XO2H + 0.1 RO2 + 0.078 FORM + 0.011 GLYD	3.21E-12	3.00E-12	-20.0	0.00	a
128	KET = 0.5 ALD2 + 0.5 C2O3 + 0.5 XO2H + 0.5 CXO3 + 0.5 MEO2 + RO2 - 2.5 PAR	Photolysis				a

Number	Reactants and Products	k_{298}	Rate Parameters			Notes
			A	E_a	B	
129	ACET = 0.38 CO + 1.38 MEO2 + 1.38 RO2 + 0.62 C2O3	Photolysis				a
130	ACET + OH = FORM + C2O3 + XO2 + RO2	1.76E-13	1.41E-12	620.6	0.00	a
131	PRPA + OH = 0.71 ACET + 0.26 ALDX + 0.26 PAR + 0.97 XO2H + 0.03 XO2N + RO2	1.07E-12	7.60E-12	585.0	0.00	a
132	PAR + OH = 0.11 ALDX + 0.76 ROR + 0.13 XO2N + 0.11 XO2H + 0.76 XO2 + RO2 - 0.11 PAR	8.10E-13	8.10E-13			c
133	ROR = 0.2 KET + 0.42 ACET + 0.74 ALD2 + 0.37 ALDX + 0.04 XO2N + 0.94 XO2H + 0.98 RO2 + 0.02 ROR - 2.7 PAR	2.15E+04	5.70E+12	5780.0	0.00	a,c
134	ROR + O2 = KET + HO2	3.78E+04	1.50E-14	200.0	0.00	a,c
135	ROR + NO2 = NTR	3.29E-11	8.60E-12	-400.0	0.00	a,c
136	ETHY + OH = 0.7 GLY + 0.7 OH + 0.3 FACD + 0.3 CO + 0.3 HO2	7.52E-13	Falloff, F=0.37 ,N=1.30			a
		k_0	5.00E-30	0.0	-1.50	
		k_∞	1.00E-12	0.0	0.00	
137	ETH + O = FORM + HO2 + CO + 0.7 XO2H + 0.7 RO2 + 0.3 OH	7.29E-13	1.04E-11	792.0	0.00	c,o
138	ETH + OH = XO2H + RO2 + 1.56 FORM + 0.22 GLYD	7.84E-12	Falloff, F=0.48 ,N=1.15			a,g
		k_0	8.60E-29	0.0	-3.10	
		k_∞	9.00E-12	0.0	-0.85	
139	ETH + O3 = FORM + 0.51 CO + 0.16 HO2 + 0.16 OH + 0.37 FACD	1.58E-18	9.10E-15	2580.0	0.00	a,g
140	ETH + NO3 = 0.5 NO2 + 0.5 NTR + 0.5 XO2H + 0.5 XO2 + RO2 + 1.125 FORM	2.10E-16	3.30E-12	2880.0	0.00	a,g
141	OLE + O = 0.2 ALD2 + 0.3 ALDX + 0.1 HO2 + 0.2 XO2H + 0.2 CO + 0.2 FORM + 0.01 XO2N + 0.21 RO2 + 0.2 PAR + 0.1 OH	3.91E-12	1.00E-11	280.0	0.00	c,o
142	OLE + OH = 0.781 FORM + 0.488 ALD2 + 0.488 ALDX + 0.976 XO2H + 0.195 XO2 + 0.024 XO2N + 1.17 RO2 - 0.73 PAR	2.86E-11	Falloff, F=0.50 ,N=1.13			a,g
		k_0	8.00E-27	0.0	-3.50	
		k_∞	3.00E-11	0.0	-1.00	
143	OLE + O3 = 0.295 ALD2 + 0.555 FORM + 0.27 ALDX + 0.15 XO2H + 0.15 RO2 + 0.334 OH + 0.08 HO2 + 0.378 CO + 0.075 GLY + 0.075 MGLY + 0.09 FACD + 0.13 AACD + 0.04 H2O2 - 0.79 PAR	1.00E-17	5.50E-15	1880.0	0.00	a,g
144	OLE + NO3 = 0.5 NO2 + 0.5 NTR + 0.48 XO2 + 0.48 XO2H + 0.04 XO2N + RO2 + 0.5 FORM + 0.25 ALD2 + 0.375 ALDX - PAR	9.54E-15	4.60E-13	1155.0	0.00	a,g
145	IOLE + O = 1.24 ALD2 + 0.66 ALDX + 0.1 XO2H + 0.1 RO2 + 0.1 CO + 0.1 PAR	2.30E-11	2.30E-11			c,o
146	IOLE + OH = 1.3 ALD2 + 0.7 ALDX + XO2H + RO2	5.99E-11	1.05E-11	-519.0	0.00	a,g
147	IOLE + O3 = 0.732 ALD2 + 0.442 ALDX + 0.128 FORM + 0.245 CO + 0.5 OH + 0.3 XO2H + 0.3 RO2 + 0.24 GLY + 0.06 MGLY + 0.29 PAR + 0.08 AACD + 0.08 H2O2	1.57E-16	4.70E-15	1013.0	0.00	a,g
148	IOLE + NO3 = 0.5 NO2 + 0.5 NTR + 0.48 XO2 + 0.48 XO2H + 0.04 XO2N + RO2 + 0.5 ALD2 + 0.625 ALDX + PAR	3.70E-13	3.70E-13			a,g
149	ISOP + OH = ISO2 + RO2	9.99E-11	2.70E-11	-390.0	0.00	a
150	ISO2 + NO = 0.117 INTR + 0.883 NO2 + 0.803 HO2 + 0.66 FORM + 0.66 ISPD + 0.08 XO2H + 0.08 RO2 + 0.05 IOLE + 0.042 GLYD + 0.115 PAR + 0.038 GLY + 0.042 MGLY + 0.093 OLE + 0.117 ALDX	8.13E-12	2.39E-12	-365.0	0.00	r,s
151	ISO2 + HO2 = 0.88 ISPX + 0.12 OH + 0.12 HO2 + 0.12 FORM + 0.12 ISPD	7.78E-12	7.43E-13	-700.0	0.00	r,s
152	ISO2 + C2O3 = 0.709 HO2 + 0.583 FORM + 0.583	1.30E-11	$k = k_{ref} * K$			r,s

Number	Reactants and Products	k ₂₉₈	Rate Parameters			Notes
			A	E _a	B	
153	ISPD + 0.071 XO2H + 0.044 IOLE + 0.037 GLYD + 0.102 PAR + 0.034 GLY + 0.037 MGLY + 0.082 OLE + 0.103 ALDX + 0.8 MEO2 + 0.2 AACD + 0.871 RO2	k(ref) K	ref = 58 1.00E+00	0.0	0.00	
	ISO2 + RO2 = 0.803 HO2 + 0.66 FORM + 0.66	3.48E-13	k = kref*K			r,s
	ISPD + 0.08 XO2H + 0.05 IOLE + 0.042 GLYD + 0.115 PAR + 0.038 GLY + 0.042 MGLY + 0.093 OLE + 0.117 ALDX + 1.08 RO2	k(ref) K	ref = 70 1.00E+00	0.0	0.00	
154	ISO2 = 0.8 HO2 + 0.04 OH + 0.04 FORM + 0.8 ISPD	1.00E+00	1.00E+00			j,t
155	ISOP + O3 = 0.6 FORM + 0.65 ISPD + 0.15 ALDX + 0.2 CXO3 + 0.35 PAR + 0.266 OH + 0.2 XO2 + 0.2 RO2 + 0.066 HO2 + 0.066 CO	1.27E-17	1.03E-14	1995.0	0.00	c
156	ISOP + NO3 = 0.35 NO2 + 0.65 INTR + 0.64 XO2H + 0.33 XO2 + 0.03 XO2N + RO2 + 0.35 FORM + 0.35 ISPD	6.74E-13	3.03E-12	448.0	0.00	u
157	ISPD + OH = 0.095 XO2N + 0.379 XO2 + 0.318 XO2H + 0.792 RO2 + 0.843 PAR + 0.379 C2O3 + 0.209 CXO3 + 0.379 GLYD + 0.24 MGLY + 0.24 FORM + 0.067 OLE + 0.079 CO + 0.028 ALDX	3.38E-11	6.31E-12	-500.0	0.00	r,s
158	ISPD + O3 = 0.02 ALD2 + 0.15 FORM + 0.225 CO + 0.85 MGLY + 0.36 PAR + 0.114 C2O3 + 0.064 XO2H + 0.064 RO2 + 0.268 OH + 0.09 HO2	7.10E-18	4.17E-15	1900.0	0.00	c
159	ISPD + NO3 = 0.643 CO + 0.282 FORM + 0.357 ALDX + 1.282 PAR + 0.85 HO2 + 0.075 CXO3 + 0.075 XO2H + 0.075 RO2 + 0.85 NTR + 0.15 HNO3	1.00E-15	1.00E-15			c
160	ISPD = 0.333 CO + 0.067 ALD2 + 0.9 FORM + 0.832 PAR + 0.333 HO2 + 0.7 XO2H + 0.7 RO2 + 0.967 C2O3	Photolysis				c,f
161	ISPD + OH = 0.904 EPOX + 0.933 OH + 0.067 ISO2 + 0.067 RO2 + 0.029 IOLE + 0.029 ALDX	7.77E-11	2.23E-11	-372.0	0.00	r,s
162	EPOX + OH = EPX2 + RO2	1.51E-11	5.78E-11	400.0	0.00	r,s
163	EPX2 + HO2 = 0.275 GLYD + 0.275 GLY + 0.275 MGLY + 1.125 OH + 0.825 HO2 + 0.375 FORM + 0.074 FACD + 0.251 CO + 2.175 PAR	7.78E-12	7.43E-13	-700.0	0.00	r,s
164	EPX2 + NO = 0.275 GLYD + 0.275 GLY + 0.275 MGLY + 0.125 OH + 0.825 HO2 + 0.375 FORM + NO2 + 0.251 CO + 2.175 PAR	8.13E-12	2.39E-12	-365.0	0.00	r,s
165	EPX2 + C2O3 = 0.22 GLYD + 0.22 GLY + 0.22 MGLY + 0.1 OH + 0.66 HO2 + 0.3 FORM + 0.2 CO + 1.74 PAR + 0.8 MEO2 + 0.2 AACD + 0.8 RO2	1.30E-11 k(ref) K	k = kref*K ref = 58 1.00E+00	0.0	0.00	a,r,s
	EPX2 + RO2 = 0.275 GLYD + 0.275 GLY + 0.275 MGLY + 0.125 OH + 0.825 HO2 + 0.375 FORM + 0.251 CO + 2.175 PAR + RO2	3.48E-13 k(ref) K	k = kref*K ref = 70 1.00E+00	0.0	0.00	a,r,s
167	INTR + OH = 0.63 XO2 + 0.37 XO2H + RO2 + 0.444 NO2 + 0.185 NO3 + 0.104 INTR + 0.592 FORM + 0.331 GLYD + 0.185 FACD + 2.7 PAR + 0.098 OLE + 0.078 ALDX + 0.266 NTR	3.10E-11	3.10E-11			r,s
168	TERP + O = 0.15 ALDX + 5.12 PAR	3.60E-11	3.60E-11			c
169	TERP + OH = 0.75 XO2H + 0.5 XO2 + 0.25 XO2N + 1.5 RO2 + 0.28 FORM + 1.66 PAR + 0.47 ALDX	6.77E-11	1.50E-11	-449.0	0.00	c
170	TERP + O3 = 0.57 OH + 0.07 XO2H + 0.69 XO2 + 0.18 XO2N + 0.94 RO2 + 0.24 FORM + 0.001 CO + 7 PAR + 0.21 ALDX + 0.39 CXO3	7.63E-17	1.20E-15	821.0	0.00	c
171	TERP + NO3 = 0.47 NO2 + 0.28 XO2H + 0.75 XO2 + 0.25 XO2N + 1.28 RO2 + 0.47 ALDX + 0.53 NTR	6.66E-12	3.70E-12	-175.0	0.00	c
172	BENZ + OH = 0.53 CRES + 0.352 BZO2 + 0.352 RO2 + 0.118 OPEN + 0.118 OH + 0.53 HO2	1.22E-12	2.30E-12	190.0	0.00	a,d,e

Number	Reactants and Products	k_{298}	Rate Parameters			Notes
			A	E_a	B	
173	BZO2 + NO = 0.918 NO2 + 0.082 NTR + 0.918 GLY + 0.918 OPEN + 0.918 HO2	9.04E-12	2.70E-12	-360.0	0.00	d,h
174	BZO2 + C2O3 = GLY + OPEN + HO2 + MEO2 + RO2	1.30E-11 k(ref) K	k = kref*K ref = 58 1.00E+00	0.0	0.00	a,d,h
175	BZO2 + HO2 =	1.49E-11	1.90E-13	-1300.0	0.00	d
176	BZO2 + RO2 = GLY + OPEN + HO2 + RO2	3.48E-13 k(ref) K	k = kref*K ref = 70 1.00E+00	0.0	0.00	a,d,h
177	TOL + OH = 0.18 CRES + 0.65 TO2 + 0.72 RO2 + 0.1 OPEN + 0.1 OH + 0.07 XO2H + 0.18 HO2	5.63E-12	1.80E-12	-340.0	0.00	a,d,e
178	TO2 + NO = 0.86 NO2 + 0.14 NTR + 0.417 GLY + 0.443 MGLY + 0.66 OPEN + 0.2 XOPN + 0.86 HO2	9.04E-12	2.70E-12	-360.0	0.00	d,h
179	TO2 + C2O3 = 0.48 GLY + 0.52 MGLY + 0.77 OPEN + 0.23 XOPN + HO2 + MEO2 + RO2	1.30E-11 k(ref) K	k = kref*K ref = 58 1.00E+00	0.0	0.00	a,d,h
180	TO2 + HO2 =	1.49E-11	1.90E-13	-1300.0	0.00	d
181	TO2 + RO2 = 0.48 GLY + 0.52 MGLY + 0.77 OPEN + 0.23 XOPN + HO2 + RO2	3.48E-13 k(ref) K	k = kref*K ref = 70 1.00E+00	0.0	0.00	a,d,h
182	XYL + OH = 0.155 CRES + 0.544 XLO2 + 0.602 RO2 + 0.244 XOPN + 0.244 OH + 0.058 XO2H + 0.155 HO2	1.85E-11	1.85E-11			d,e,p
183	XLO2 + NO = 0.86 NO2 + 0.14 NTR + 0.221 GLY + 0.675 MGLY + 0.3 OPEN + 0.56 XOPN + 0.86 HO2	9.04E-12	2.70E-12	-360.0	0.00	d,h
184	XLO2 + HO2 =	1.49E-11	1.90E-13	-1300.0	0.00	d
185	XLO2 + C2O3 = 0.26 GLY + 0.77 MGLY + 0.35 OPEN + 0.65 XOPN + HO2 + MEO2 + RO2	1.30E-11 k(ref) K	k = kref*K ref = 58 1.00E+00	0.0	0.00	a,d,h
186	XLO2 + RO2 = 0.26 GLY + 0.77 MGLY + 0.35 OPEN + 0.65 XOPN + HO2 + RO2	3.48E-13 k(ref) K	k = kref*K ref = 70 1.00E+00	0.0	0.00	a,d,h
187	CRES + OH = 0.06 CRO + 0.12 XO2H + HO2 + 0.13 OPEN + 0.732 CAT1 + 0.06 CO + 0.06 XO2N + 0.18 RO2 + 0.06 FORM	4.12E-11	1.70E-12	-950.0	0.00	d
188	CRES + NO3 = 0.3 CRO + HNO3 + 0.24 XO2 + 0.36 XO2H + 0.48 ALDX + 0.24 FORM + 0.24 MGLY + 0.12 OPEN + 0.1 XO2N + 0.7 RO2 + 0.24 CO	1.40E-11	1.40E-11			d
189	CRO + NO2 = CRON	2.10E-12	2.10E-12			d
190	CRO + HO2 = CRES	5.50E-12	5.50E-12			d
191	CRON + OH = CRNO	1.53E-12	1.53E-12			d
192	CRON + NO3 = CRNO + HNO3	3.80E-12	3.80E-12			d
193	CRNO + NO2 = 2 NTR	2.10E-12	2.10E-12			d
194	CRNO + O3 = CRN2	2.86E-13	2.86E-13			d
195	CRN2 + NO = CRNO + NO2	8.50E-12	2.54E-12	-360.0	0.00	d
196	CRN2 + HO2 = CRPX	1.88E-11	2.40E-13	-1300.0	0.00	d
197	CRPX = CRNO + OH	Photolysis				a,d
198	CRPX + OH = CRN2	3.59E-12	1.90E-12	-190.0	0.00	d
199	XOPN = CAO2 + 0.7 HO2 + 0.7 CO + 0.3 C2O3 + RO2	Photolysis				d,p
200	XOPN + OH = CAO2 + MGLY + XO2H + RO2	9.00E-11	9.00E-11			d,p
201	XOPN + O3 = 1.2 MGLY + 0.5 OH + 0.6 C2O3 + 0.1 ALD2 + 0.5 CO + 0.3 XO2H + 0.3 RO2	2.02E-17	1.08E-16	500.0	0.00	d,p

Number	Reactants and Products	k ₂₉₈	Rate Parameters			Notes
			A	E _a	B	
202	XOPN + NO ₃ = 0.5 NO ₂ + 0.5 NTR + 0.45 XO ₂ H + 0.45 XO ₂ + 0.1 XO ₂ N + RO ₂ + 0.25 OPEN + 0.25 MGLY	3.00E-12	3.00E-12			d,p
203	OPEN = OPO ₃ + HO ₂ + CO	Photolysis				d,p
204	OPEN + OH = 0.6 OPO ₃ + 0.4 CAO ₂ + 0.4 RO ₂	4.40E-11	4.40E-11			d,p
205	OPEN + O ₃ = 1.4 GLY + 0.24 MGLY + 0.5 OH + 0.12 C ₂ O ₃ + 0.08 FORM + 0.02 ALD ₂ + 1.98 CO + 0.56 HO ₂	1.01E-17	5.40E-17	500.0	0.00	d,p
206	OPEN + NO ₃ = OPO ₃ + HNO ₃	3.80E-12	3.80E-12			d,p
207	CAT ₁ + OH = CAO ₂ + RO ₂	7.00E-11	7.00E-11			d
208	CAT ₁ + NO ₃ = CRO + HNO ₃	1.70E-10	1.70E-10			d
209	CAO ₂ + NO = 0.86 NO ₂ + 0.14 NTR + 1.2 HO ₂ + 0.344 FORM + 0.344 CO	8.50E-12	2.54E-12	-360.0	0.00	d
210	CAO ₂ + HO ₂ =	1.88E-11	2.40E-13	-1300.0	0.00	d
211	CAO ₂ + C ₂ O ₃ = HO ₂ + 0.4 GLY + MEO ₂ + RO ₂	1.30E-11	k = kref*K			d
		k(ref)	ref = 58			
		K	1.00E+00	0.0	0.00	
212	CAO ₂ + RO ₂ = HO ₂ + 0.4 GLY + RO ₂	3.48E-13	k = kref*K			d
		k(ref)	ref = 70			
		K	1.00E+00	0.0	0.00	
213	OPO ₃ + NO = NO ₂ + XO ₂ H + RO ₂ + ALDX	1.00E-11	1.00E-11			d
214	OPO ₃ + NO ₂ = OPAN	1.16E-11	k = kref*K			d
		k(ref)	ref = 62			
		K	1.00E+00	0.0	0.00	
215	OPAN = OPO ₃ + NO ₂	9.92E-05	Falloff, F=0.30 ,N=1.00			d
		k ₀	4.60E-04	11280.0	0.00	
		k _∞	2.24E+16	13940.0	0.00	
216	OPO ₃ + HO ₂ = 0.41 PACD + 0.15 AACD + 0.15 O ₃ + 0.44 ALDX + 0.44 XO ₂ H + 0.44 RO ₂ + 0.44 OH	1.39E-11	k = kref*K			d
		k(ref)	ref = 57			
		K	1.00E+00	0.0	0.00	
217	OPO ₃ + C ₂ O ₃ = MEO ₂ + XO ₂ + ALDX + 2 RO ₂	1.55E-11	k = kref*K			d
		k(ref)	ref = 59			
		K	1.00E+00	0.0	0.00	
218	OPO ₃ + RO ₂ = 0.8 XO ₂ H + 0.8 RO ₂ + 0.8 ALDX + 0.2 AACD	1.30E-11	k = kref*K			d
		k(ref)	ref = 58			
		K	1.00E+00	0.0	0.00	

Table notes:

k₂₉₈ is the rate constant at 298 K and 1 atmosphere using units molecules cm⁻³ and s⁻¹

See Table 2-7 for species names

See Table 2-8 for information on photolysis reactions

a	IUPAC: Atkinson et al., (2010)	h	Arey et al. (2009)	o	Cvetanovic (1987)
b	JPL: Sander et al., (2006)	i	Hu et al. (2007)	p	Calvert et al. (2002)
c	CB05: Yarwood et al (2005)	j	Archibald et al. (2010)	q	Feierabend et al. (2009)
d	CB05-TU: Whitten et al., 2010)	k	Hjorth et al. (1992)	r	Paulot et al. (2009a)
e	Bloss et al. (2005)	l	Kaiser and Wu (1977)	s	Paulot et al. (2009b)
f	SAPRC-99: Carter (2000)	m	Jeffries et al. (2002)	t	Peeters et al. (2009)
g	Calvert et al. (2000)	n	Herron (1988)	u	Perring et al. (2009)

Table 2-8. Model species names for CB6.

Species	Description
AACD	Acetic acid
ACET	Acetone
ALD2	Acetaldehyde
ALDX	Propionaldehyde and higher aldehydes
BENZ	Benzene
BZO2	Peroxy radical from OH addition to benzene
C2O3	Acetylperoxy radical
CAO2	Peroxy radical from aromatic degradation products
CAT1	Methyl-catechols
CH4	Methane
CO	Carbon monoxide
CRES	Cresols
CRN2	Peroxy radical from nitro-cresol
CRNO	Alkoxy radical from nitro-cresols
CRO	Alkoxy radical from cresol
CRON	Nitro-cresols
CRPX	Nitro-cresol hydroperoxides
CXO3	C3 and higher acylperoxy radicals
EPOX	Epoxide formed from ISPX reaction with OH
EPX2	Peroxy radical from EPOX reaction with OH
ETH	Ethene
ETHA	Ethane
ETHY	Ethyne
ETOH	Ethanol
FACD	Formic acid
FORM	Formaldehyde
GLY	Glyoxal
GLYD	Glycolaldehyde
H2O2	Hydrogen peroxide
HCO3	Adduct from HO2 plus formaldehyde
HNO3	Nitric acid
HO2	Hydroperoxy radical
HONO	Nitrous acid
INTR	Organic nitrates from ISO2 reaction with NO
IOLE	Internal olefin carbon bond (R-C=C-R)
ISO2	Peroxy radical from OH addition to isoprene
ISOP	Isoprene
ISPD	Isoprene product (lumped methacrolein, methyl vinyl ketone, etc.)
ISPX	Hydroperoxides from ISO2 reaction with HO2
KET	Ketone carbon bond (C=O)
M	Air
MEO2	Methylperoxy radical
MEOH	Methanol
MEPX	Methylhydroperoxide
MGLY	Methylglyoxal
N2O5	Dinitrogen pentoxide
NO	Nitric oxide
NO2	Nitrogen dioxide
NO3	Nitrate radical
NTR	Organic nitrates
O	Oxygen atom in the $O^3(P)$ electronic state
O1D	Oxygen atom in the $O^1(D)$ electronic state

Species	Description
O2	Oxygen
O3	Ozone
OH	Hydroxyl radical
OLE	Terminal olefin carbon bond (R-C=C)
OPAN	Peroxyacyl nitrate (PAN compound) from OPO3
OPEN	Aromatic ring opening product (unsaturated dicarbonyl)
OPO3	Peroxyacyl radical from OPEN
PACD	Peroxyacetic and higher peroxydicarboxylic acids
PAN	Peroxyacetyl Nitrate
PANX	C3 and higher peroxyacyl nitrate
PAR	Paraffin carbon bond (C-C)
PNA	Peroxynitric acid
PRPA	Propane
RO2	Operator to approximate total peroxy radical concentration
ROOH	Higher organic peroxide
ROR	Secondary alkoxy radical
SO2	Sulfur dioxide
SULF	Sulfuric acid (gaseous)
TERP	Monoterpenes
TO2	Peroxy radical from OH addition to TOL
TOL	Toluene and other monoalkyl aromatics
XLO2	Peroxy radical from OH addition to XYL
XO2	NO to NO2 conversion from alkylperoxy (RO2) radical
XO2H	NO to NO2 conversion (XO2) accompanied by HO2 production
XO2N	NO to organic nitrate conversion from alkylperoxy (RO2) radical
XOPN	Aromatic ring opening product (unsaturated dicarbonyl)
XYL	Xylene and other polyalkyl aromatics

2.3 REACTION RATE CHANGES FROM CB05

The rates for inorganic reactions included in CB6 (reactions 1-51) are compared to CB05 in Table 2-9 at 298 K and 1 atmosphere. Ten of the 51 reactions compared are photolysis reaction and they are discussed separately below. One reaction ($O + O_3$) was not included in CB05. Of the remaining 40 reactions, there was no change in rate constant for 14 reactions and the change was smaller than 5% for another 8 reactions. Notable changes include:

- 5% increase in the rate constant for the $OH + NO_2$ reaction which will tend to shorten the atmospheric lifetime of NO_x and thereby reduce ozone production in NO_x -limited conditions.
- 60% decrease in the rate constant for the $N_2O_5 + H_2O$ reaction (and elimination of the $N_2O_5 + H_2O + H_2O$ reaction) which will prolong the atmospheric lifetime of NO_x at night. As discussed above, heterogeneous reaction between N_2O_5 and H_2O may offset this change and should be accounted for when CB6 is used in atmospheric models.
- 11% increase in the rate constant for $O(^1D)$ reaction with M (i.e., $O(^1D)$ quenching) and 3% decrease in the rate constant for $O(^1D)$ reaction with H_2O to produce OH. Both of these changes will reduce production of OH from O_3 photolysis.

- 32% increase in the rate constant for reaction of OH with NO to form HONO which is partially offset by 23% increase in the rate constant of the reaction of OH with HONO.

Table 2-9. Comparison of CB6 to CB05 rate constants for inorganic reactions.

CB6 Number	CB6 Reactants and Products	k ₂₉₈		Change
		CB05	CB6	
1	NO ₂ = NO + O	Photolysis		
2	O + O ₂ + M = O ₃ + M	6.10E-34	5.78E-34	-5.2%
3	O ₃ + NO = NO ₂	1.95E-14	1.73E-14	-11.7%
4	O + NO + M = NO ₂ + M	6.75E-32	1.01E-31	49.6%
5	O + NO ₂ = NO	1.02E-11	1.03E-11	0.9%
6	O + NO ₂ = NO ₃	3.28E-12	2.11E-12	-35.8%
7	O + O ₃ =	N/A	7.96E-15	N/A
8	O ₃ = O	Photolysis		
9	O ₃ = O ₁ D	Photolysis		
10	O ₁ D + M = O + M	2.96E-11	3.28E-11	10.9%
11	O ₁ D + H ₂ O = 2 OH	2.20E-10	2.14E-10	-2.7%
12	O ₃ + OH = HO ₂	7.25E-14	7.25E-14	0.0%
13	O ₃ + HO ₂ = OH	1.93E-15	2.01E-15	4.3%
14	OH + O = HO ₂	3.29E-11	3.47E-11	5.5%
15	HO ₂ + O = OH	5.87E-11	5.73E-11	-2.5%
16	OH + OH = O	1.88E-12	1.48E-12	-21.3%
17	OH + OH = H ₂ O ₂	6.29E-12	5.25E-12	-16.6%
18	OH + HO ₂ =	1.11E-10	1.11E-10	0.0%
19	HO ₂ + HO ₂ = H ₂ O ₂	2.92E-12	2.90E-12	-0.7%
20	HO ₂ + HO ₂ + H ₂ O = H ₂ O ₂	6.58E-30	6.53E-30	-0.7%
21	H ₂ O ₂ = 2 OH	Photolysis		
22	H ₂ O ₂ + OH = HO ₂	1.70E-12	1.70E-12	0.0%
23	H ₂ O ₂ + O = OH + HO ₂	1.70E-15	1.70E-15	0.0%
24	NO + NO + O ₂ = 2 NO ₂	1.95E-38	1.95E-38	0.0%
25	HO ₂ + NO = OH + NO ₂	8.10E-12	8.54E-12	5.4%
26	NO ₂ + O ₃ = NO ₃	3.23E-17	3.52E-17	9.1%
27	NO ₃ = NO ₂ + O	Photolysis		
28	NO ₃ = NO	Photolysis		
29	NO ₃ + NO = 2 NO ₂	2.65E-11	2.60E-11	-1.9%
30	NO ₃ + NO ₂ = NO + NO ₂	6.56E-16	6.56E-16	0.0%
31	NO ₃ + O = NO ₂	1.00E-11	1.70E-11	70.0%
32	NO ₃ + OH = HO ₂ + NO ₂	2.20E-11	2.00E-11	-9.1%
33	NO ₃ + HO ₂ = OH + NO ₂	3.50E-12	4.00E-12	14.3%
34	NO ₃ + O ₃ = NO ₂	1.00E-17	1.00E-17	0.0%
35	NO ₃ + NO ₃ = 2 NO ₂	2.28E-16	2.28E-16	0.0%
36	NO ₃ + NO ₂ = N ₂ O ₅	1.18E-12	1.24E-12	5.3%
37	N ₂ O ₅ = NO ₃ + NO ₂	5.28E-02	4.46E-02	-15.6%
38	N ₂ O ₅ = NO ₂ + NO ₃	Photolysis		
39	N ₂ O ₅ + H ₂ O = 2 HNO ₃	2.50E-22	1.00E-22	-60.0%
40	NO + OH = HONO	7.41E-12	9.77E-12	32.0%
41	NO + NO ₂ + H ₂ O = 2 HONO	5.00E-40	5.00E-40	0.0%
42	HONO + HONO = NO + NO ₂	1.00E-20	1.00E-20	0.0%
43	HONO = NO + OH	Photolysis		
44	HONO + OH = NO ₂	4.86E-12	5.98E-12	23.0%
45	NO ₂ + OH = HNO ₃	1.05E-11	1.06E-11	1.4%
46	HNO ₃ + OH = NO ₃	1.54E-13	1.54E-13	0.0%
47	HNO ₃ = OH + NO ₂	Photolysis		
48	HO ₂ + NO ₂ = PNA	1.38E-12	1.38E-12	0.0%
49	PNA = HO ₂ + NO ₂	8.31E-02	8.31E-02	0.0%
50	PNA = 0.59 HO ₂ + 0.59 NO ₂ + 0.41 OH + 0.41 NO ₃	Photolysis		
51	PNA + OH = NO ₂	3.24E-12	3.24E-12	0.0%

Note: k₂₉₈ is the rate constant at 298 K and 1 atmosphere using units molecules cm⁻³ and s⁻¹

The rates for photolysis reactions included in both CB6 and CB05 are compared in Table 2-10 for an altitude of 1 km at 60 degree zenith angle with ozone column of 300 Dobson Units. The photolysis rates change for 5 of 19 reactions compared. Notable changes include:

- 7% increase in the rate of NO₂ photolysis which will tend to increase O₃ formation.
- 23% increase in the rate of formaldehyde photolysis to radical products which will tend to increase O₃ formation under VOC-limited conditions.

Table 2-10. Comparison of CB6 and CB05 photolysis reaction rates.

CB6 Number	Photolysis of	CB05		CB6		Percent Change
		source	J (min ⁻¹)	source	J (min ⁻¹)	
1	NO ₂	SAPRC99	4.20E-01	IUPAC10	4.49E-01	7%
8	O ₃ to O(3P)	IUPAC05	2.15E-02	IUPAC10	2.15E-02	0%
9	O ₃ to O(1D)	IUPAC05	6.75E-04	IUPAC10	6.75E-04	0%
27	NO ₃ to NO ₂	SAPRC99	9.76E+00	NASA06	1.01E+01	3%
28	NO ₃ to NO	SAPRC99	1.04E+00	NASA06	1.25E+00	20%
43	HONO	IUPAC05	7.53E-02	IUPAC10	7.53E-02	0%
21	H ₂ O ₂	SAPRC99	2.80E-04	IUPAC10	2.80E-04	0%
50	PNA	IUPAC05	1.90E-04	IUPAC10	1.90E-04	0%
47	HNO ₃	IUPAC05	1.91E-05	IUPAC10	1.91E-05	0%
38	N ₂ O ₅	IUPAC05	1.86E-03	IUPAC10	1.85E-03	0%
92	NTR	IUPAC05	7.91E-05	IUPAC10	7.91E-05	0%
88	MEPX	SAPRC99	2.01E-04	IUPAC10	1.98E-04	-1%
97	FORM to H + HCO	SAPRC99	1.05E-03	IUPAC10	1.33E-03	27%
98	FORM to H ₂ + CO	SAPRC99	1.79E-03	IUPAC10	1.76E-03	-2%
108	ALD2	SAPRC99	1.33E-04	IUPAC10	1.32E-04	0%
56	PAN	IUPAC05	2.58E-05	IUPAC10	2.58E-05	0%
112	ALDX	SAPRC99	5.21E-04	SAPRC99	5.21E-04	0%
119	MGLY	IUPAC05	1.09E-02	IUPAC10	1.09E-02	0%
160	ISPD	SAPRC97	7.13E-05	SAPRC97	7.13E-05	0%

Note: Comparison for altitude of 1 km at 60 degree zenith angle with ozone column of 300 Dobson Units

3. MECHANISM EVALUATION

3.1 INTRODUCTION

This section describes the evaluation of CB6 using environmental chamber data. The mechanism design and implementation was described in Chapter 2. Following this introduction, Section 3.2 describes evaluation methods and chamber experimental data used to evaluate the CB6 mechanism. Then Section 3.3 presents charts and tables that document the performance evaluation of CB6. Section 3.4 presents the overall summary of mechanism performance and suggests future studies.

3.2. DATA AND METHODS USED IN EVALUATING CB6

3.2.1. Evaluating CB6 using a hierarchical approach

Many components describing atmospheric photooxidation reactions (e.g., CO chemistry, acetaldehyde chemistry, toluene chemistry) consist of an entire chemical mechanism (e.g., CB6). As a result, interactions between these different components make it difficult to (1) test each component of a chemical mechanism and (2) systematically evaluate the entire chemical mechanism while minimizing compensating errors by these interactions. One approach to dealing with this challenge is applying a concept of hierarchical mechanism evaluation (Whitten, 1983), which was used in this project for evaluating CB6 as shown in Figure 3-1.

Figure 3-1 presents a hierarchical approach for evaluating CB6 using chamber simulations with chamber data. For example, first, the CO chemistry in CB6 was evaluated using CO-NO_x chamber experiments. Second, the FORM chemistry was evaluated using HCHO-NO_x chamber experiments while building on the evaluated CO chemistry. The ALD2 and PAN chemistries were evaluated together using CH₃CHO-NO_x experiments. The chemistries of ALDX (a model species similar to ALD2 but for higher aldehydes (e.g., CH₃CH₂CHO (propanal))) and PANX (a species similar to PAN but formed from higher aldehydes) were indirectly evaluated by using chamber experiments of terminal and internal alkenes (OLE and IOLE) due to lack of suitable chamber data.

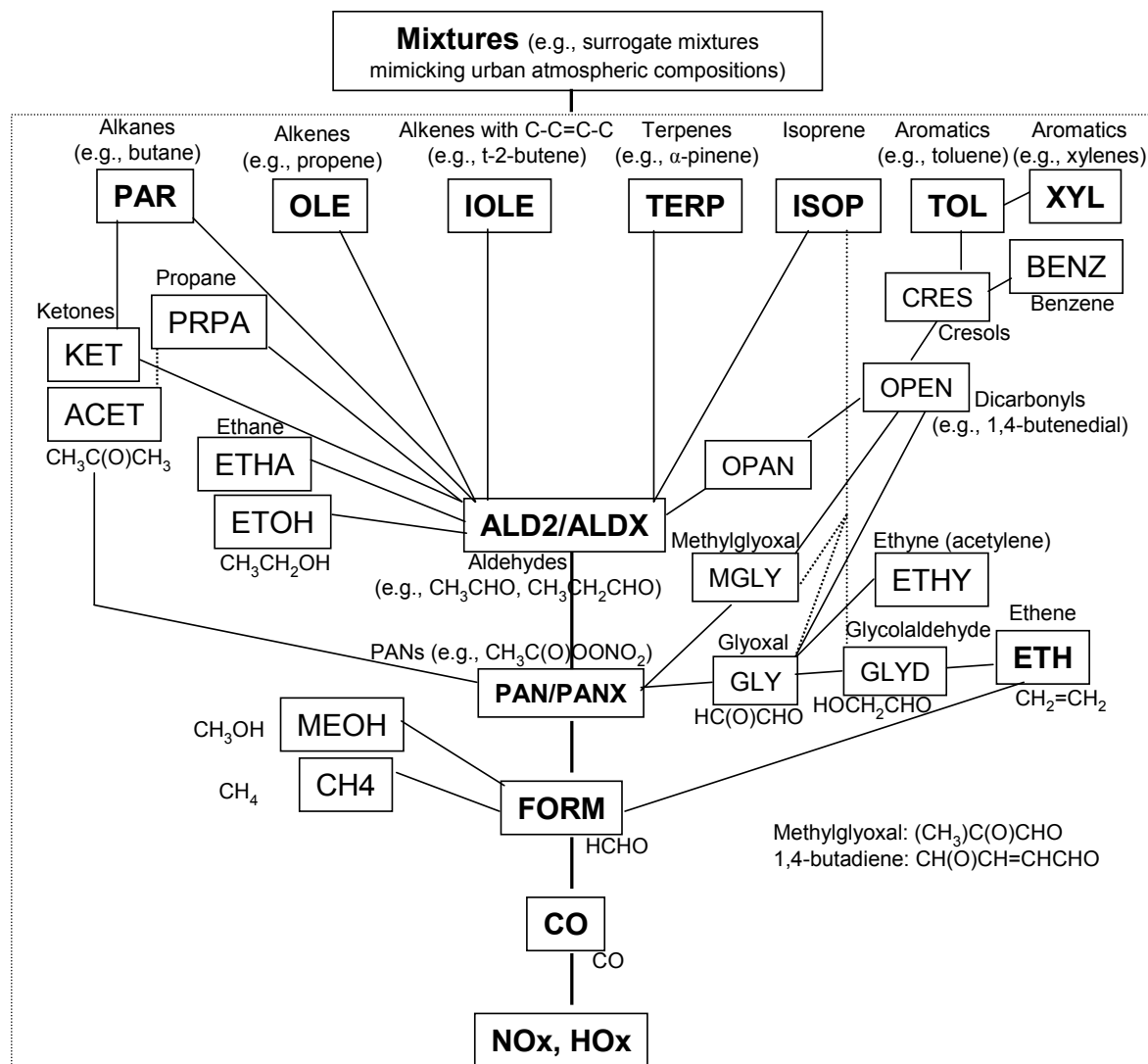


Figure 3-1. Schematic diagram showing a hierarchical approach to evaluating CB6.

Note: Key CB species and backbone chemistry parts are displayed in bold.

Several components (e.g., CH_4 , MEOH, ETOH, ETHA and ETHY chemistries) do not influence higher-level chemistries (e.g., PAR, OLE, IOLE, ISOP, TERP, TOL and XYL chemistries) as shown in Figure 3-1. Therefore, the limited number of available chamber experiments for testing chemistries of these low-reactivity species (e.g., MEOH) does not lead to a significant flaw to the CB6 evaluation work described subsequently in this chapter.

The ETH (ethene) chemistry and ACET (acetone) chemistry were evaluated after evaluating the chemistries of CO, FORM and PAN, and the PRPA (propane) chemistry was evaluated separately from other alkanes (PAR). The chemistries of KET (ketones) and BENZ (benzene) were evaluated after evaluating ALD2 chemistry. After evaluating the ALD2 and KET chemistries, the chemistries of PAR, OLE, IOLE, ISOP, TERP and TOL were evaluated in parallel. The XYL chemistry was evaluated after testing the TOL chemistry in CB6 (Figure 3-1).

3.2.2. Environmental chambers and chamber data used for evaluating CB6

The CB6 mechanism was evaluated by simulating chamber experiments in which mixtures of VOC and NO_x were irradiated to form ozone. A database of experiments compiled by the University of California at Riverside (UCR) was the basis for the evaluation. Most UCR chamber data except data for very recent experiments and TVA chamber data for around 60 experiments are available in a chamber database that is managed by William Carter at UCR and publicly available <http://www.cert.ucr.edu/~carter/SAPRC/SAPRCfiles.htm>. Chamber experimental data for ~2000 experiments are available in the UCR chamber database (Carter, 2010). Chamber data used for this study are the chamber experimental data in this UCR database (version of April 23, 2010).

Various types of chamber experimental data produced by the University of California at Riverside (UCR) and the Tennessee Valley Authority (TVA)) were used in this study. An overview of various environmental chambers at UCR and TVA is given in Table 3-1. Environmental chamber data were measured at 8 different environmental chambers: EC, ETC, OTC (outdoor), DTC, XTC, CTC and EPA (7 chambers at UCR); TVA (chamber at TVA) (Table 3-1).

In the past, a database of chamber experiments compiled by the University of North Carolina (UNC) has been used to evaluate Carbon Bond mechanisms. However, the UNC research team informed us that the chamber light model which calculates spectral actinic flux for the chamber experiments contains an error. As a result, this evaluation used only chamber data compiled by UCR which includes experiments performed at UCR and the Tennessee Valley Authority (TVA).

Table 3-1. An overview of environmental chambers at UCR and TVA used for mechanism evaluation (Heo, 2009).

Chamber	Chamber ID	Reactor type	Reactor volume (m ³)	Light source	Relative humidity	Operation period
<i>Indoor chamber</i>						
Evacuatable Chamber at UCR	EC	single	~5.8	xenon arc	~50%	1975-84
Ernie's Teflon Chamber at UCR	ETC	single	~3.0	blacklight	dry (< 5%)	1989-93
Dividable Teflon Chamber at UCR	DTC	dual	~5.0 (X 2)	blacklight	dry (< 5%)	1993-99
Xenon arc Teflon Chamber at UCR	XTC	single	~5.0	xenon arc	dry (< 5%)	1993
CE-CERT Teflon Chamber at UCR	CTC (11-82 ^a)	single	~5.0	xenon arc	dry (< 5%)	1994-95
CE-CERT Teflon Chamber at UCR (rebuilt)	CTC (>82 ^a)	dual	~2.5 (X 2)	xenon arc	dry (< 5%)	1995-99
UCR EPA chamber	EPA	dual	~90 (X 2)	argon arc/blacklight	dry (< 1%)	2003-present
TVA indoor chamber	TVA	single	~28	3 types including blacklight	~15%	1993-95
<i>Outdoor chamber</i>						
Outdoor Teflon Chamber at UCR	OTC	dual	~20 (X 2)	sunlight	dry (< 5%)	1992-93

^aRun number of the chamber experiment.

References: Dodge (2000), Carter (2000 and 2010), Carter et al. (2005).

In a chamber experiment, a test compound (e.g., ethene and toluene) is injected as a “single” test compound with NO_x (and optionally with CO), or injected with other related compounds as a mixture (e.g., as an alkene “mixture”). Experiments of “single test compound – NO_x” or “special mixture – NO_x” are useful in testing each component of CB6 (e.g., ALD2 chemistry or ETH chemistry). On the other hand, for testing CB6 overall, “surrogate mixture - NO_x” experiments are useful. In a surrogate-mixture experiment, a mixture simulating a target atmospheric composition (e.g., an urban mixture) is injected. In this study, all three types of chamber experiments were used: “single test compound – NO_x”, “special mixture – NO_x” and “surrogate mixture – NO_x”.

The need of selecting chamber experiments useful for evaluating CB6 originates from chamber effects (e.g., wall reactions such as NO_x offgassing and chamber-dependent radical formation) which are difficult to describe accurately (Dodge, 2000; Heo, 2009). In order to minimize the impact of wall effects on CB6 evaluation, chamber experiments that are expected to have been significantly influenced by chamber effects were not be used whenever possible.

In selecting UCR and TVA experiments in the UCR chamber database, criteria on the ratio of O₃ formed to NO oxidized ($\text{Max}(\text{O}_3)/[\text{NO}]_0$), the initial NO_x level ($[\text{NO}_x]_0$) and the chamber light source (whether a blacklight light source was used or not) were used as follows:

Criteria generally applied for selecting single test compound - NO_x experiments:

1. $\text{Max}(\text{O}_3)/[\text{NO}]_0 \geq 1$.
2. $[\text{NO}_x]_0 \geq 10$ ppb.
3. Exclude blacklight-used experiments when an aromatic compound (e.g., toluene) was injected.
4. $[\text{NO}_x]_0 < 300$ ppb for testing most compounds.

Criteria generally applied for selecting VOC mixture - NO_x experiments:

1. $\text{Max}(\text{O}_3)/[\text{NO}]_0 \geq 1$.
2. $[\text{NO}_x]_0 \geq 10$ ppb.
3. Exclude blacklight-used experiments when an aromatic compound was injected.
4. $[\text{NO}_x]_0 < 200$ ppb.

After applying these criteria to UCR and TVA experiments, with some exceptions stated as notes in Table 3-2, 194 experiments of “single test compound – NO_x” or “special mixture – NO_x” and 145 experiments of “surrogate mixture – NO_x” were selected from around 2000 experiments in the UCR chamber database (Tables 3-2 and 3-3). Table 3-2 summarizes 194 chamber experiments used for testing single components of CB6 (e.g., CO) and Table 3-3 summarizes 145 surrogate-mixture experiments used for testing interactions of various components of CB6 and testing the performance of CB6 in simulating O₃ against VOCs – NO_x mixtures. Tables A-1 and A-2 in the Appendix provide additional details for the experiments summarized in Tables 3-2 and 3-3, respectively.

In evaluating CB6, non-blacklight chamber experiments were preferred in order to utilize light conditions most relevant to the atmosphere and thereby minimize the consequences of uncertain photolysis data. However, in some cases only backlight simulations were available and therefore had to be utilized to evaluate MEOH (methanol), ETOH (ethanol), ETHA (ethane) and PRPA (propane). The uncertainty introduced by blacklights is suggested by the results for ethene

(ETH). The ETH chemistry of CB6 showed significantly different performance in simulating Max(O₃) against non-blacklight experiments and blacklight experiments: average model errors (see Section 3.3.5) for 11 non-blacklight experiments and 22 blacklight experiments were -13% ($\pm 17\%$) and +28% ($\pm 17\%$).

Table 3-2. Summary of 194 UCR and TVA chamber experiments of single test compounds and special mixtures used for evaluating CB6.^a

Group	CB6 Species	Test compound	Experiment type ^b	Number of experiments per compound [total (blacklight)] ^c	Number of experiments per CB6 species [total (mixture)] ^d	Note
1	CO	CO	single	33	33	
2	FORM	HCHO	single	9	9	
3	CH4	CH ₄	-	0	0	
4	MEOH	CH ₃ OH	IR	2 (2)	2 (2)	1
5	ETH	ethene	single	11	11	2
6	ALD2	CH ₃ CHO	single	8	8	
7	ETOH	C ₂ H ₅ OH	IR	3 (3)	3 (3)	3
8	ACET	CH ₃ C(O)CH ₃	single	4	4	
9	KET	CH ₃ C(O)C ₂ H ₅ (MEK ^e)	single	2	2	
10	ETHA	ethane	IR	5 (5)	5 (5)	4
11	ALDX	higher aldehydes	-	0	0	5
12	PAR	n-butane	single	3	5	6
		n-butane/2,3-dimethyl butane	mixture	2		
13	OLE	propene	single	47	48	
		1-butene	single	1		
14	IOLE	trans-2-butene	single	3	3	
15	TOL	toluene	single	18	20	
		ethylbenzene	single	2		
16	XYL	o-xylene (o-XYL)	single	4	27	
		m-XYL	single	15		
		p-XYL	single	2		
		123-trimethyl benzene (123-TMB)	single	2		
		124-TMB	single	2		
		135-TMB	single	2		
17	ISOP	isoprene	single	6	6	
18	TERP	α -pinene	single	1	2	7
		β -pinene	single	1		
19	PRPA	propane	IR	2 (2)	2 (2)	8
20	BENZ	benzene	single	2	2	
21	ETHY	ethyne (acetylene)	single	2	2	
Total				194 (12)	194 (12)	

^aA test compound was injected as a "single" test compound with NO_x (and optionally with CO), injected excessively relative to other co-injected compounds (e.g., in "Incremental Reactivity (IR)" style experiments), or injected with other related compounds (e.g., as an alkane "mixture"). "Opt" is "optional" PRPA, BENZ, ACTY and BOLE are optional (Opt) model species for propane, benzene, acetylene and branched olefins (e.g., isobutene), respectively.

^b"Single", "IR" and "mixture" mean "injected as a single test compound", "injected in an IR style", and "injected as a mixture with other closely related compounds (e.g., as an alkane mixture)".

^cTotal number of blacklight experiments in the parentheses.

^dTotal number of selected experiments for each CB species (e.g., ALD2, PAR and XYL) and total number of "test compound – other VOCs – NO_x" experiments in the parentheses.

^eMEK is methyl ethyl ketone.

^fOnly two blacklight/mixture type experiments were available for testing the MEOH chemistry of CB6.

^g22 blacklight experiments were also used to compare ETH performance for non-blacklight and blacklight experiments.

^hOnly three blacklight/mixture type experiments were available for testing the ETOH chemistry of CB6.

ⁱOnly five blacklight/mixture type experiments were available for testing the ETHA chemistry of CB6.

⁵No experiment was available for specifically testing the ALDX chemistry of CB6. 1-Butene – NOx experiments can be indirectly used.

⁶For testing the PAR chemistry of CB6, two mixture-type experiments where n-butane and 2,3-dimethyl butane were both injected were used as well as 3 experiments where n-butane was injected in presence of NOx (NO and NO2).

⁷Blacklight experiments were also used to provide supplementary information. 14 blacklight terpene – NOx experiments were used: α -pinene (4), β -pinene (1), 3-carene (3), d-limonene (3) and sabinene (3).

⁸Only two blacklight/mixture type experiments were used for testing the PRPA (propane) chemistry of CB6.

Table 3-3. 145 non-blacklight surrogate mixture experiments used for evaluating CB6.^a

Group	Description	Subgroup ^b	VOC/NOx ratio and initial [NOx] _o	Number of experiments
Group 1	Incomplete surrogate without aromatics (Surg-NA)	Surg-NA Vary	Variable VOC/NOx; [NOx] _o < 200 ppb	2
Group 2	Incomplete surrogate but with TOL or XYL	-	-	<i>Sub-total: 57</i>
		Surg-7 MIR2	Low VOC/NOx; [NOx] _o < 100 ppb	21
		Surg-7 LN2	[NOx] _o < 100 ppb	26
		ECsrg-7	[NOx] _o < 100 ppb	2
		TVA srg-1	[NOx] _o ~ 50 ppb	8
Group 3	Full surrogate			<i>Sub-total: 86</i>
		Surg-8 MIR2	Low VOC/NOx; [NOx] _o < 100 ppb	10
		Surg-8 LN1	100 ppb < [NOx] _o < 200 ppb	19
		Surg-8 LN2	[NOx] _o < 100 ppb	9
		Surg-8 Vary	Variable VOC/NOx; [NOx] _o < 200 ppb	43
		TVA srg-2	[NOx] _o < 100 ppb	5
Total				145

^aSurg-8, Surg-7, Surg-NA, TVAsrg-2 and ECsrg-7 experiments contains at least 7 different VOCs, at least one in each class (alkanes, alkenes, aromatics).

^bSurg-8: 8-component VOC mixture (n-butane, n-octane, ethene, propene, trans-2-butene, toluene, m-xylene, HCHO) with NOx. Surg-7: Surg-8 without HCHO.

Surg-NA: Surg-8 without aromatics (toluene, m-xylene) and HCHO.

TVAsrg-1: mixtures of n-butane, 2-methyl butane, ethene, propene, toluene and HCHO.

TVAsrg-2: complex mixtures of alkanes, alkenes and aromatics.

ECsrg-7: EC chamber experiments using 7-component surrogate (n-butane, 2,3-dimethyl butane, ethene, propene, t-2-butene, toluene, m-xylene).

MIR1, MIR2, LN1, LN2 and Vary are acronyms stating experimental conditions related to the VOC/NOx ratio and initial NOx level as follows: MIR1: Low VOC/NOx, MIR (maximum incremental reactivity)-like conditions. NOx 300-500 ppb. MIR2: Low VOC/NOx, MIR-like conditions, NOx < 100 ppb. LN1: Lower NOx conditions, NOx > 100 ppb. LN2: Lower NOx, NOx < 50 ppb. Vary: Non-standard ROG/NOx. Conditions varied.

3.2.3. Environmental chamber simulations for evaluating CB6

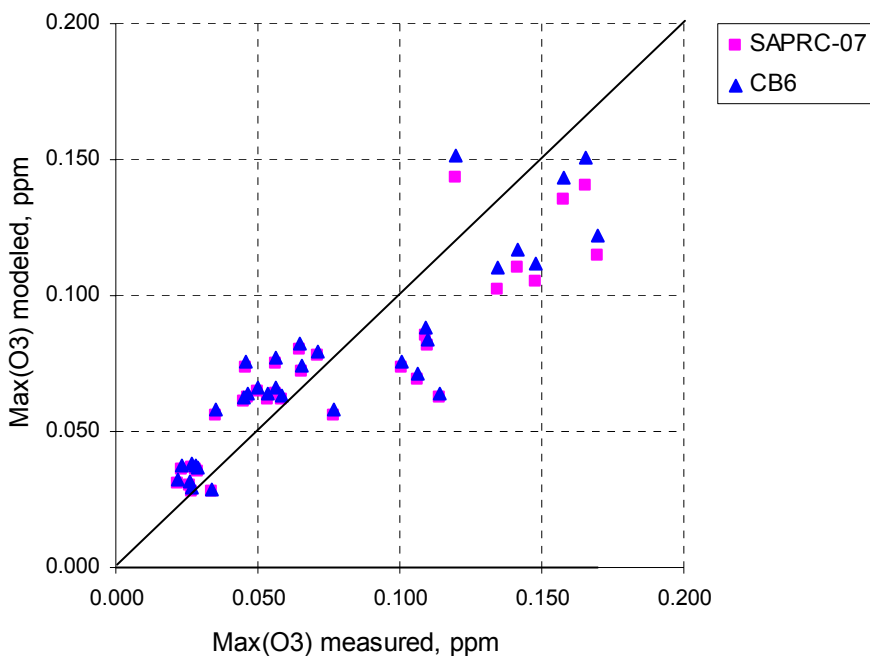
Chamber simulations were performed using the SAPRC software that has been used for evaluating the Statewide Air Pollution Research Center (SAPRC) mechanism and the Carbon Bond (CB) mechanism (Carter, 2000 and 2010; Yarwood et al., 2005; Whitten et al., 2010). The reactions of CB6 were implemented in the format compatible with the SAPRC software. Then, CB6 was evaluated (1) first against single compound – NOx experiments using the hierarchical approach (Figure 3-1) and (2) against surrogate mixture – NOx experiments to evaluate CB6 against experiments where major components of urban atmospheres (e.g., n-butane, n-octane, ethene, propene, trans-2-butene, toluene, m-xylene) were injected. 194 experiments were used for testing each component of CB6, and 145 experiments were used for testing the overall performance of CB6 against surrogate mixture experiments.

Performance metrics that were used for evaluating CB6 include the following: The maximum ozone concentration ($\text{Max}(\text{O}_3)$), Maximum $\text{D}(\text{O}_3\text{-NO})$, and NO_x crossover time (i.e., the time when the NO_2 concentration becomes equal to the NO concentration). Means and standard deviations of these metrics were used to characterize performance over multiple experiments, especially performance against surrogate mixture experiments.

The metric $\text{D}(\text{O}_3\text{-NO})$, defined as $([\text{O}_3] - [\text{NO}])_{t=t} - ([\text{O}_3] - [\text{NO}])_{t=0}$, quantifies the amount of O_3 formed and NO oxidized during an experiment) and is useful even when there is no significant O_3 production (Carter and Atkinson, 1987). $\text{Max}(\text{O}_3)$ and $\text{Max}(\text{D}(\text{O}_3\text{-NO}))$ are useful because a primary goal of condensed chemical mechanisms for urban/regional photochemical models is accurate prediction of maximum ozone concentrations; however, these metrics do not provide information on the rate of ozone formation. The NO_x crossover time contains information on the rate of NO oxidation into NO_2 , which accompanies O_3 formation. Therefore, the NO_x crossover time is a useful performance metric and was also used in this study as a metric for evaluating the performance of CB6.

Running chamber simulations with CB6 requires wall mechanisms that characterize chamber-dependent effects such as chamber-dependent radical sources and NO_x offgasing from chamber walls. For CB6, wall mechanisms that were used for evaluating SAPRC-07 by William Carter at UCR were used based on two facts: (1) the rate constant for reaction $\text{OH} + \text{NO}_2 = \text{HNO}_3$, the most important radical sink under most chamber conditions, is the same between CB6 and SAPRC-07; (2) chamber simulation results against 33 $\text{CO} - \text{NO}_x$ experiments (for details, see Table A-1) are similar between CB6 and SAPRC-07 (Figure 3-2 and Table 3-4). The $\text{CO} - \text{NO}_x$ chemical system is most sensitive to chamber-dependent radical sources. However, chemical systems (such as propene - NO_x and surrogate mixture - NO_x) that have a significant internal radical source (e.g., photolysis of FORM) are relatively insensitive to chamber-dependent radical sources.

(a)



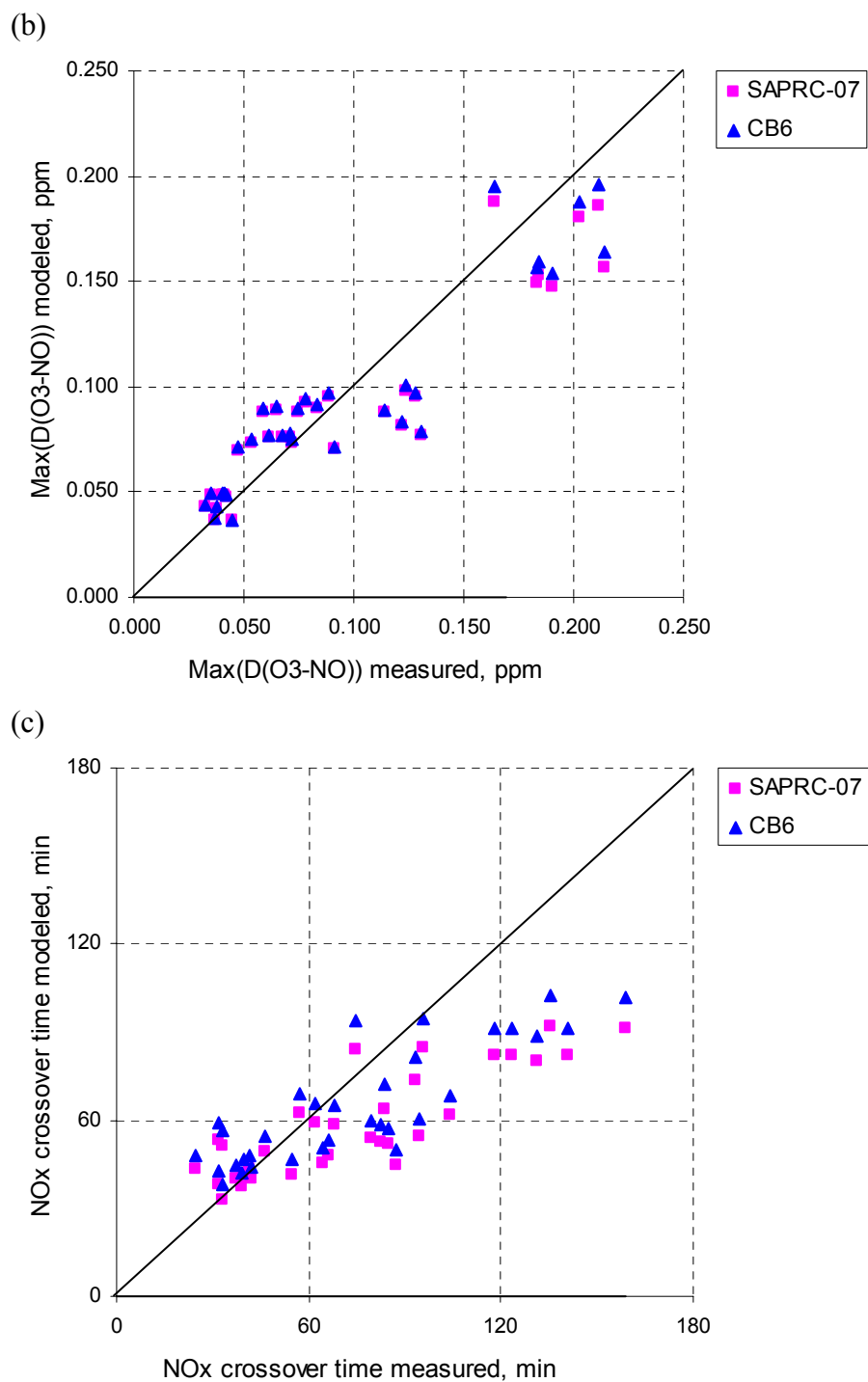


Figure 3-2. Mechanism performance comparison between CB6 and SAPRC-07 against 33 CO - NOx experiments: (a) Max(O₃), (b) Max(D(O₃-NO)), (c) NOx crossover time.

Note: D(O₃-NO) is $([O_3] - [NO])_{t=t} - ([O_3] - [NO])_{t=0}$; $[NO_2] = [NO]$ at the NOx crossover time.

Table 3-4. Summary of model errors for CB6 and SAPRC-07 against 33 CO - NOx experiments.

	Max(O ₃) [%]		Max(D(O ₃ -NO) [%])		NOx crossover time [min]	
	CB6	SAPRC-07	CB6	SAPRC-07	CB6	SAPRC-07
Average	11	7	6	4	-10	-16
Std. dev.	31	30	25	25	23	24

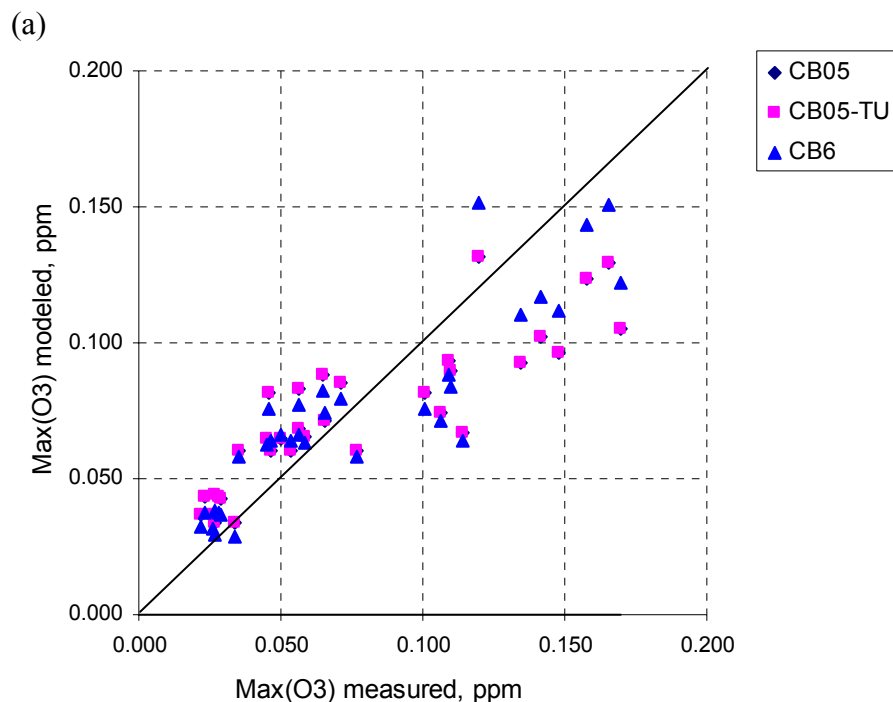
3.3. CHAMBER SIMULATION RESULTS FOR CB6

This section provides chamber simulation results for testing each component of the CB6 chemical mechanism against 194 chamber experiments listed in Table 3-2 (in Section 3.2) and Table A-1 (in the Appendix) and for testing the overall performance of CB6 against 145 surrogate mixture experiments listed in Tables 3-3 and A-2.

Three metrics, $\text{Max}(\text{O}_3)$, $\text{Max}(\text{D}(\text{O}_3\text{-NO}))$ and the NO_x crossover time were used as mechanism performance metrics. In this work, $\text{Max}(\text{O}_3)$ is defined as the highest maximum O_3 concentration by the end of the experiment but not later than 6 hours since the start of the experiment because chamber data after hour of 6 were not gathered and are not quality-assured in most cases. $\text{D}(\text{O}_3\text{-NO})$ represents the amount of O_3 formed and NO oxidized since irradiation and is defined as $([\text{O}_3] - [\text{NO}])_{t=t} - ([\text{O}_3] - [\text{NO}])_{t=0}$. The NO_x crossover time characterizes the rate of NO oxidation and O_3 formation and is defined as the time when the NO_2 concentration becomes equal to the NO concentration ($[\text{NO}_2]_t = [\text{NO}]_t$ at the NO_x crossover time).

In following subsections, $\text{Max}(\text{O}_3)$, $\text{Max}(\text{D}(\text{O}_3\text{-NO}))$ and the NO_x crossover times will be presented as mechanism performance metrics for testing each component of CB6 from CO to ETHY (ethyne, $\text{CH}\equiv\text{CH}$) listed in Table 3-2 and the entire CB6 chemical mechanism. Model errors of $\text{Max}(\text{O}_3)$ and $\text{Max}(\text{D}(\text{O}_3\text{-NO}))$ were calculated as $(\text{model} - \text{experimental})/\text{experimental}$ in units of parts per million (ppm); model errors of NO_x crossover times were calculated as $(\text{model} - \text{experimental})$ in units of minutes (min). For comparison of CB6 with CB05 and CB05-TU, simulation results for CB05 and CB05-TU are also presented in following subsections.

3.3.1. CO: 33 experiments with carbon monoxide.



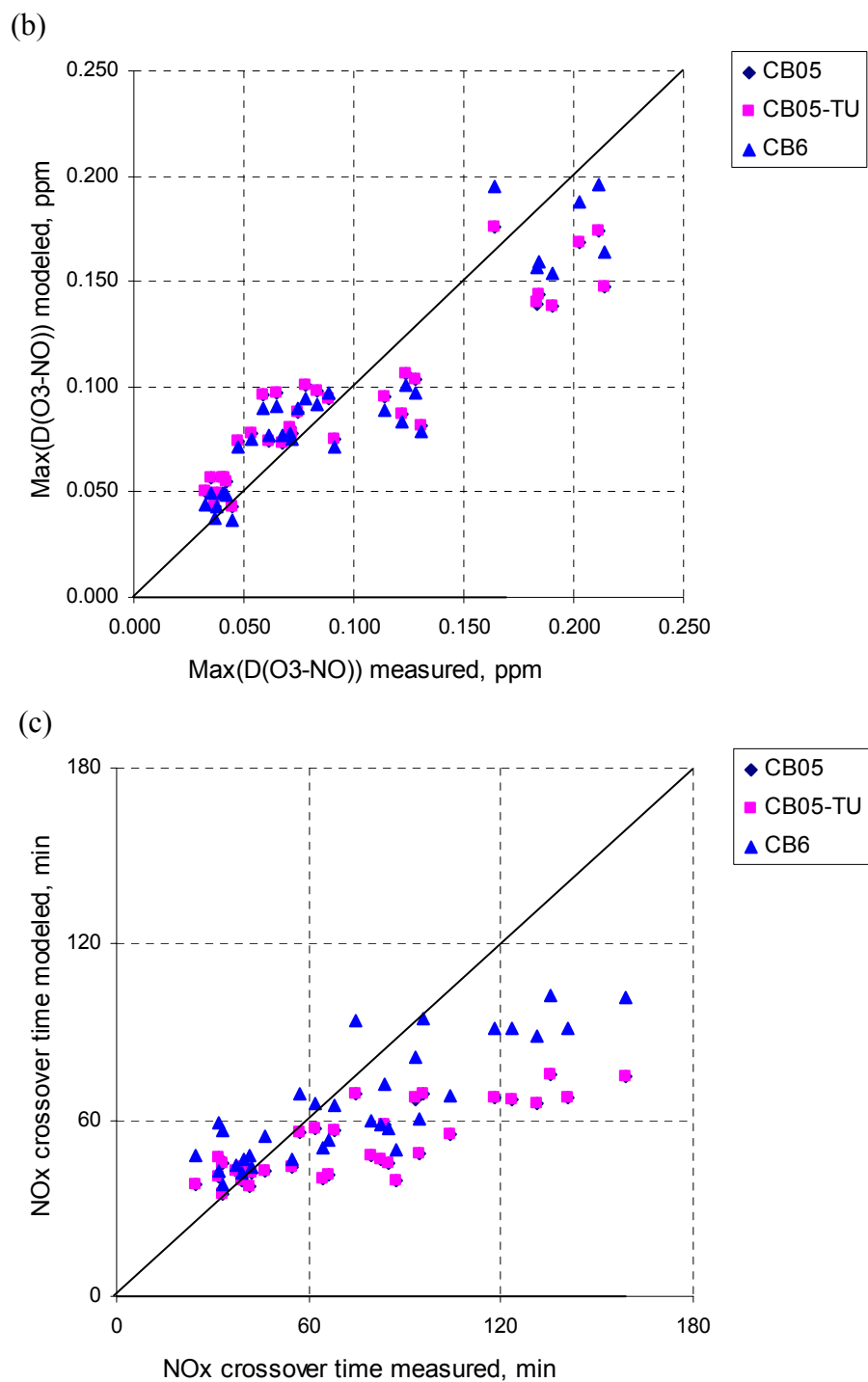


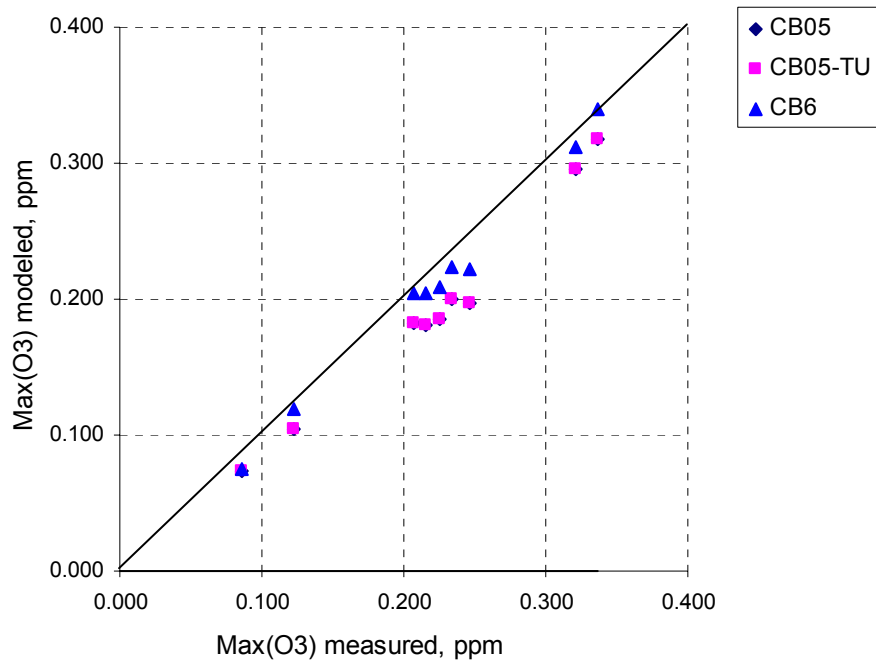
Figure 3-3. Mechanism performance against 33 CO - NO_x experiments: (a) Max(O₃), (b) Max(D(O₃-NO)), (c) NO_x crossover time.

Table 3-5. Summary of model errors for 33 CO - NO_x experiments.

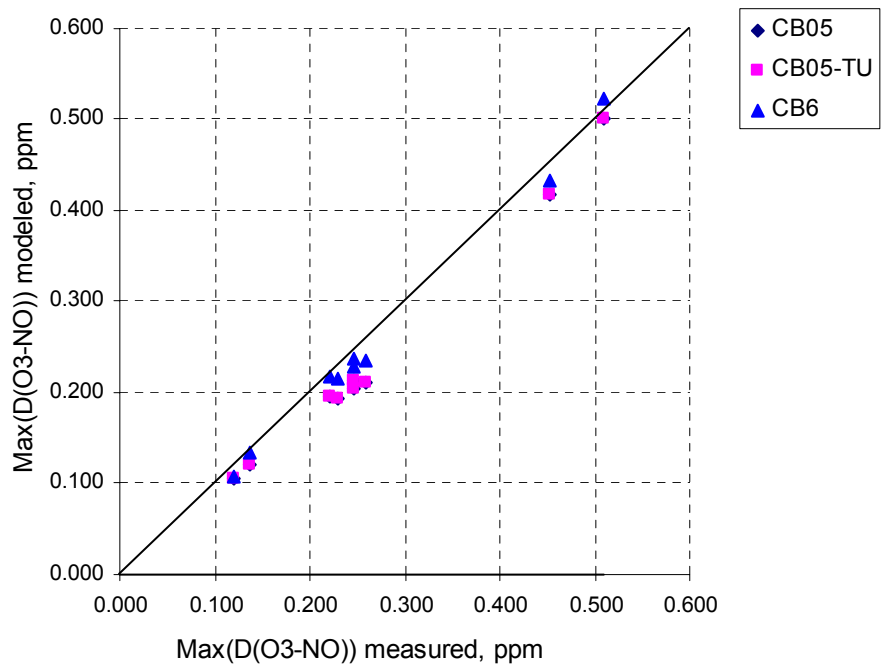
	Max(O ₃) [%]			Max(D(O ₃ -NO) [%]			NO _x crossover time [min]		
	CB05	CB05-TU	CB6	CB05	CB05-TU	CB6	CB05	CB05-TU	CB6
Average	15	15	11	10	10	6	-23	-23	-10
Std. dev.	38	38	31	30	30	25	27	27	23

3.3.2. FORM: 9 experiments with formaldehyde.

(a)



(b)



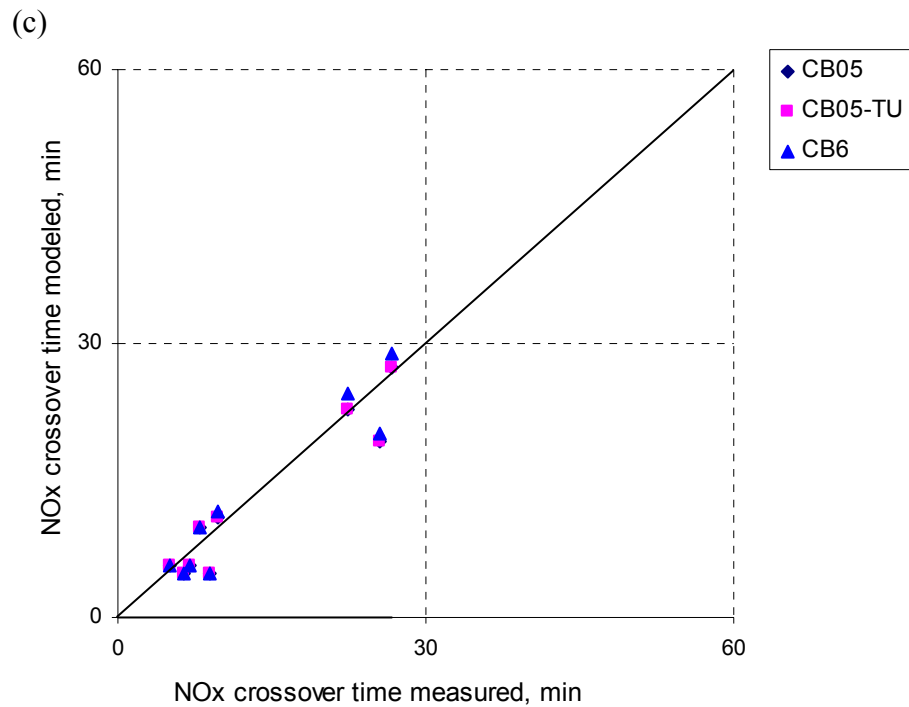


Figure 3-4. Mechanism performance against 9 FORM - NO_x experiments: (a) Max(O₃), (b) Max(D(O₃-NO)), (c) NO_x crossover time.

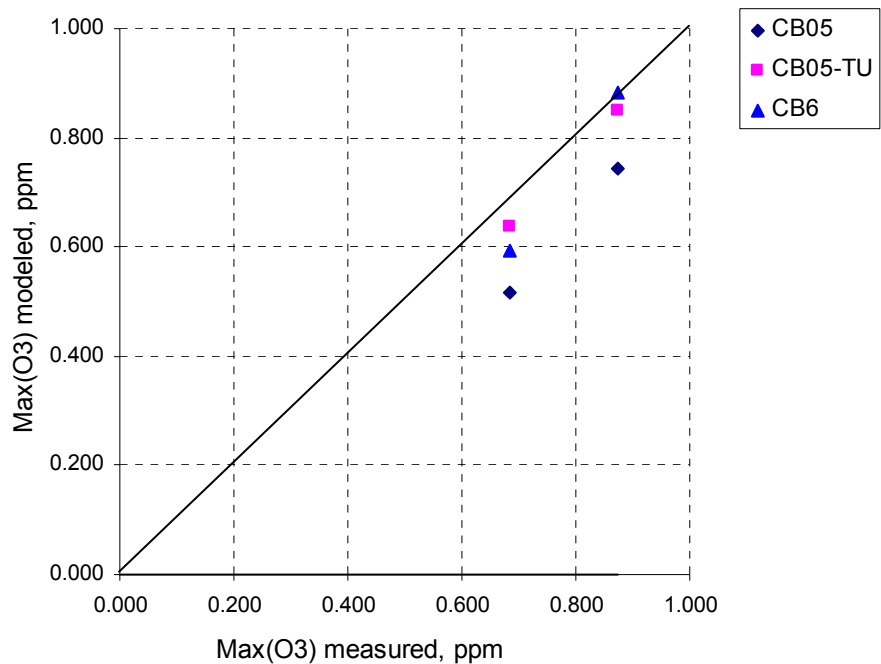
Table 3-6. Summary of model errors for 9 FORM - NO_x experiments.

	Max(O ₃) [%]			Max(D(O ₃ -NO) [%]			NO _x crossover time [min]		
	CB05	CB05-TU	CB6	CB05	CB05-TU	CB6	CB05	CB05-TU	CB6
Average	-14	-14	-5	-12	-12	-4	-1	-1	0
Std. dev.	4	5	5	5	5	4	3	3	3

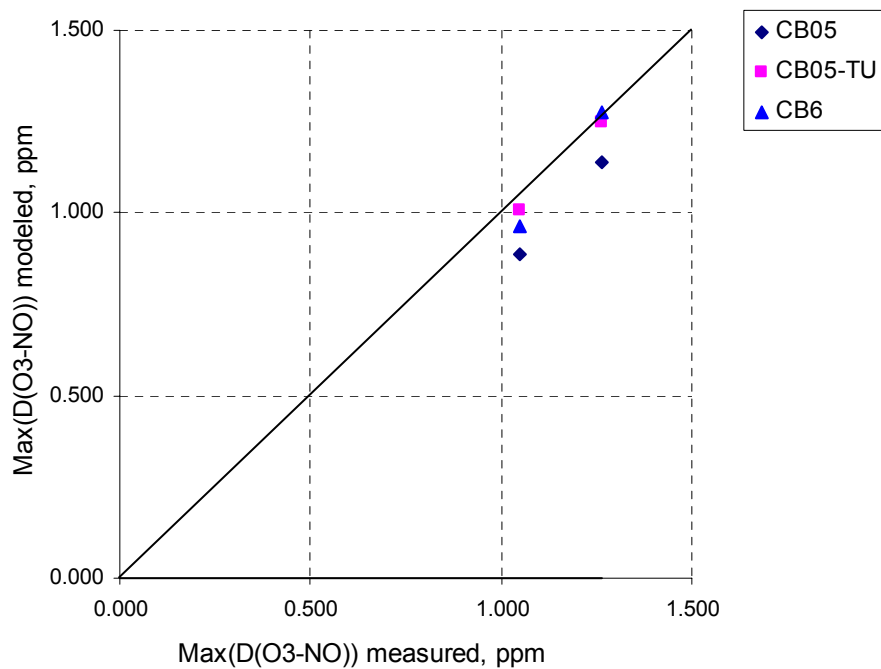
3.3.3. CH₄: no suitable experiments available.

3.3.4. MEOH: 2 experiments using blacklights and VOC mixtures containing methanol.

(a)



(b)



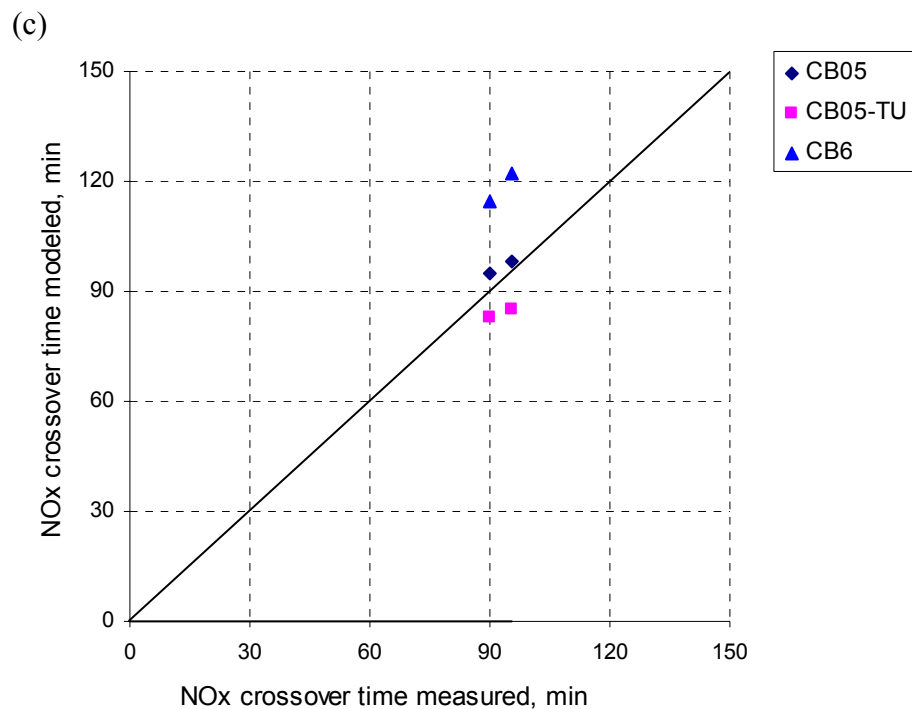


Figure 3-5. Mechanism performance against 2 blacklight MEOH - other VOCs - NOx experiments: (a) Max(O₃), (b) Max(D(O₃-NO)), (c) NOx crossover time.

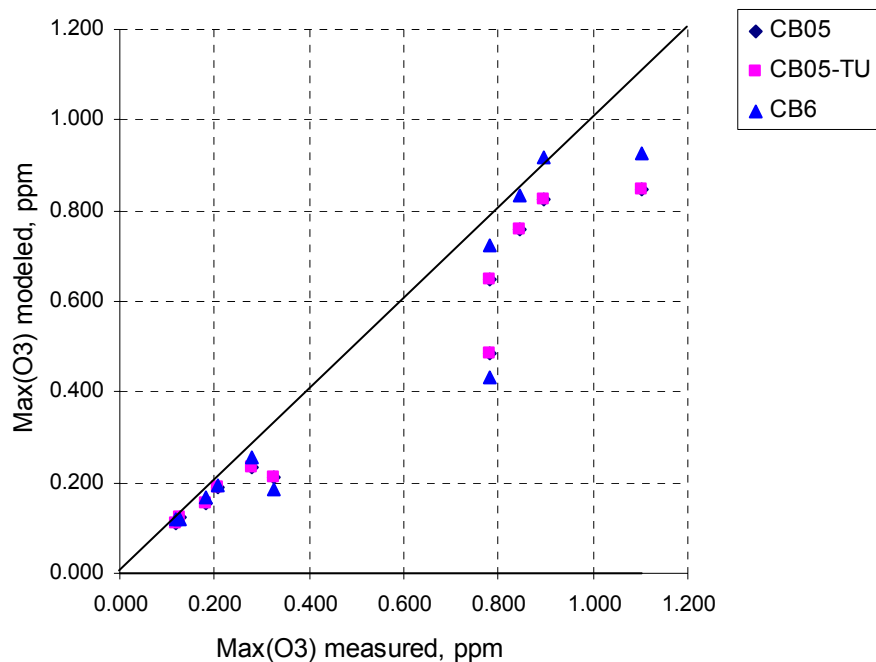
Table 3-7. Summary of model errors for 2 blacklight MEOH - other VOCs - NOx experiments.

	Max(O ₃) [%]			Max(D(O ₃ -NO) [%]			NOx crossover time [min]		
	CB05	CB05-TU	CB6	CB05	CB05-TU	CB6	CB05	CB05-TU	CB6
Average	-20	-5	-6	-13	-3	-4	4	-9	26
Std. dev.	7	3	10	4	2	6	2	3	1

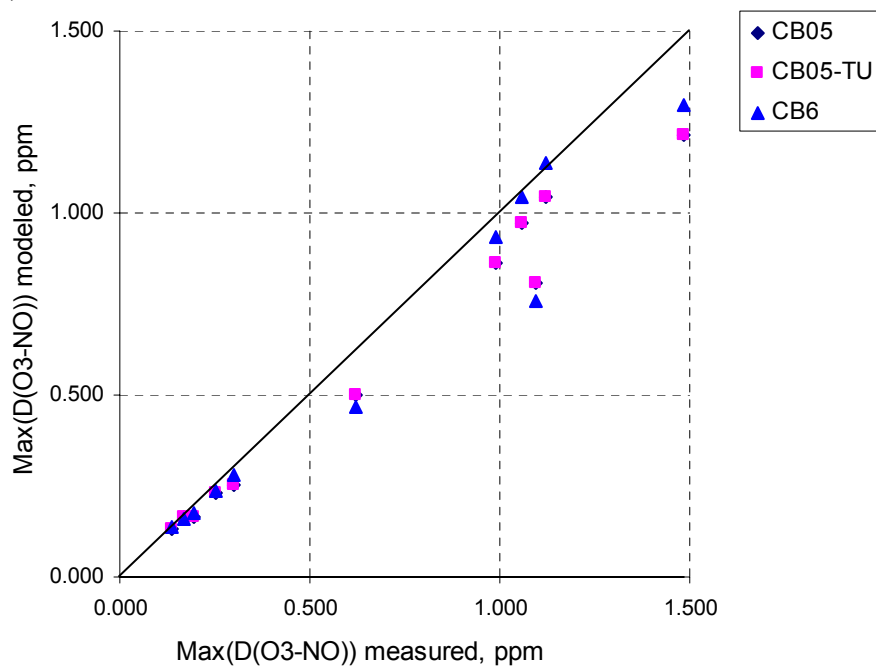
3.3.5. ETH: 11 non-blacklight experiments with ethene (22 blacklight experiments for comparison only).

3.3.5a. ETH: 11 non-blacklight experiments.

(a)



(b)



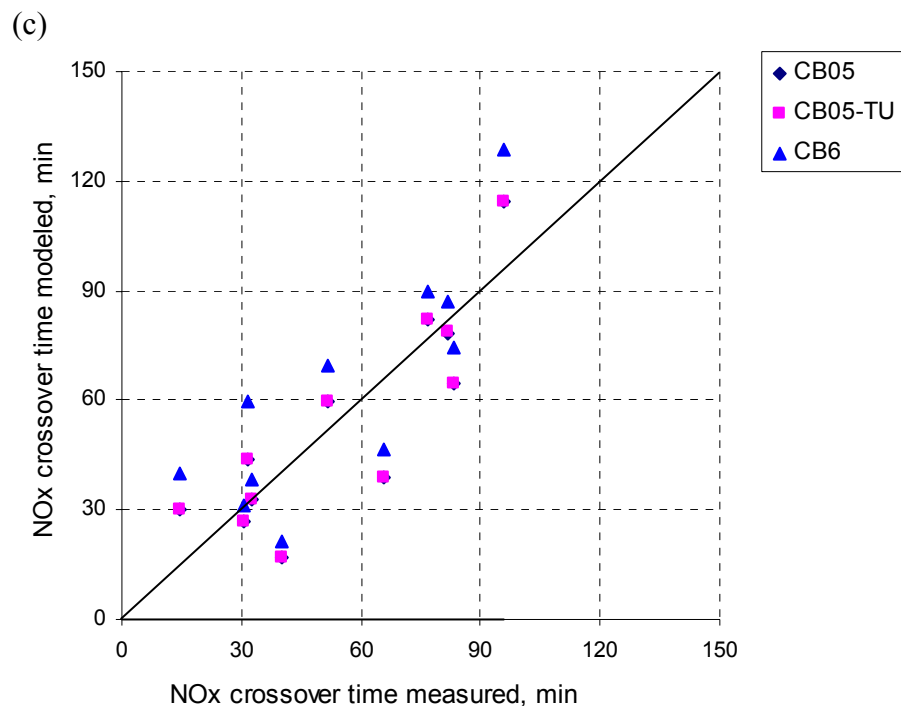


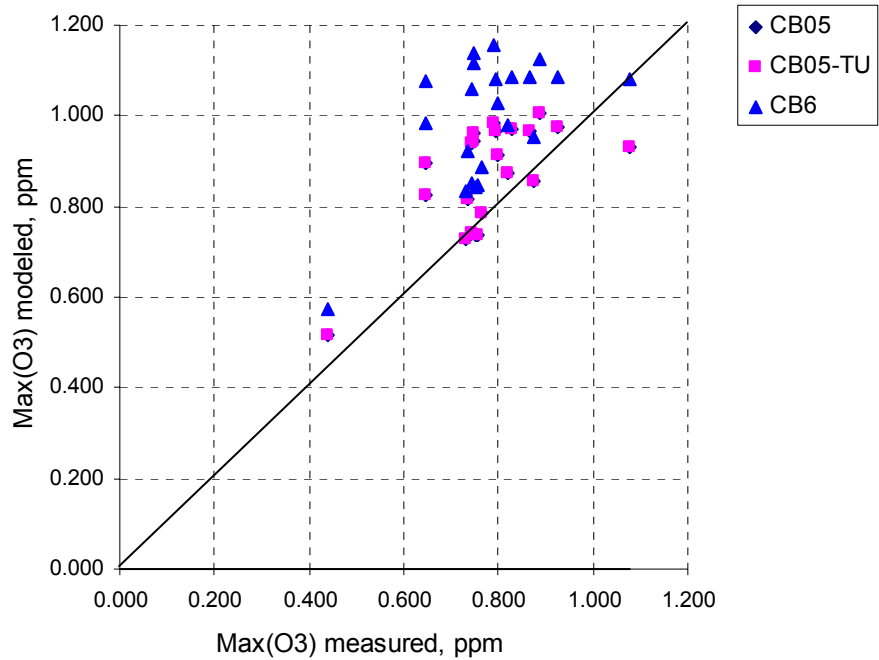
Figure 3-6a. Mechanism performance against 11 non-blacklight ETH - NOx experiments: (a) Max(O₃), (b) Max(D(O₃-NO)), (c) NOx crossover time.

Table 3-8a. Summary of model errors for 11 non-blacklight ETH - NOx experiments.

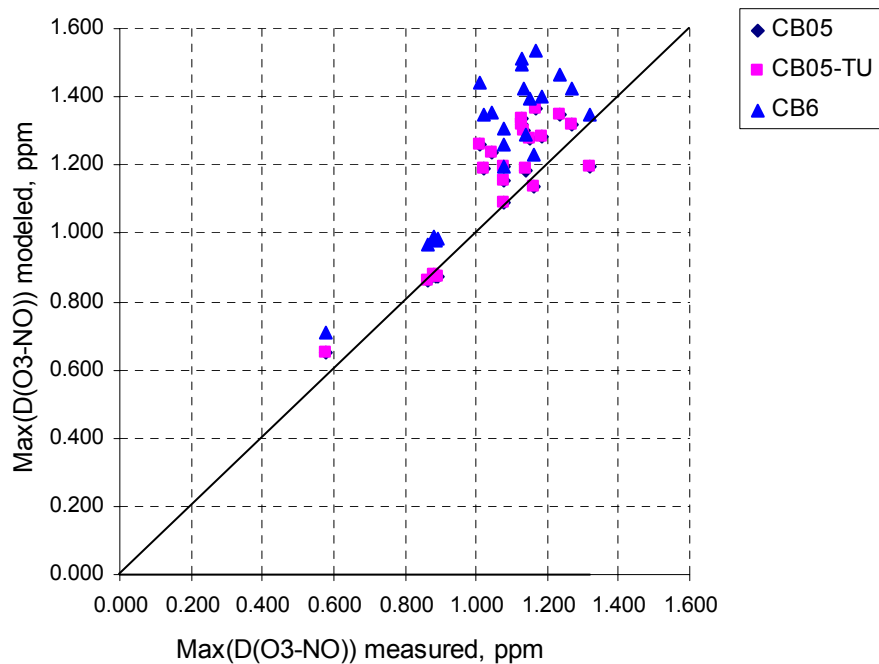
	Max(O ₃) [%]			Max(D(O ₃ -NO) [%])			NOx crossover time [min]		
	CB05	CB05-TU	CB6	CB05	CB05-TU	CB6	CB05	CB05-TU	CB6
Average	-16	-16	-12	-12	-12	-9	-1	-1	8
Std. dev.	12	12	16	7	7	10	16	16	18

3.3.5b. ETH: 22 blacklight experiments.

(a)



(b)



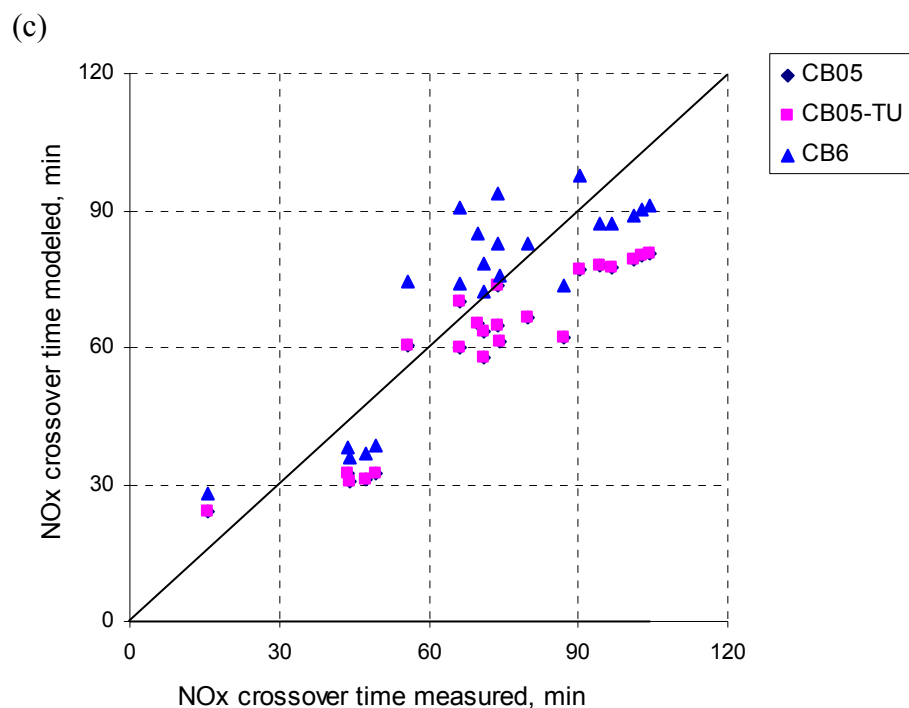


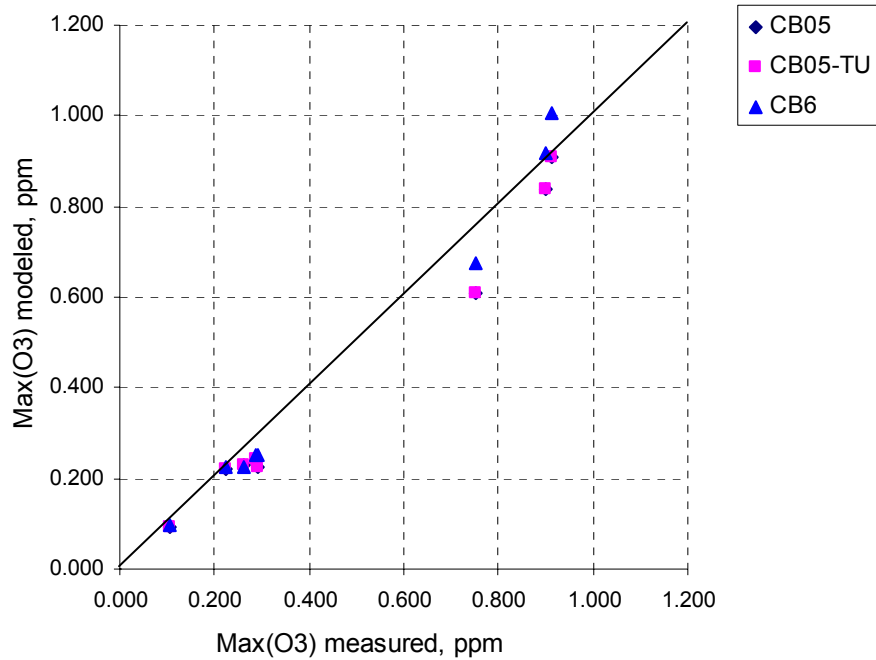
Figure 3-6b. Mechanism performance against 22 blacklight ETH - NOx experiments: (a) $\text{Max}(\text{O}_3)$, (b) $\text{Max}(\text{D}(\text{O}_3\text{-NO}))$, (c) NOx crossover time.

Table 3-8b. Summary of model errors for 22 blacklight ETH - NOx experiments.

	$\text{Max}(\text{O}_3)$ [%]			$\text{Max}(\text{D}(\text{O}_3\text{-NO}))$ [%]			NOx crossover time [min]		
	CB05	CB05-TU	CB6	CB05	CB05-TU	CB6	CB05	CB05-TU	CB6
Average	12	12	28	8	8	20	-11	-11	1
Std. dev.	13	13	17	9	9	11	9	9	12

3.3.6. ALD2: 8 experiments with acetaldehyde.

(a)



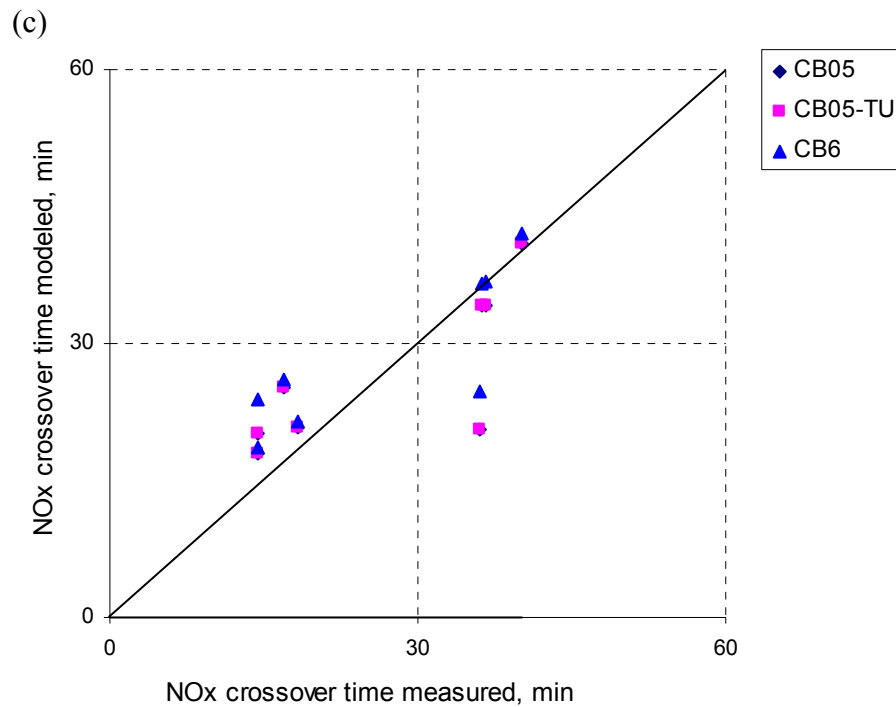


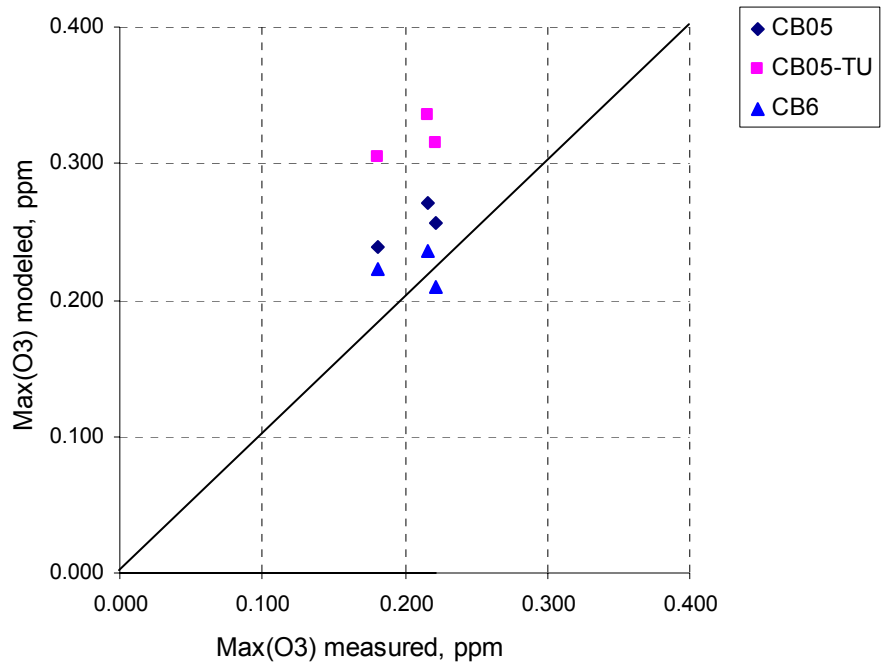
Figure 3-7. Mechanism performance against 8 ALD2 - NO_x experiments: (a) Max(O₃), (b) Max(D(O₃-NO)), (c) NO_x crossover time.

Table 3-9. Summary of model errors for 8 ALD2-NO_x experiments.

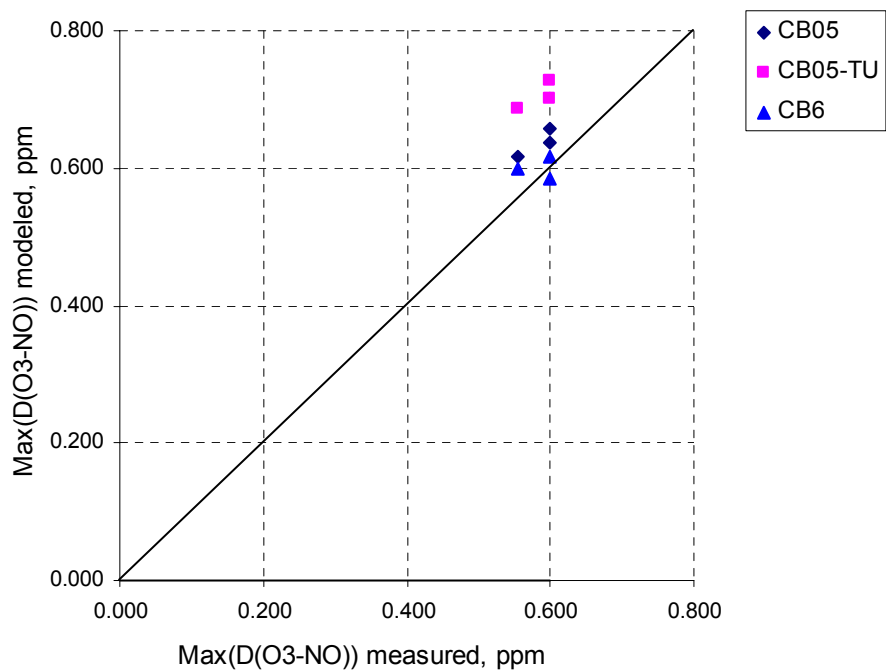
	Max(O ₃) [%]			Max(D(O ₃ -NO) [%]			NO _x crossover time [min]		
	CB05	CB05-TU	CB6	CB05	CB05-TU	CB6	CB05	CB05-TU	CB6
Average	-12	-12	-6	-9	-9	-4	0	0	2
Std. dev.	8	8	9	5	5	6	7	7	6

3.3.7. ETOH: 3 experiments using blacklights and VOC mixtures containing ethanol.

(a)



(b)



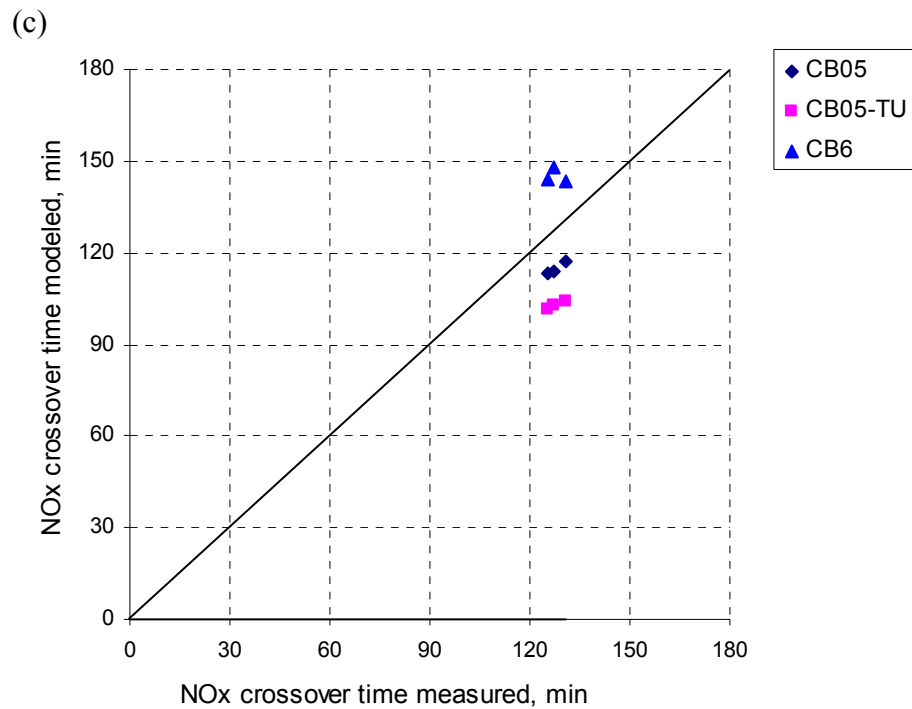


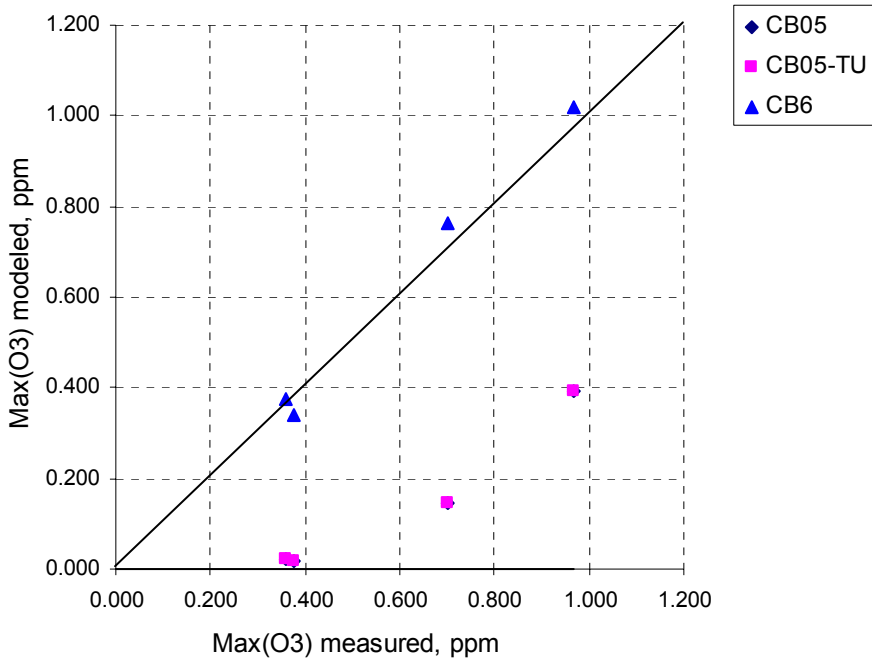
Figure 3-8. Mechanism performance against 3 blacklight ETOH - other VOCs - NOx experiments: (a) Max(O₃), (b) Max(D(O₃-NO)), (c) NOx crossover time.

Table 3-10. Summary of model errors for 3 blacklight ETOH -other VOCs - NOx experiments.

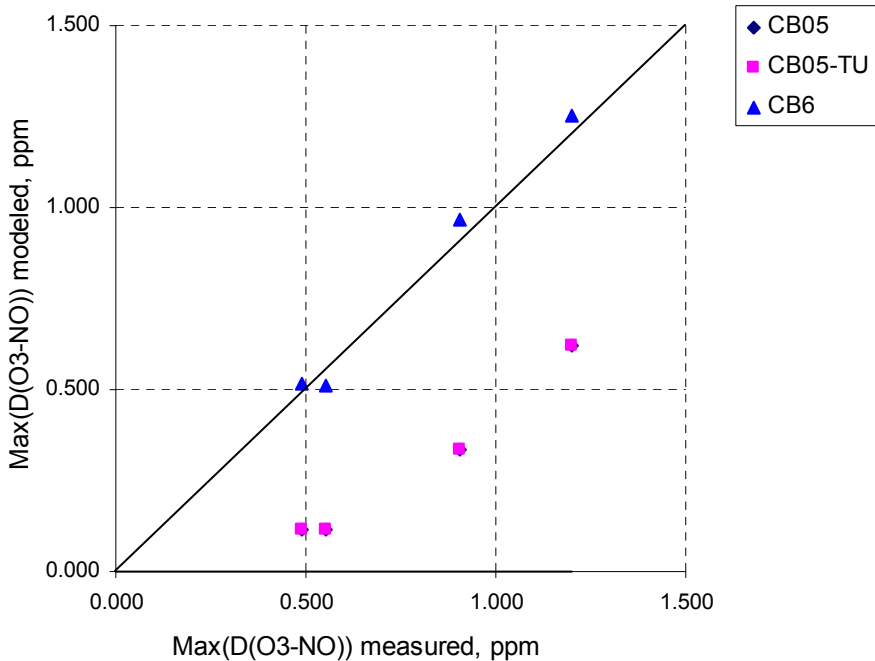
	Max(O ₃) [%]			Max(D(O ₃ -NO) [%]			NOx crossover time [min]		
	CB05	CB05-TU	CB6	CB05	CB05-TU	CB6	CB05	CB05-TU	CB6
Average	24	55	9	9	21	3	-13	-25	17
Std. dev.	8	13	14	3	4	5	1	2	4

3.3.8. ACET: 4 experiments with acetone.

(a)



(b)



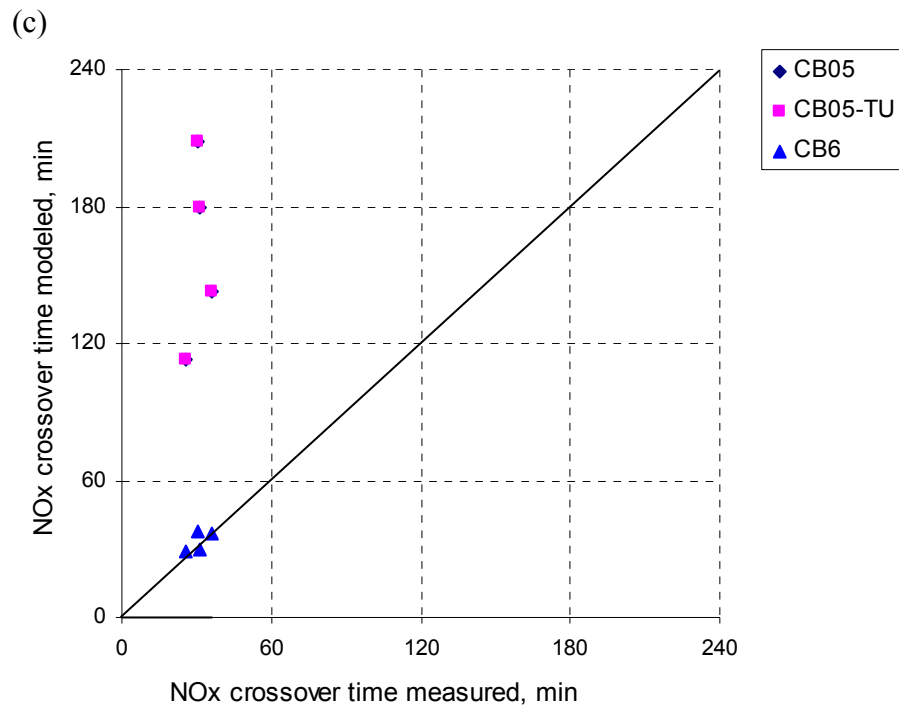


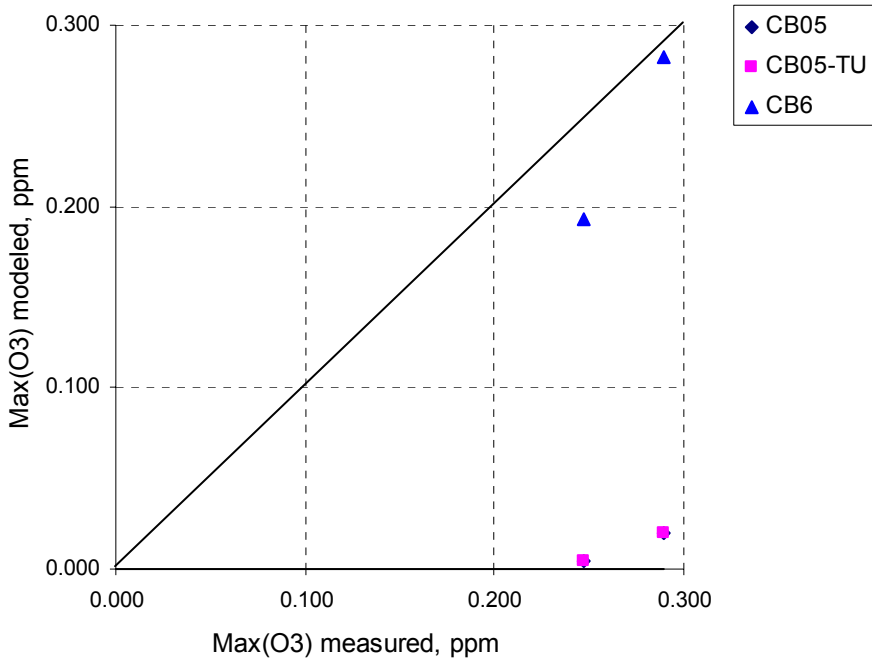
Figure 3-9. Mechanism performance against 4 ACET - NOx experiments: (a) Max(O₃), (b) Max(D(O₃-NO)), (c) NOx crossover time.

Table 3-11. Summary of model errors for 4 ACET - NOx experiments.

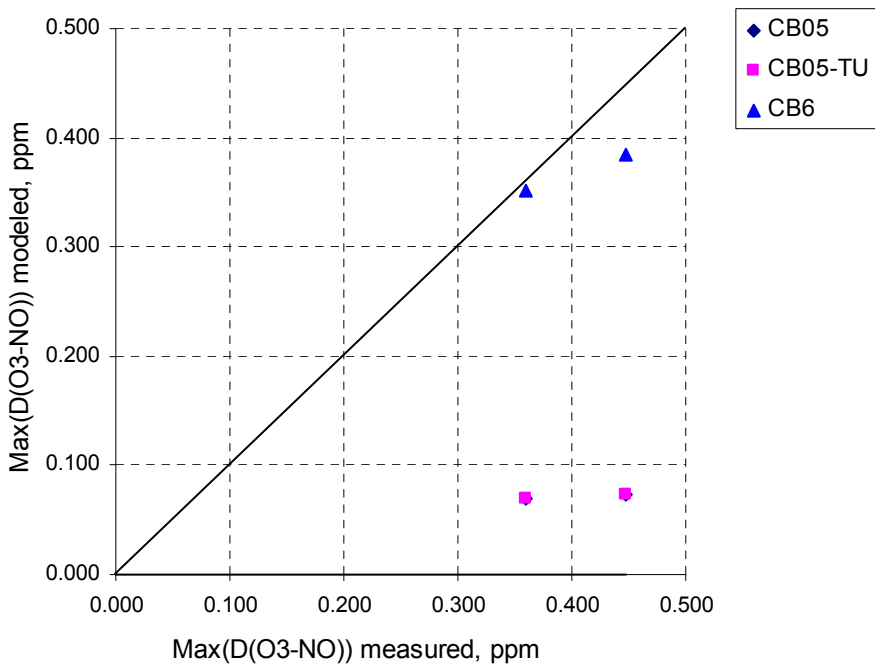
	Max(O ₃) [%]			Max(D(O ₃ -NO) [%]			NOx crossover time [min]		
	CB05	CB05-TU	CB6	CB05	CB05-TU	CB6	CB05	CB05-TU	CB6
Average	-82	-82	2	-66	-66	2	130	130	2
Std. dev.	17	17	8	14	14	7	41	41	4

3.3.9. KET: 2 experiments with methyl ethyl ketone (MEK).

(a)



(b)



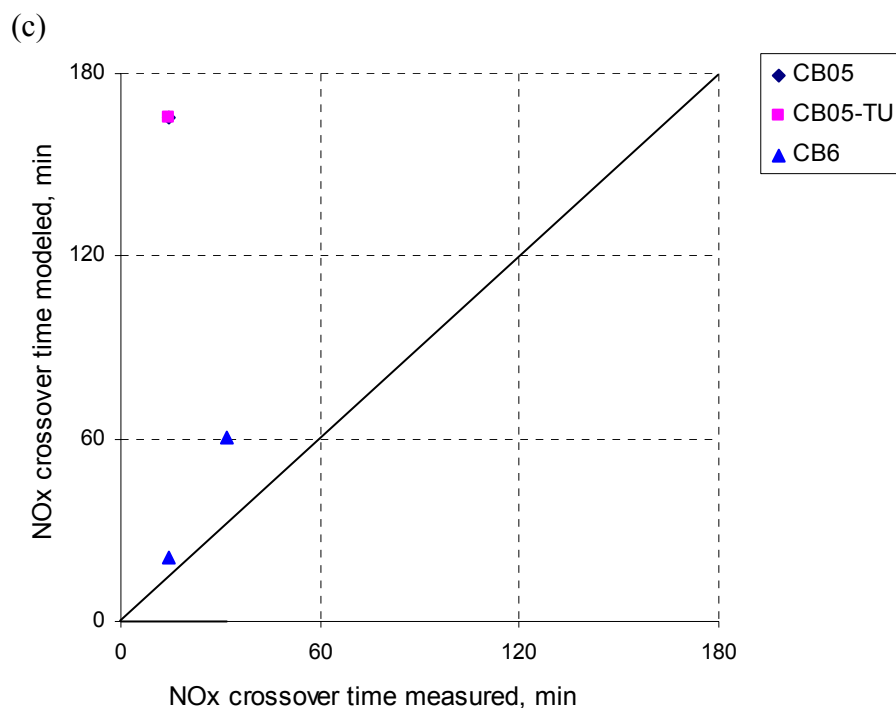


Figure 3-10. Mechanism performance against 2 Methyl Ethyl Ketone (MEK) - NOx experiments: (a) Max(O₃), (b) Max(D(O₃-NO)), (c) NOx crossover time.

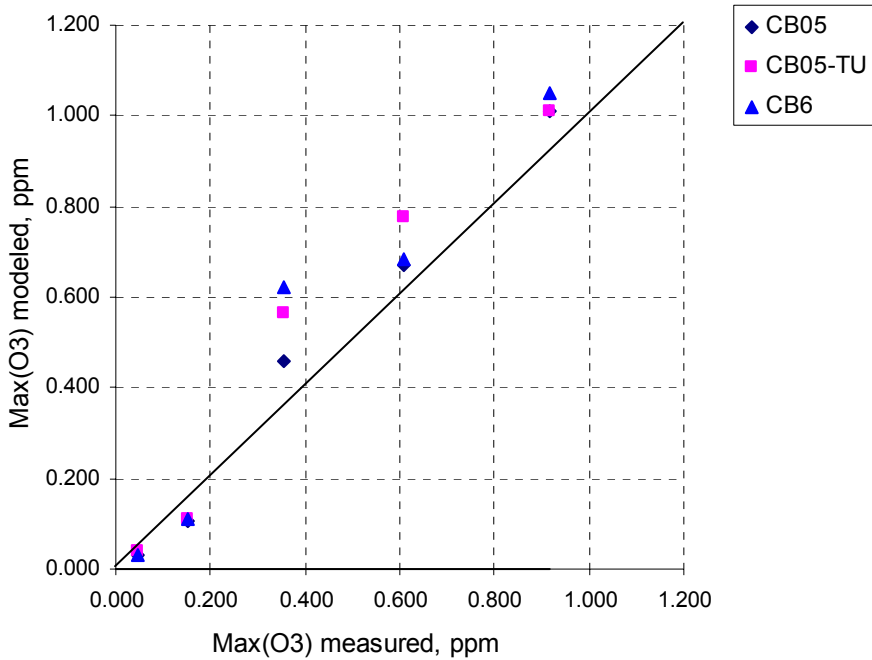
Table 3-12. Summary of model errors for 2 Methyl Ethyl Ketone - NOx experiments.^a

	Max(O ₃) [%]			Max(D(O ₃ -NO) [%])			NOx crossover time [min]		
	CB05	CB05-TU	CB6	CB05	CB05-TU	CB6	CB05	CB05-TU	CB6
Average	-96	-96	-12	-82	-82	-8	^a	^a	18
Std. dev.	3	3	14	2	2	8	^a	^a	15

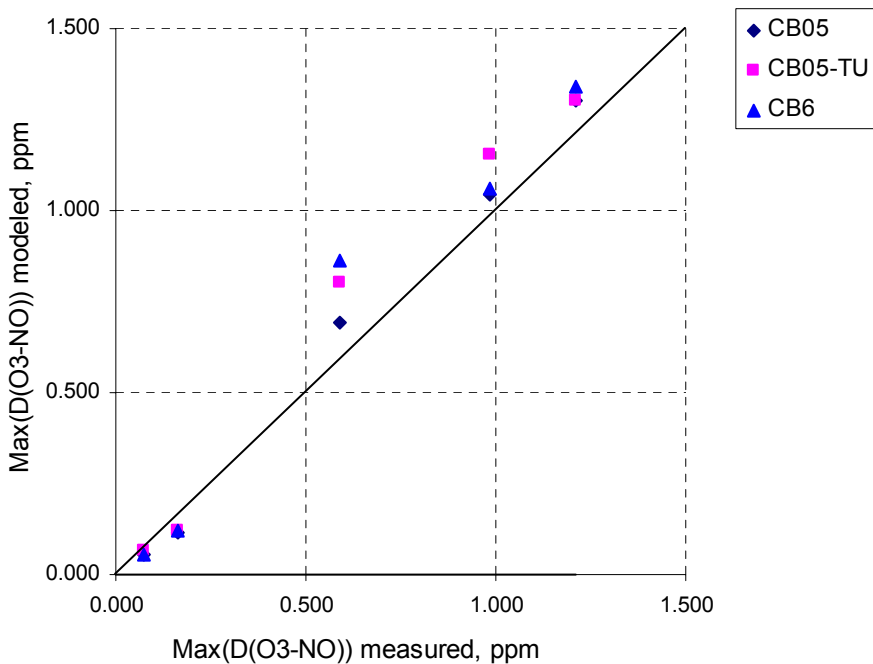
^aCB05 and CB05-TU did not show NOx crossovers by hour of 6 for experiment CTC178A, one of the two experiments selected for testing KET chemistry.

3.3.10. ETHA: 5 experiments using blacklights and VOC mixtures containing ethane.

(a)



(b)



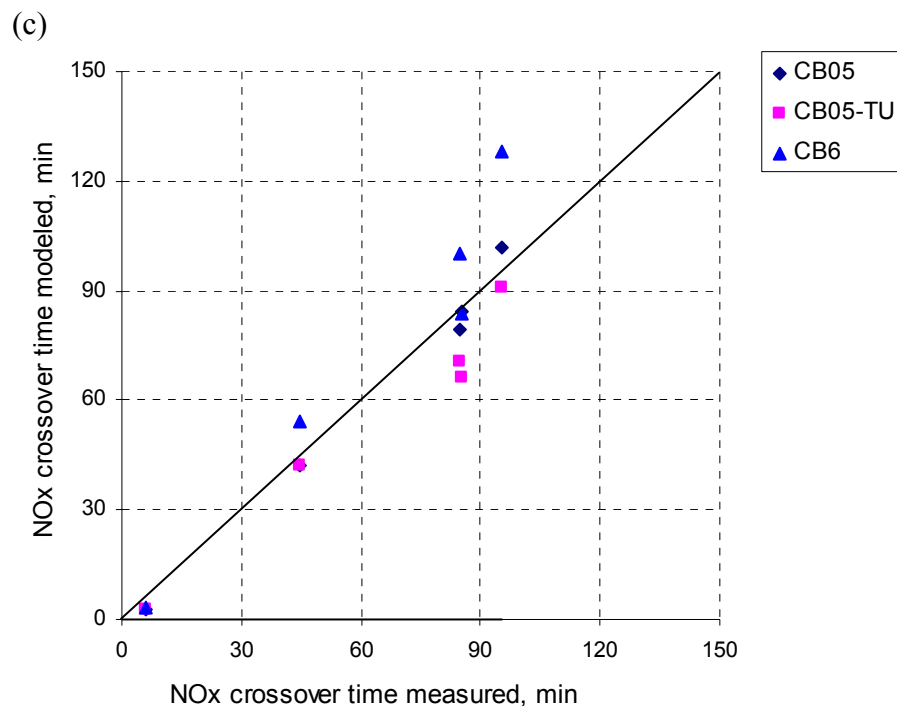


Figure 3-11. Mechanism performance against 2 blacklight ETHA - other VOCs - NOx experiments: (a) Max(O₃), (b) Max(D(O₃-NO)), (c) NOx crossover time. Note: ETHA is ethane.

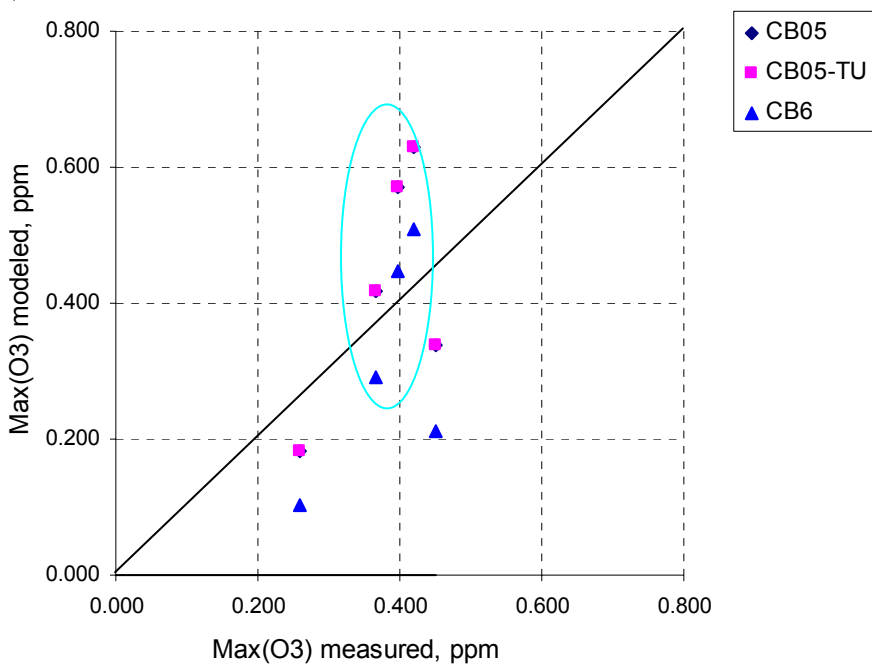
Table 3-13. Summary of model errors for 2 blacklight ETHA - other VOCs - NOx experiments.

	Max(O ₃) [%]			Max(D(O ₃ -NO) [%])			NOx crossover time [min]		
	CB05	CB05-TU	CB6	CB05	CB05-TU	CB6	CB05	CB05-TU	CB6
Average	-2	12	10	-4	3	1	-1	-9	11
Std. dev.	27	33	42	21	29	24	5	7	15

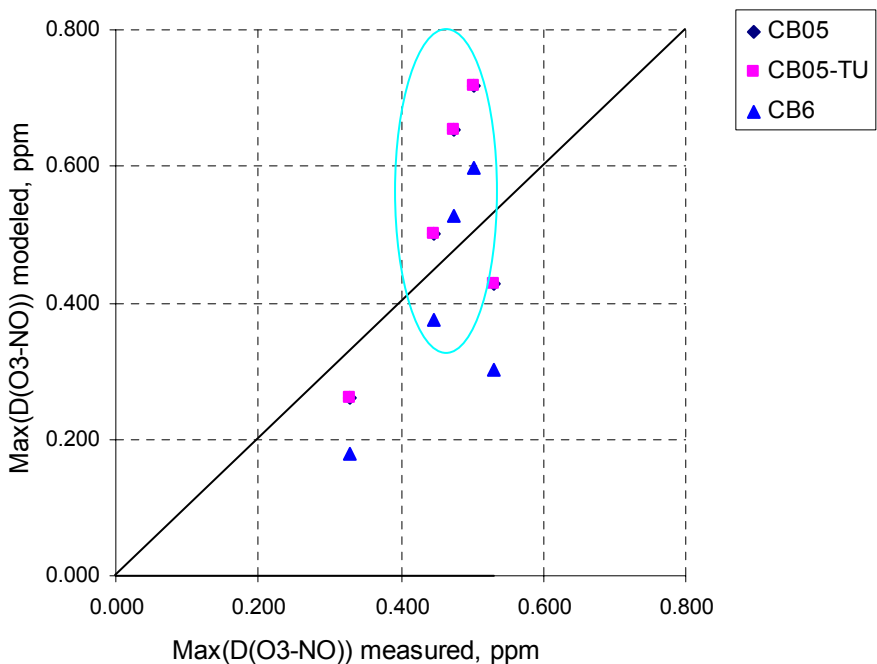
3.3.11. ALDX: no suitable experiments available for higher aldehydes.

3.3.12. PAR: 5 experiments in total, 3 with n-butane and 2 with n-butane plus 2,3-dimethyl butane.

(a)



(b)



(c)

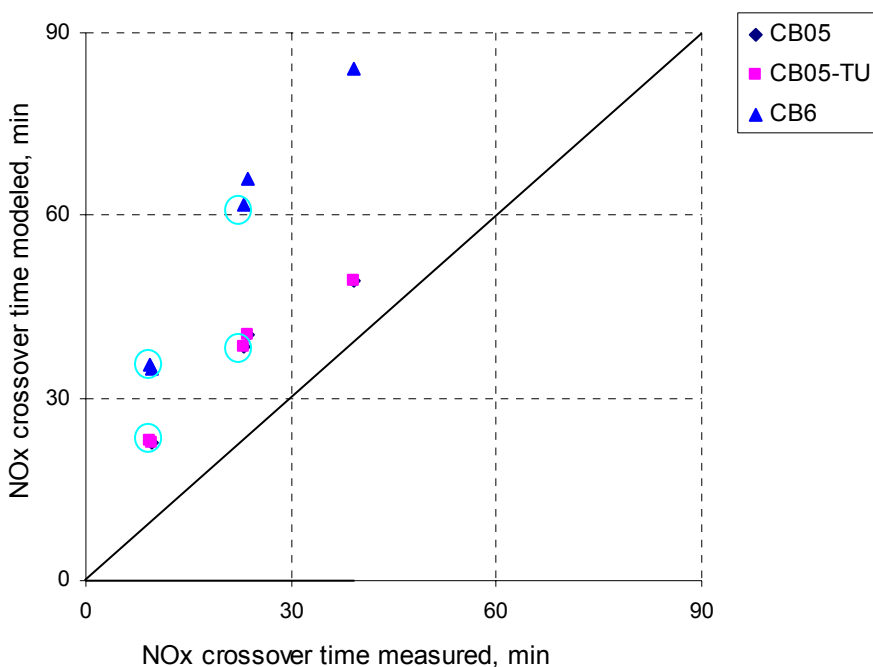


Figure 3-12. Mechanism performance against 5 PAR - NO_x experiments: (a) Max(O₃), (b) Max(D(O₃-NO)), (c) NO_x crossover time.

Note: model results for three n-butane – NO_x experiments are circled.

Table 3-14a. Summary of model errors for 5 PAR - NO_x experiments.

	Max(O ₃) [%]			Max(D(O ₃ -NO) [%])			NO _x crossover time [min]		
	CB05	CB05-TU	CB6	CB05	CB05-TU	CB6	CB05	CB05-TU	CB6
Average	11	11	-20	11	11	-15	14	14	35
Std. dev.	37	37	37	30	30	30	2	2	9

Table 3-14b. Summary of model errors only for 3 n-Butane - NO_x experiments.^a

	Max(O ₃) [%]			Max(D(O ₃ -NO) [%])			NO _x crossover time [min]		
	CB05	CB05-TU	CB6	CB05	CB05-TU	CB6	CB05	CB05-TU	CB6
Average	36	36	5	31	31	5	14	14	30
Std. dev.	19	19	22	16	16	18	1	1	7

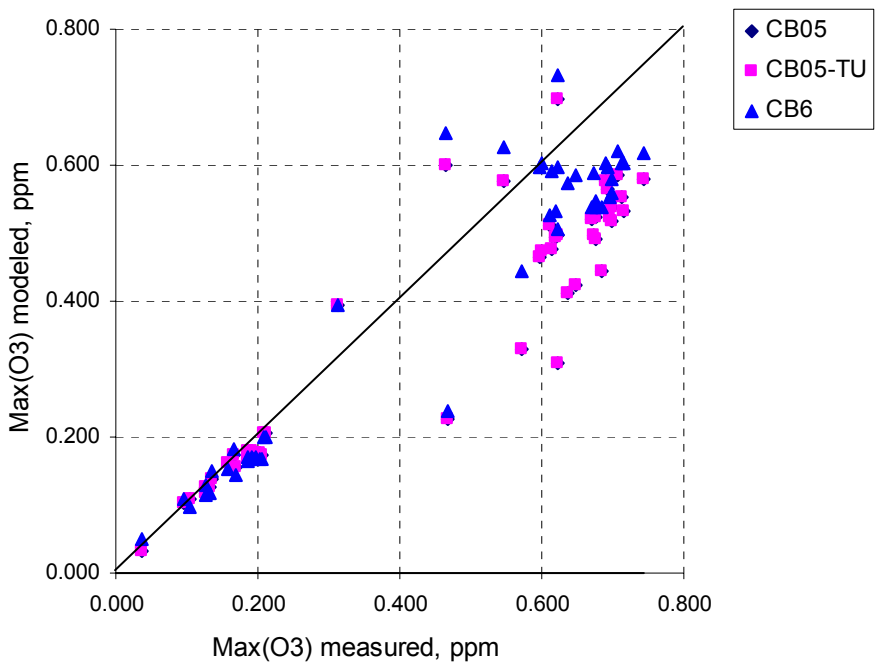
^amodel results for three n-butane – NO_x experiments are circled in Figure 3-11.

Table 3-14c. Summary of model errors only for 2 n-Butane/2,3-Dimethyl Butane/NO_x experiments.

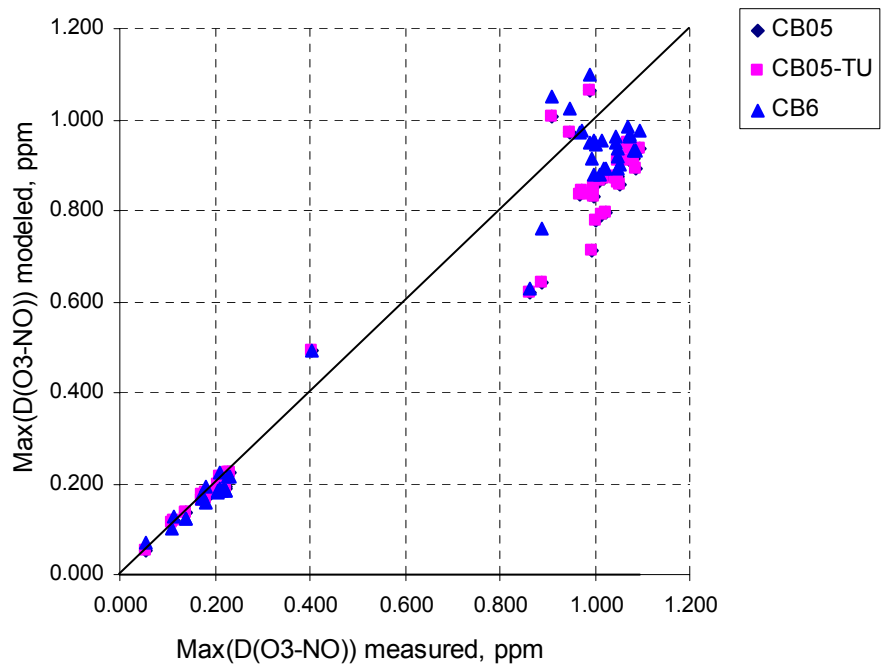
	Max(O ₃) [%]			Max(D(O ₃ -NO) [%])			NO _x crossover time [min]		
	CB05	CB05-TU	CB6	CB05	CB05-TU	CB6	CB05	CB05-TU	CB6
Average	-27	-27	-57	-20	-20	-45	13	13	44
Std. dev.	3	3	5	1	1	2	5	5	2

3.3.13. OLE: 48 experiments in total, 47 with propene and 1 with 1-butene.

(a)



(b)



(c)

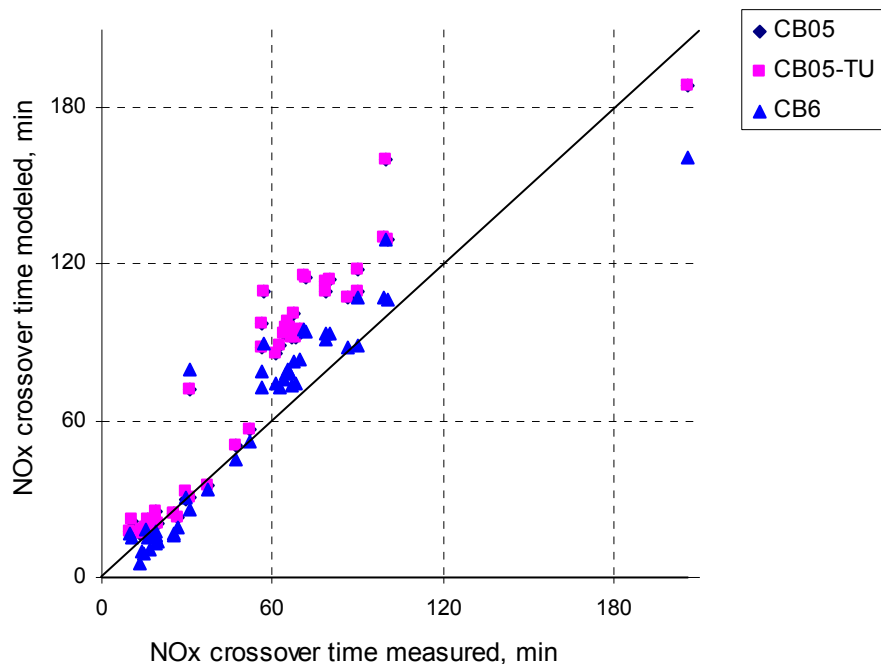


Figure 3-13. Mechanism performance against 48 OLE - NOx experiments: (a) $\text{Max}(\text{O}_3)$, (b) $\text{Max}(\text{D}(\text{O}_3\text{-NO}))$, (c) NOx crossover time.

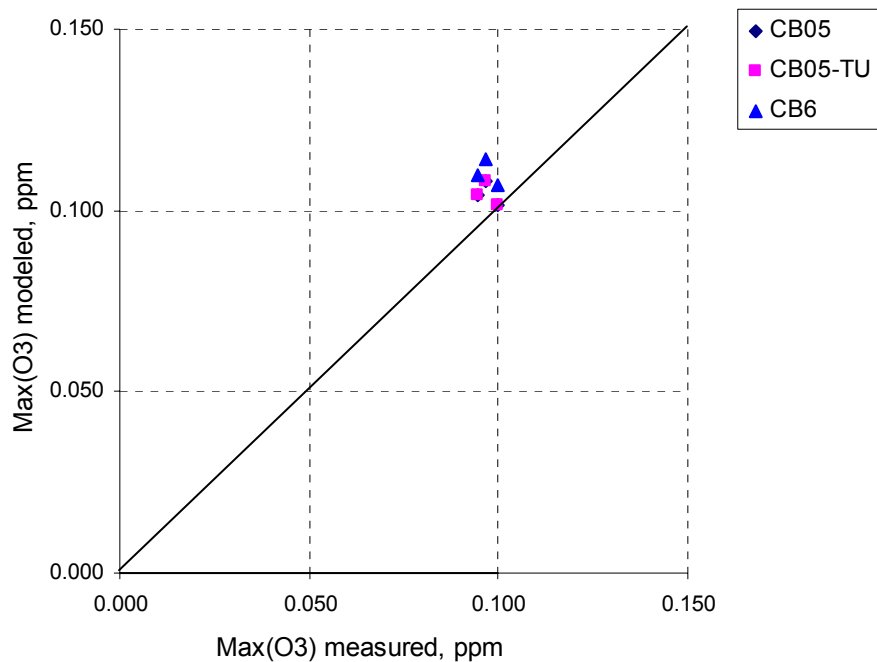
Table 3-15. Summary of model errors for 48 OLE - NOx experiments.^a

	$\text{Max}(\text{O}_3)$ [%]			$\text{Max}(\text{D}(\text{O}_3\text{-NO}))$ [%]			NOx crossover time [min]		
	CB05	CB05-TU	CB6	CB05	CB05-TU	CB6	CB05	CB05-TU	CB6
Average	-14	-14	-7	-10	-10	-6	18	18	6
Std. dev.	17	17	16	10	10	11	18	17	14

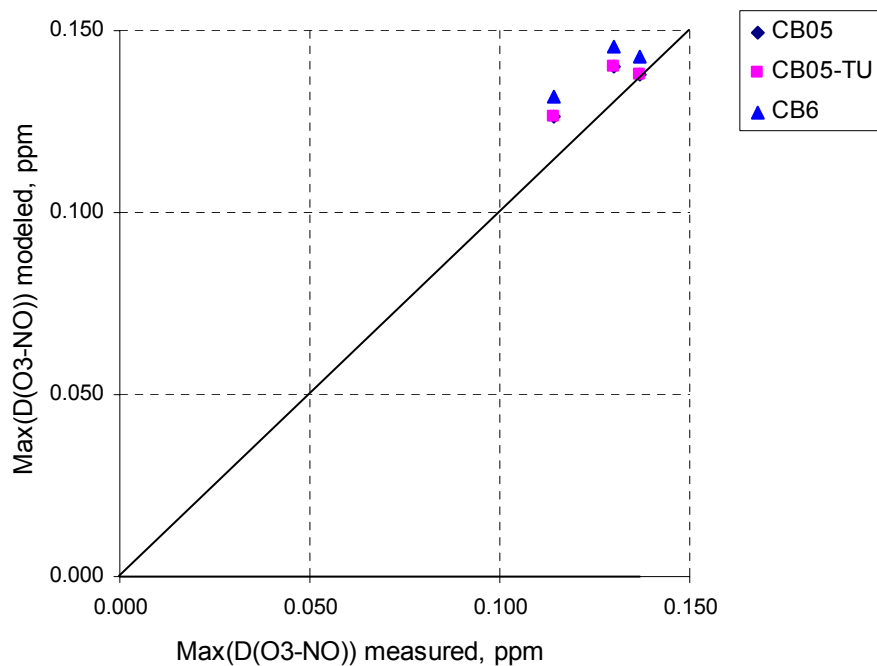
^a47 Propene-NOx experiments and one 1-butene-NOx experiment.

3.3.14. IOLE: 3 experiments with trans-2-butene.

(a)



(b)



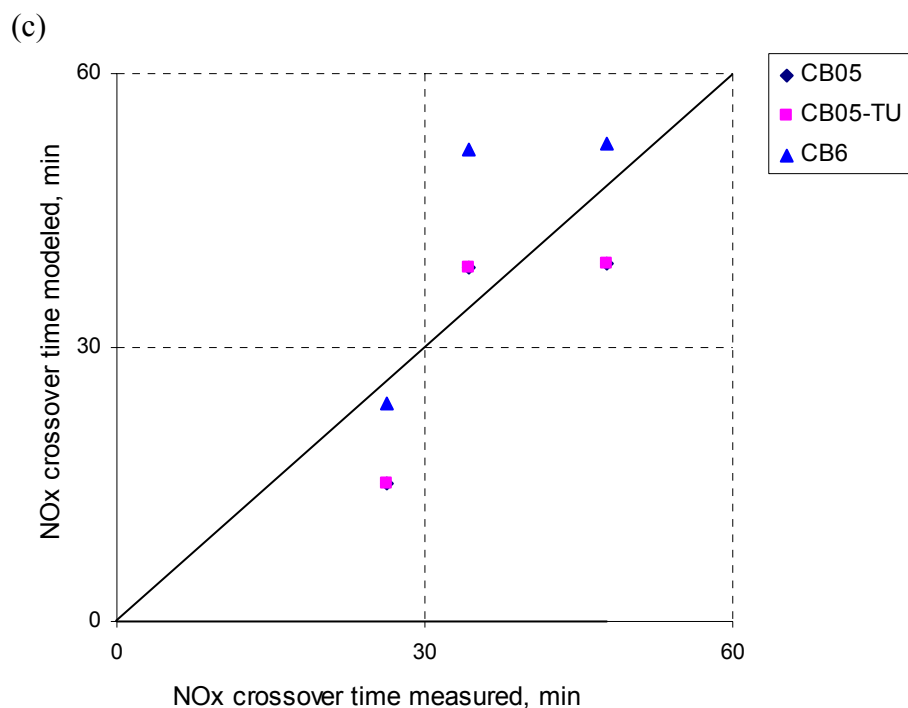


Figure 3-14. Mechanism performance against 3 IOLE - NOx experiments: (a) $\text{Max}(\text{O}_3)$, (b) $\text{Max}(\text{D}(\text{O}_3\text{-NO}))$, (c) NOx crossover time.

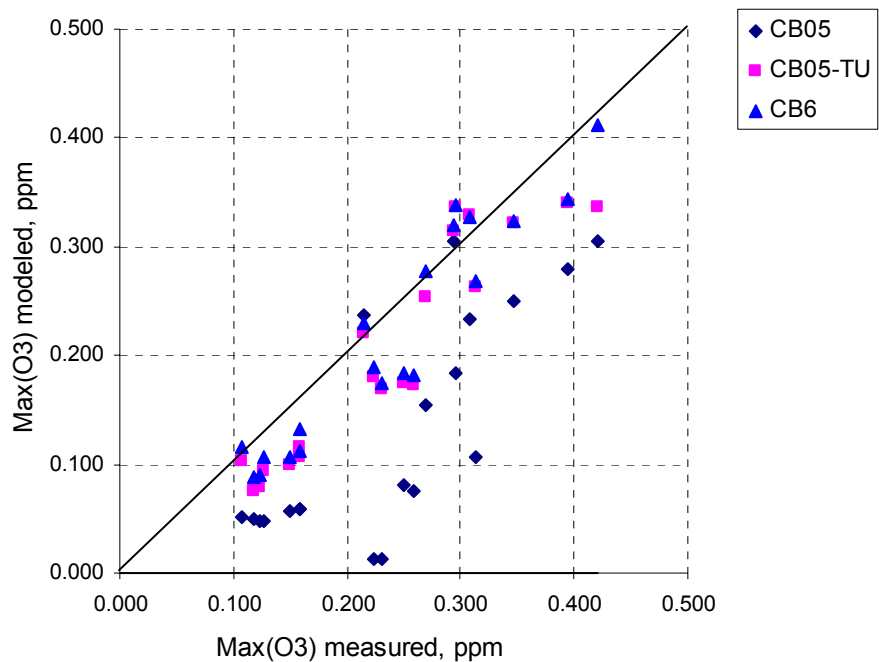
Table 3-16. Summary of model errors for 3 IOLE-NOx experiments.^a

	Max(O_3) [%]			Max(D($\text{O}_3\text{-NO}$)) [%]			NOx crossover time [min]		
	CB05	CB05-TU	CB6	CB05	CB05-TU	CB6	CB05	CB05-TU	CB6
Average	8	8	14	6	6	11	-5	-5	7
Std. dev.	6	6	6	5	5	5	8	8	10

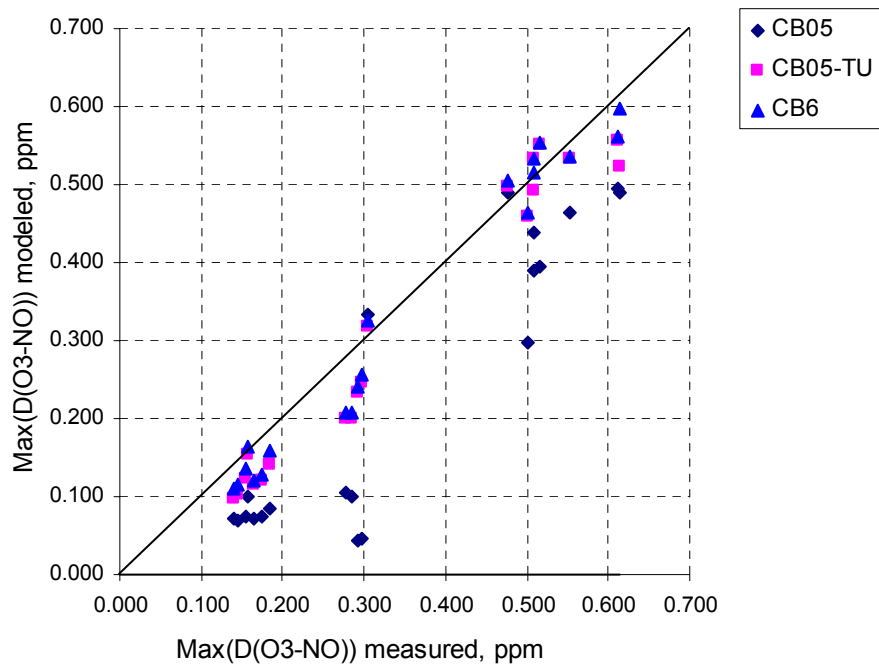
^a3 trans-2-butene – NOx experiments.

3.3.15. TOL: 20 experiments in total, 18 with toluene and 2 with ethyl benzene.

(a)



(b)



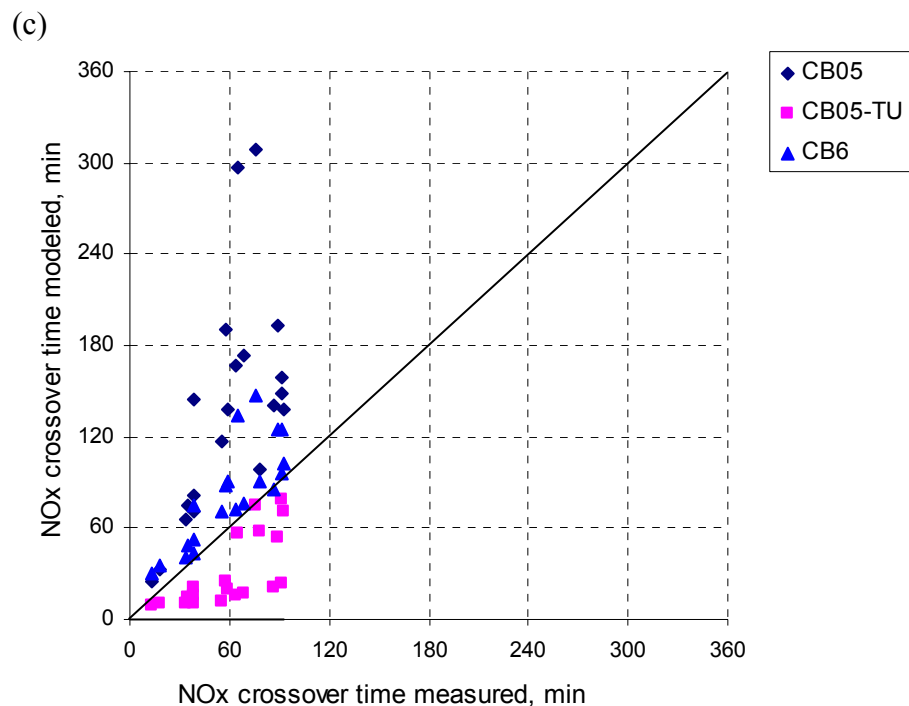


Figure 3-15. Mechanism performance against 20 TOL - NOx experiments: (a) $\text{Max}(\text{O}_3)$, (b) $\text{Max}(\text{D}(\text{O}_3\text{-NO}))$, (c) NOx crossover time.

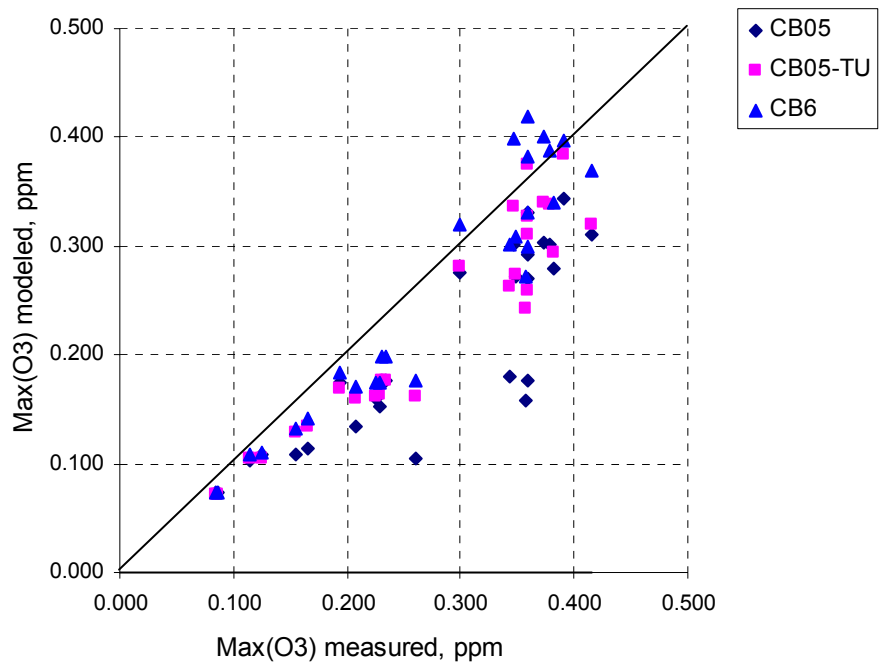
Table 3-17. Summary of model errors for 20 TOL-NOx experiments.^a

	$\text{Max}(\text{O}_3)$ [%]			$\text{Max}(\text{D}(\text{O}_3\text{-NO}))$ [%]			NOx crossover time [min]		
	CB05	CB05-TU	CB6	CB05	CB05-TU	CB6	CB05	CB05-TU	CB6
Average	-49	-17	-11	-40	-14	-10	79	-29	22
Std. dev.	28	16	15	26	14	12	63	19	20

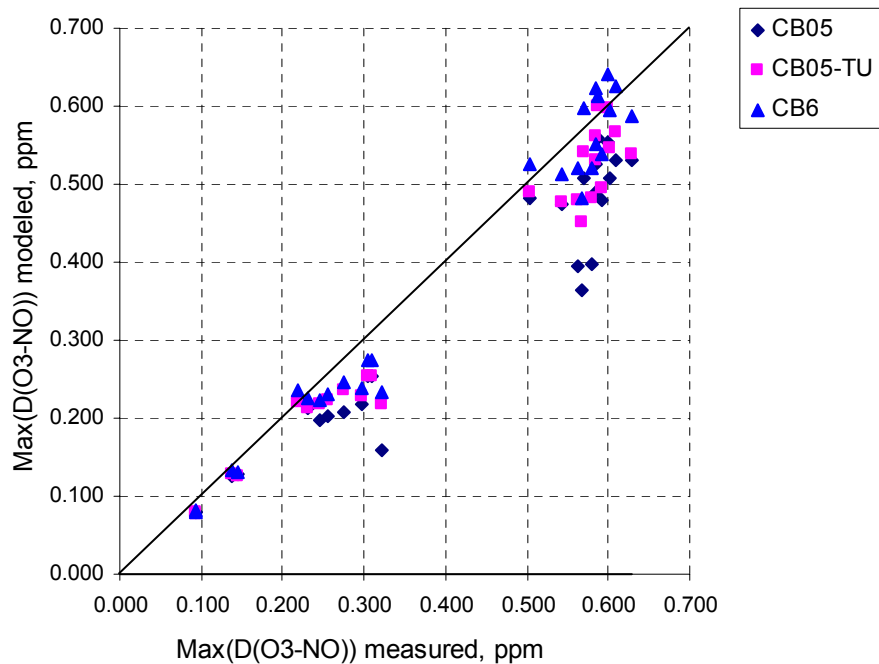
^a18 toluene - NOx experiments, and 2 ethyl benzene - NOx experiments.

3.3.16. XYL: 27 experiments in total, 4 with o-xylene, 15 with m-xylene, 2 with p-xylene, 2 with 1,2,3-trimethylbenzene, 2 with 1,2,4-trimethylbenzene and 2 with 1,3,5-trimethylbenzene.

(a)



(b)



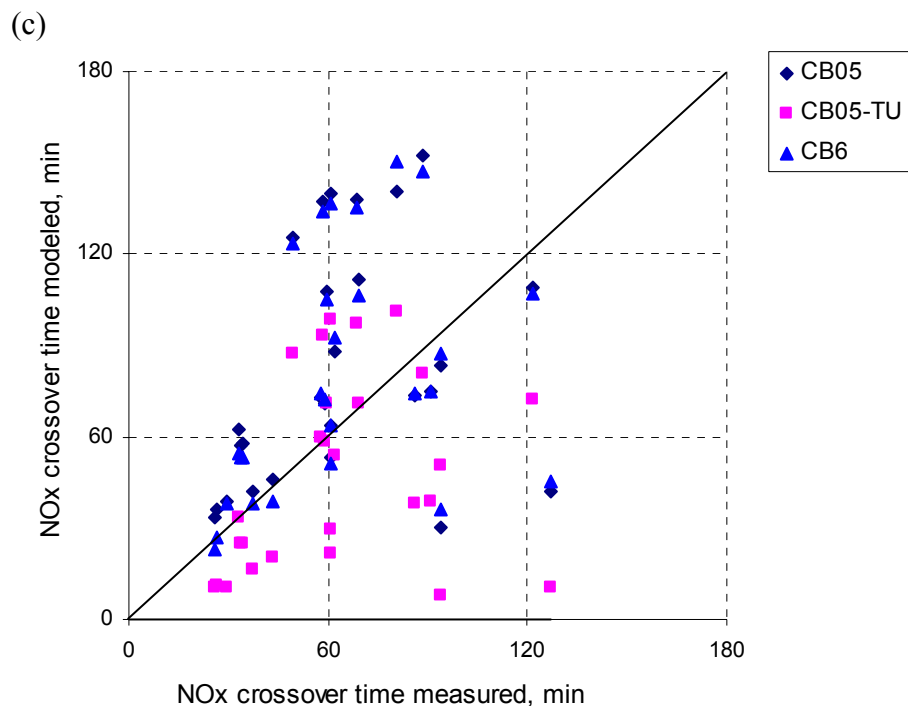


Figure 3-16. Mechanism performance against 27 XYL - NOx experiments: (a) $\text{Max}(\text{O}_3)$, (b) $\text{Max}(\text{D}(\text{O}_3\text{-NO}))$, (c) NOx crossover time.

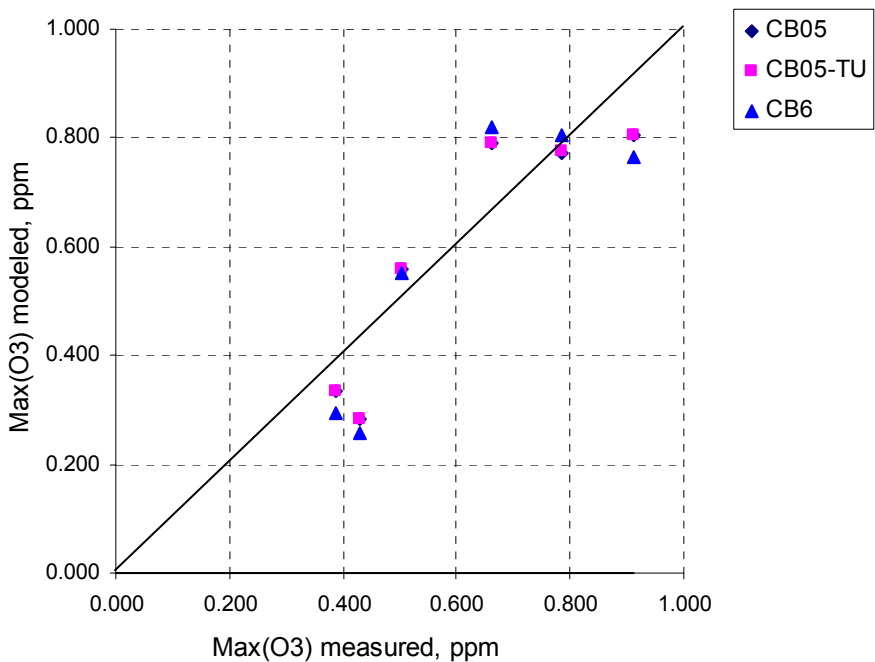
Table 3-18. Summary of model errors for 27 XYL-NOx experiments.^a

	$\text{Max}(\text{O}_3)$ [%]			$\text{Max}(\text{D}(\text{O}_3\text{-NO}))$ [%]			NOx crossover time [min]		
	CB05	CB05-TU	CB6	CB05	CB05-TU	CB6	CB05	CB05-TU	CB6
Average	-25	-17	-9	-17	-12	-6	18	-15	16
Std. dev.	14	10	12	11	8	9	40	36	39

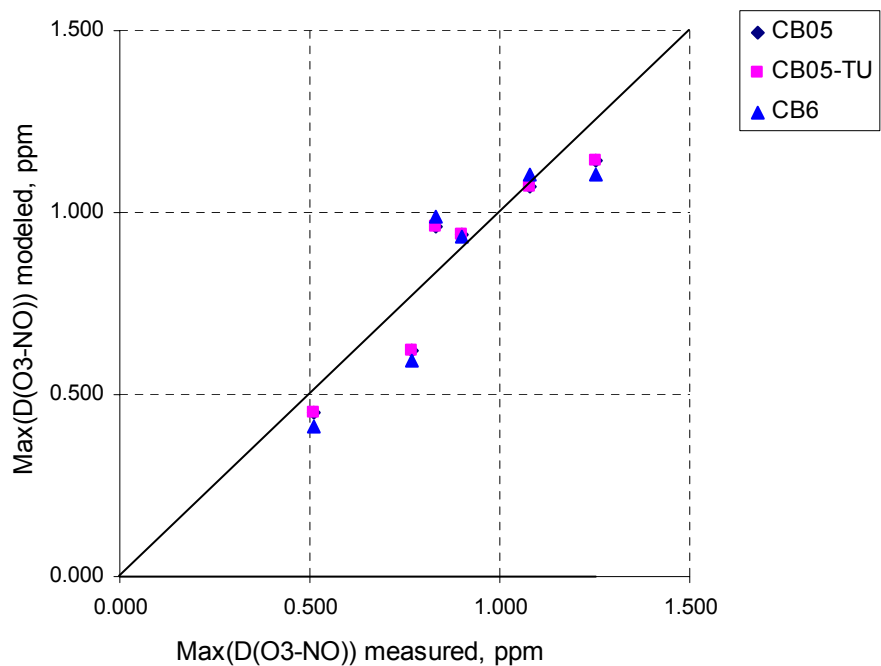
^a4, 15 and 2 experiments for o-xylene (o-XYL), m-XYL and p-XYL; 2 experiments for each of 123-trimethyl benzene (TMB), 124-TMB and 135-TMB.

3.3.17. ISOP: 6 experiments with isoprene.

(a)



(b)



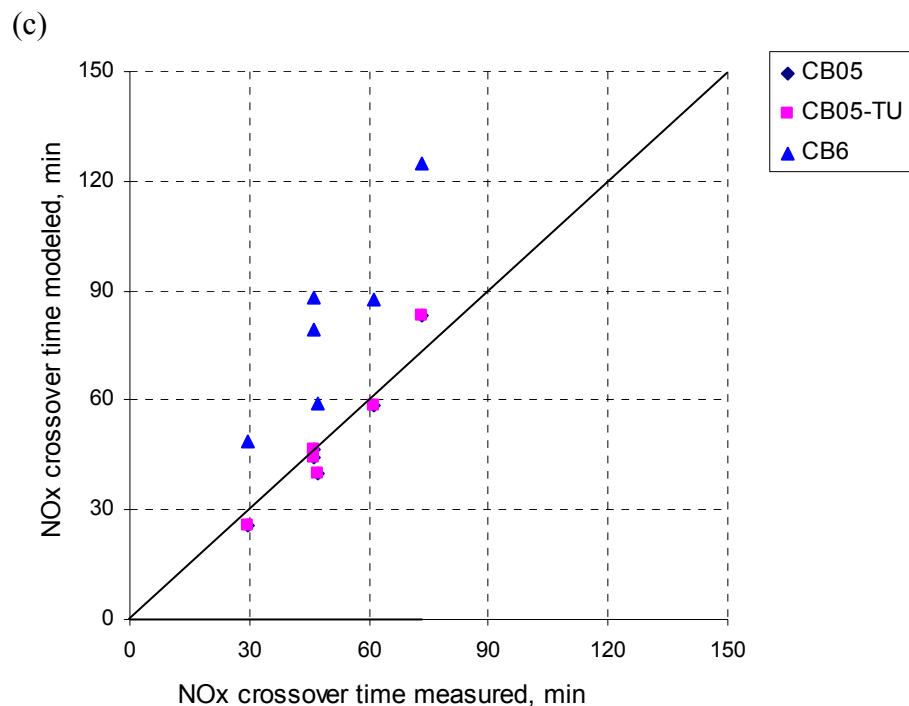


Figure 3-17. Mechanism performance against 6 ISOP - NO_x experiments: (a) Max(O₃), (b) Max(D(O₃-NO)), (c) NO_x crossover time.

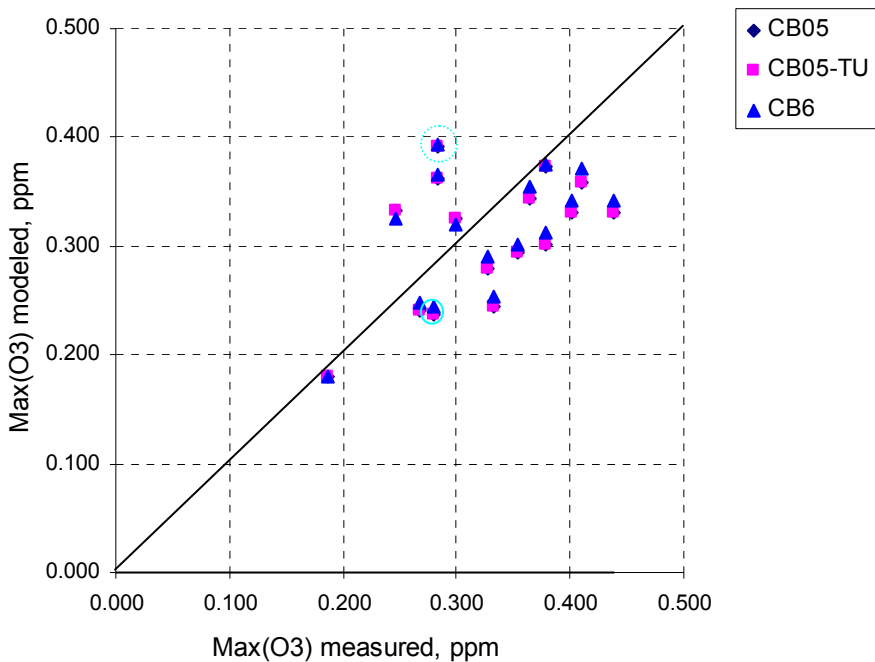
Note: ISOP is isoprene.

Table 3-19. Summary of model errors for 6 isoprene - NO_x experiments.

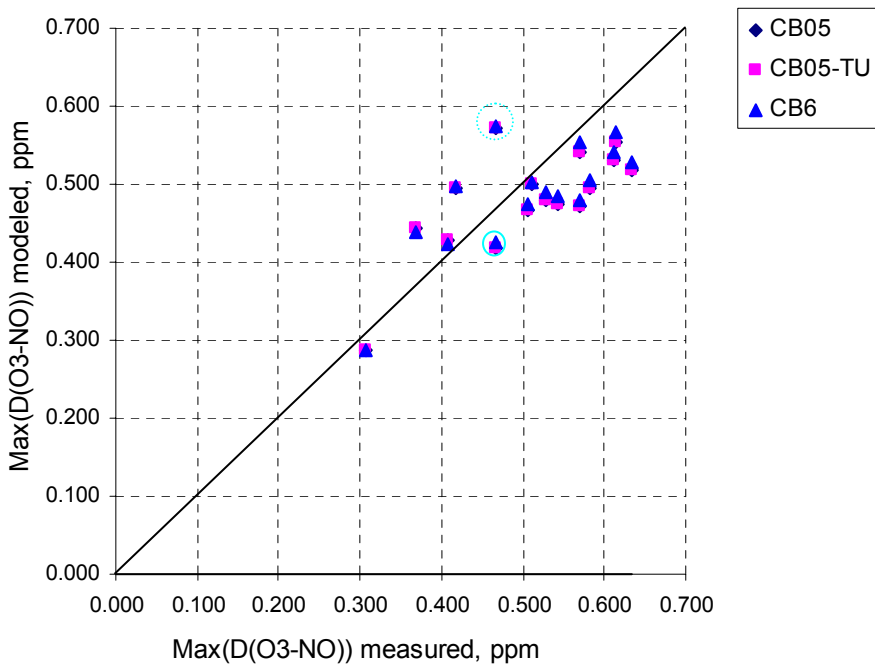
	Max(O ₃) [%]			Max(D(O ₃ -NO) [%])			NO _x crossover time [min]		
	CB05	CB05-TU	CB6	CB05	CB05-TU	CB6	CB05	CB05-TU	CB6
Average	-5	-5	-7	-3	-3	-5	-1	-1	31
Std. dev.	19	19	23	12	12	16	6	6	15

3.3.18. TERP: 2 non-blacklight experiments, 1 with α -pinene and 1 with β -pinene (1)); 14 blacklight experiments with α -pinene (4), β -pinene (1), 3-carene (3), d-limonene (3) and sabinene (3) for additional information.

(a)



(b)



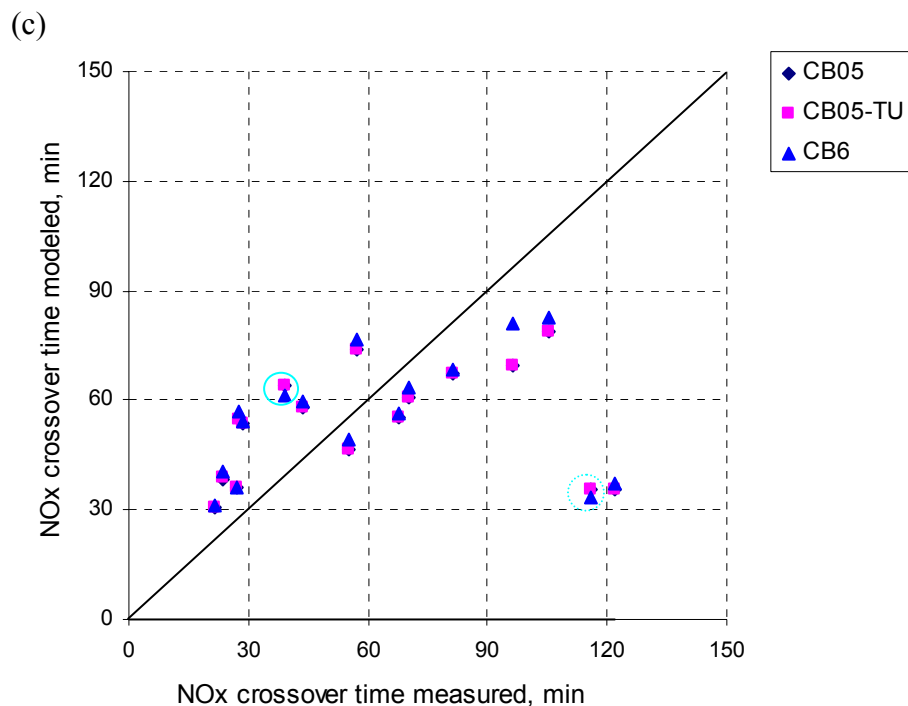


Figure 3-18. Mechanism performance against 2 non-blacklight and 14 blacklight terpene (TERP) - NO_x experiments: (a) Max(O₃), (b) Max(D(O₃-NO)), (c) NO_x crossover time.

Note: Results for one non-blacklight α -pinene – NO_x experiment and one non-blacklight β -pinene are surrounded by solid circles and by broken circles.

Table 3-20a. Summary of model errors for 2 non-blacklight terpene-NO_x experiments.^a

	Max(O ₃) [%]			Max(D(O ₃ -NO) [%])			NO _x crossover time [min]		
	CB05	CB05-TU	CB6	CB05	CB05-TU	CB6	CB05	CB05-TU	CB6
Average	12	12	13	6	6	7	-28	-28	-30
Std. dev.	38	38	37	23	23	22	75	75	74

^aOne for α -pinene, and one for β -pinene.

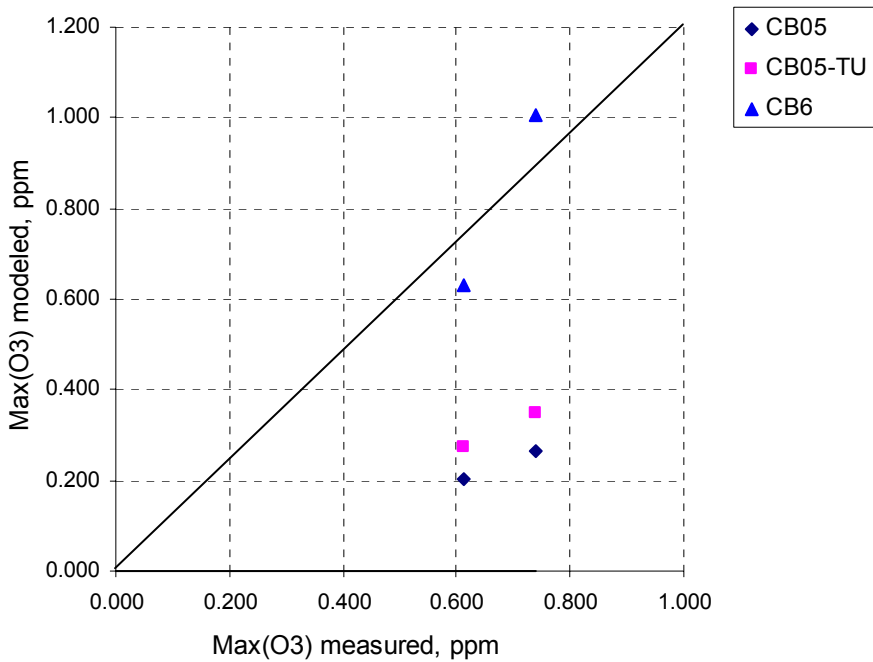
Table 3-20b. Summary of model errors for 14 blacklight terpene-NO_x experiments.^a

	Max(O ₃) [%]			Max(D(O ₃ -NO) [%])			NO _x crossover time [min]		
	CB05	CB05-TU	CB6	CB05	CB05-TU	CB6	CB05	CB05-TU	CB6
Average	-6	-6	-4	-5	-5	-4	-5	-5	-2
Std. dev.	18	19	17	12	12	11	30	30	29

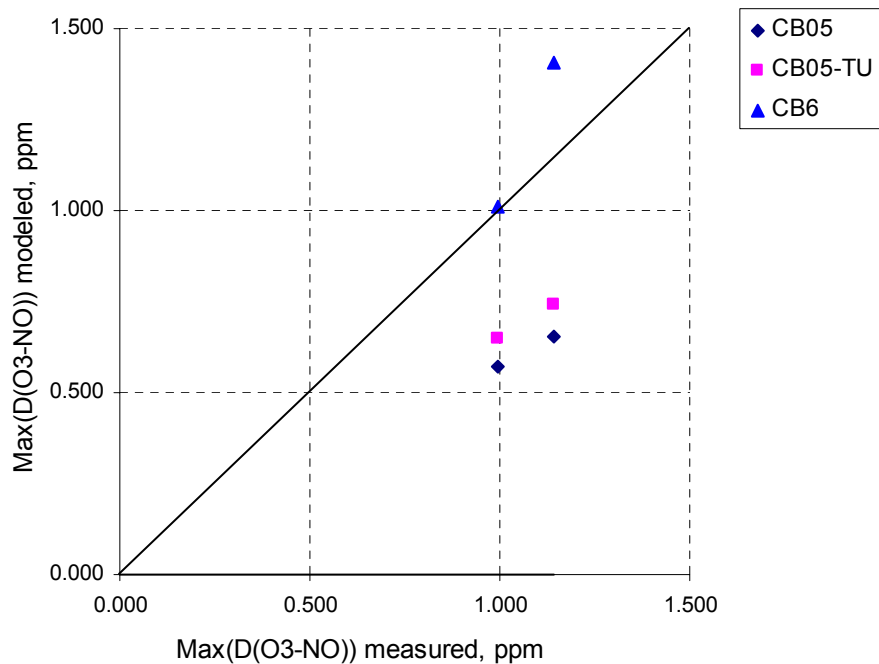
^a4 experiments for α -pinene, 1 experiment for β -pinene, and 3 experiments for each of 3-carene, d-limonene and sabinene.

3.3.19. PRPA: 2 experiments using blacklights and VOC mixtures containing propane.

(a)



(b)



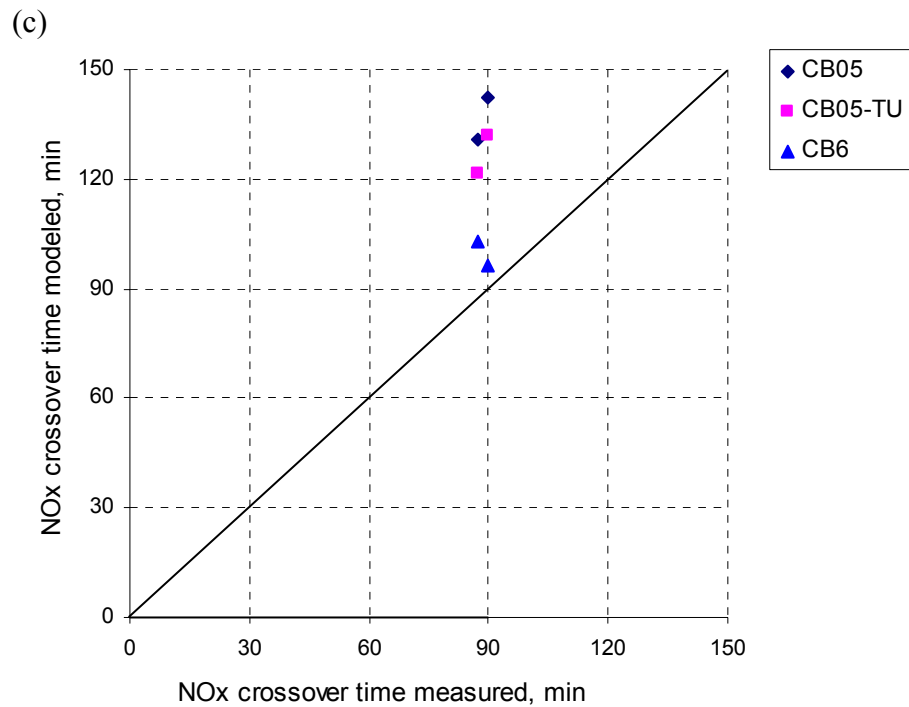


Figure 3-19. Mechanism performance against 2 blacklight PRPA - other VOCs - NOx experiments: (a) Max(O₃), (b) Max(D(O₃-NO)), (c) NOx crossover time.
Note: PRPA is propene.

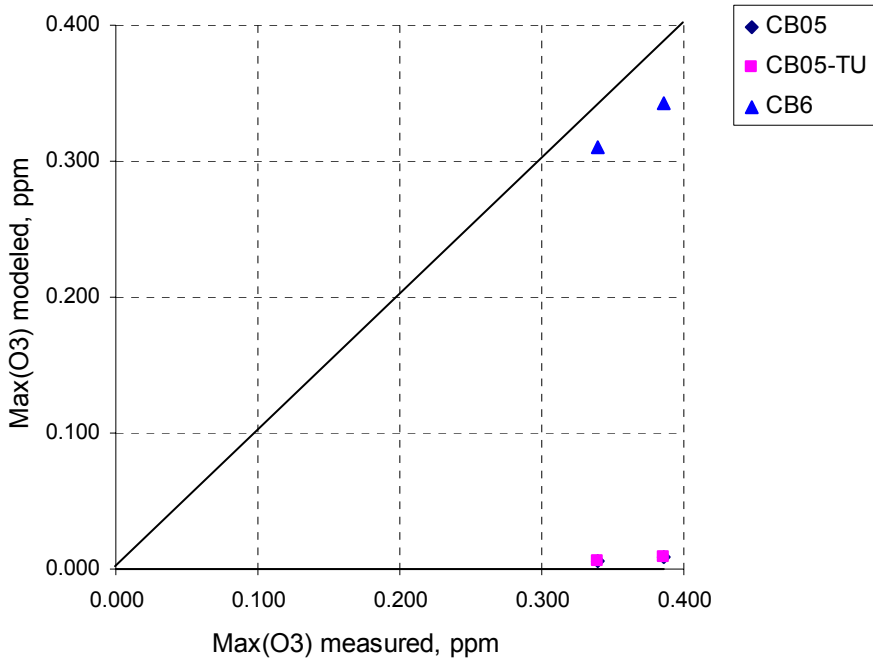
Table 3-21. Summary of model errors for 2 blacklight PRPA - other VOCs - NOx experiments.^a

	Max(O ₃) [%]			Max(D(O ₃ -NO) [%])			NOx crossover time [min]		
	CB05	CB05-TU	CB6	CB05	CB05-TU	CB6	CB05	CB05-TU	CB6
Average	-65	-54	20	-43	-35	13	48	38	11
Std. dev.	2	2	24	0	0	16	6	6	7

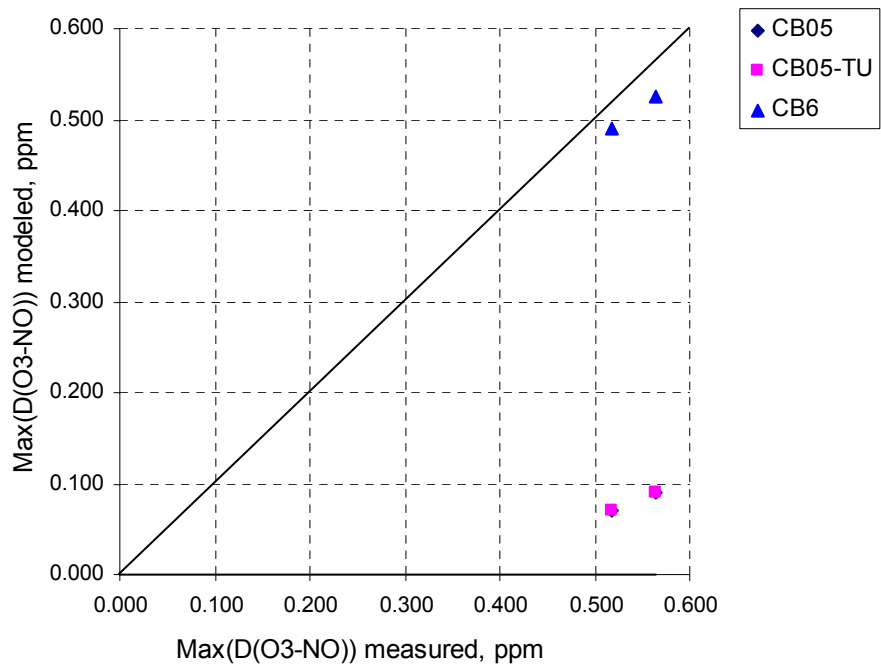
^aPRPA is "propane".

3.3.20. BENZ: 2 experiments for benzene.

(a)



(b)



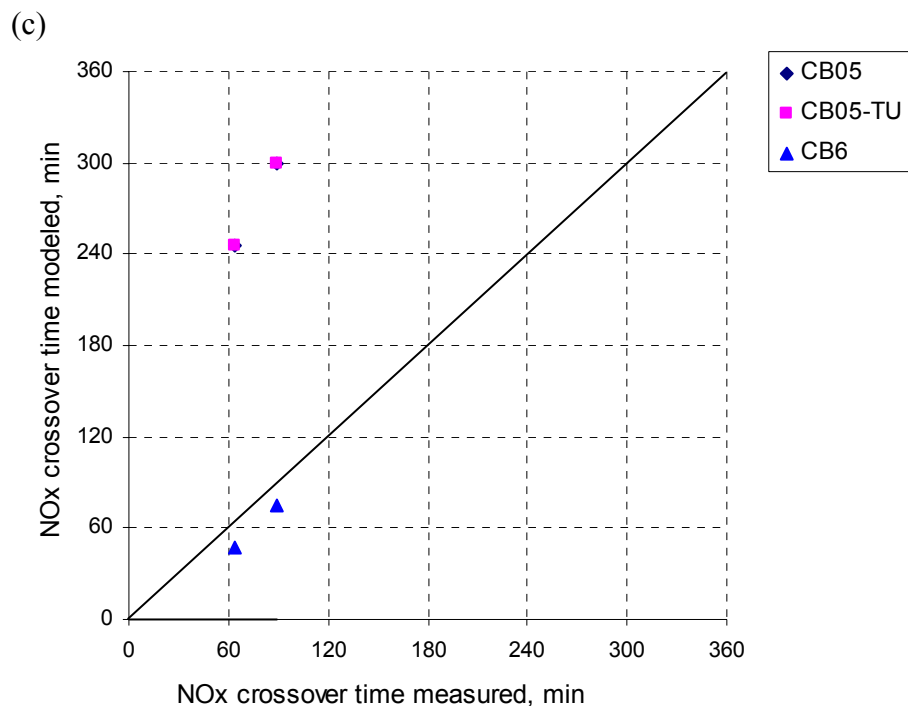


Figure 3-20. Mechanism performance against 2 BENZ - NO_x experiments: (a) Max(O₃), (b) Max(D(O₃-NO)), (c) NO_x crossover time.
Note: BENZ is benzene.

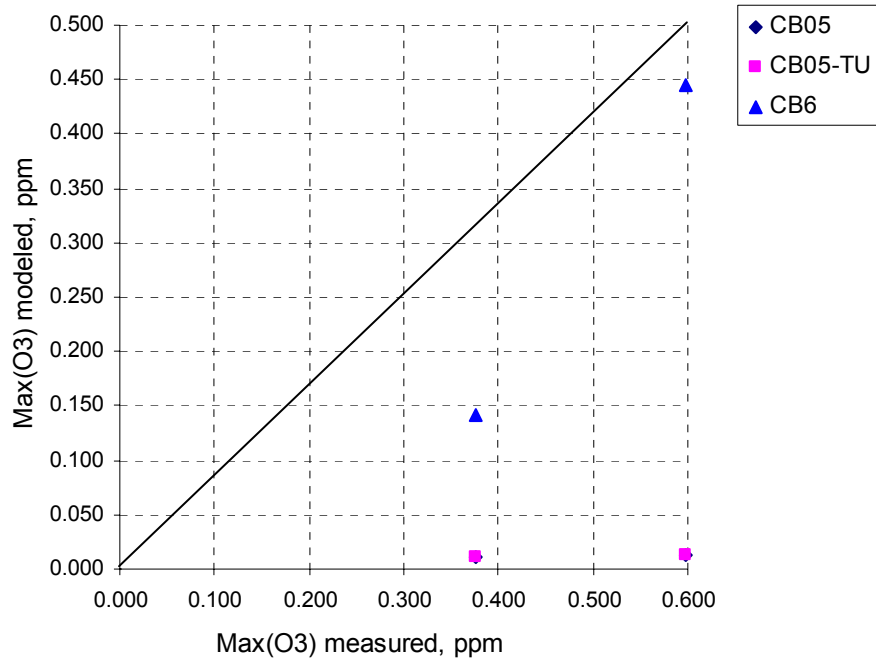
Table 3-22. Summary of model errors for 2 BENZ - NO_x experiments.^a

	Max(O ₃) [%]			Max(D(O ₃ -NO) [%])			NO _x crossover time [min]		
	CB05	CB05-TU	CB6	CB05	CB05-TU	CB6	CB05	CB05-TU	CB6
Average	-98	-98	-10	-85	-85	-6	196	196	-15
Std. dev.	0	0	2	2	2	1	20	20	2

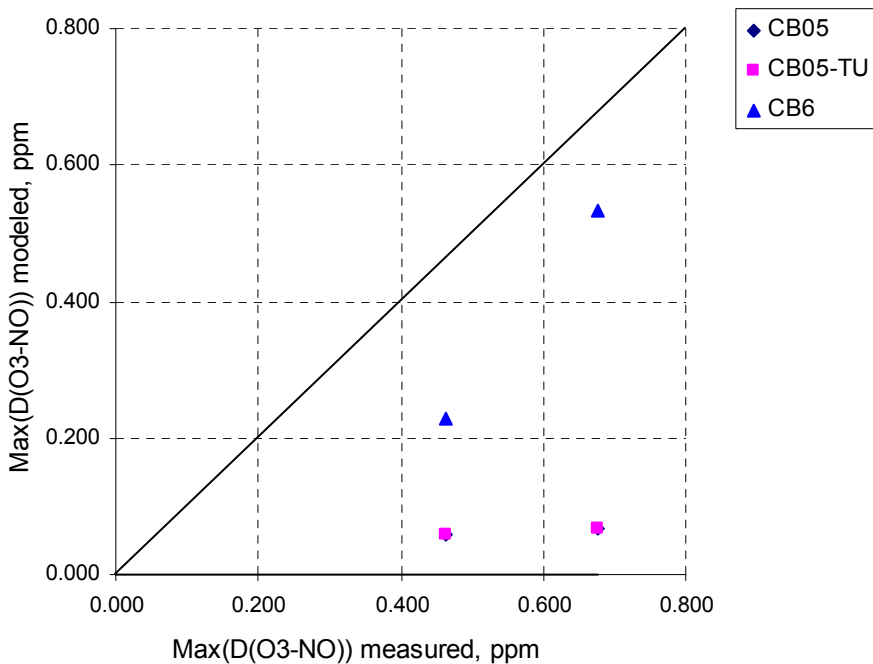
^aBENZ is "benzene".

3.3.21. ETHY: 2 experiments for ethyne (acetylene).

(a)



(b)



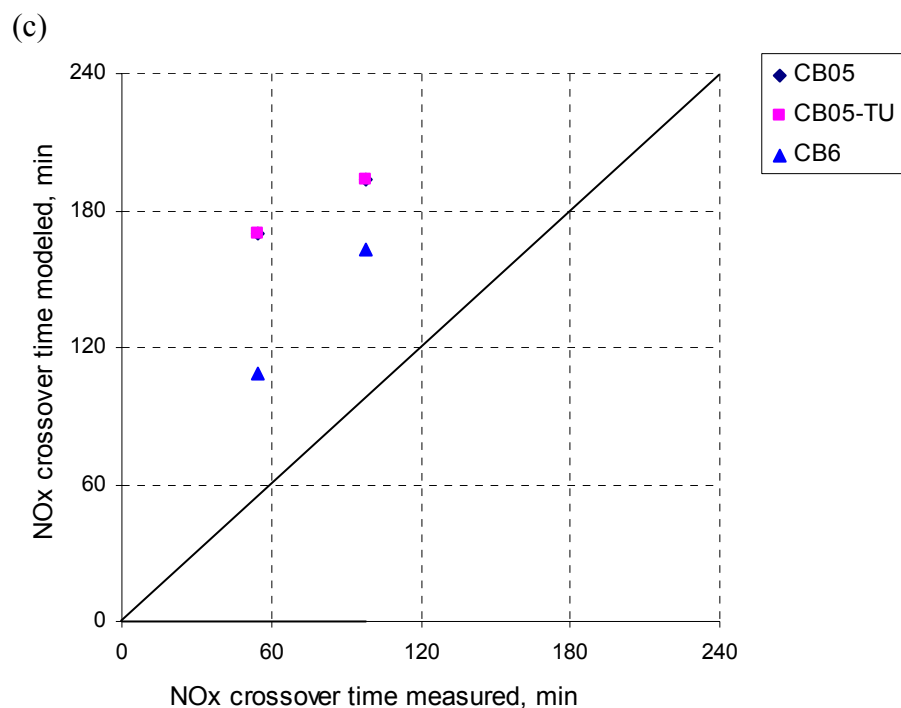


Figure 3-21. Mechanism performance against 2 ETHY - NO_x experiments: (a) Max(O₃), (b) Max(D(O₃-NO)), (c) NO_x crossover time.
Note: ETHY is ethyne (acetylene).

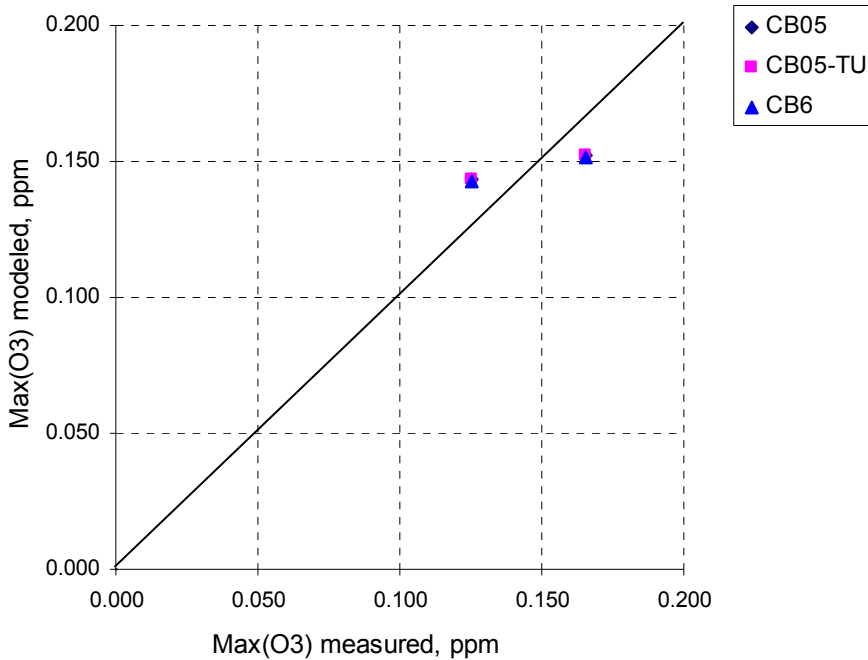
Table 3-23. Summary of model errors for 2 ETHY - NO_x experiments.^a

	Max(O ₃) [%]			Max(D(O ₃ -NO) [%])			NO _x crossover time [min]		
	CB05	CB05-TU	CB6	CB05	CB05-TU	CB6	CB05	CB05-TU	CB6
Average	-97	-97	-44	-89	-89	-36	106	106	60
Std. dev.	1	1	26	2	2	21	14	14	8

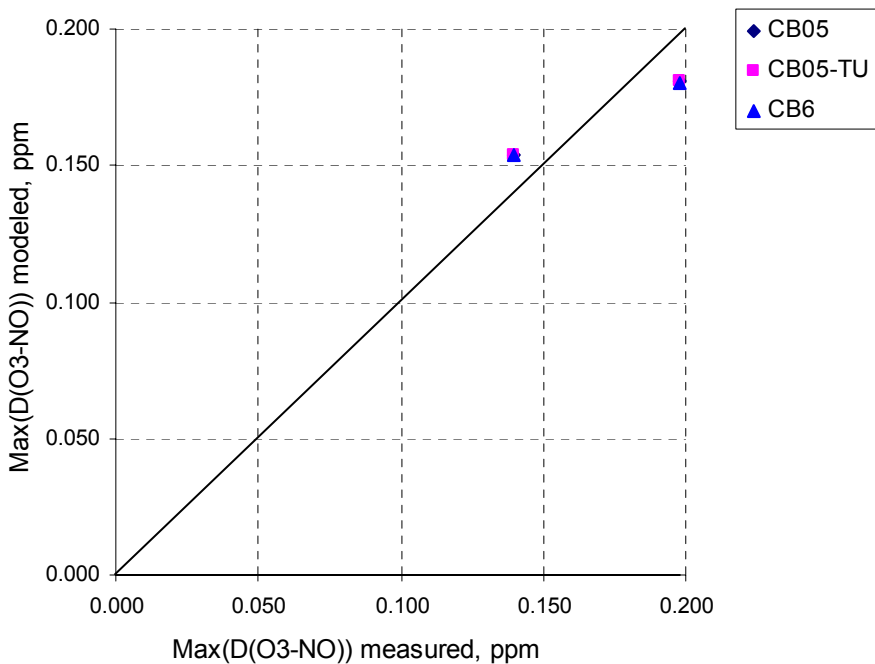
^aETHY is ethyne (acetylene).

3.3.22. Surrogate mixtures: 145 experiments in total.**3.3.22a. Incomplete surrogate mixtures excluding TOL, XYL and FORM (Surg-NA):** 2 experiments.

(a)



(b)



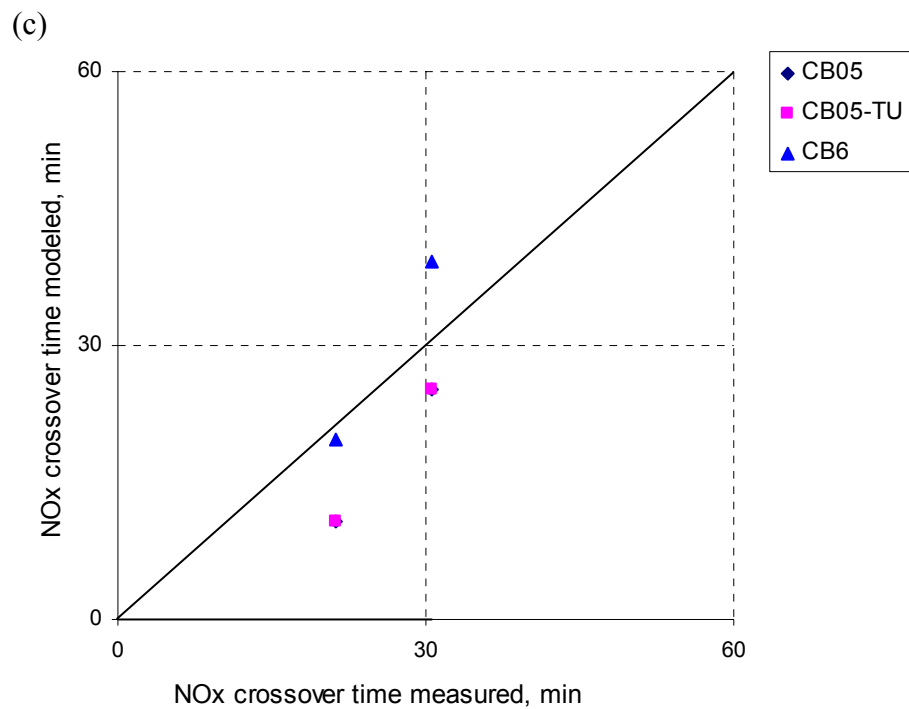


Figure 3-22. Mechanism performance against 2 Surg-NA type VOC mixture - NOx experiments: (a) Max(O₃), (b) Max(D(O₃-NO)), (c) NOx crossover time.

Note: Surg-NA type mixtures are incomplete surrogate mixtures excluding TOL, XYL and FORM.

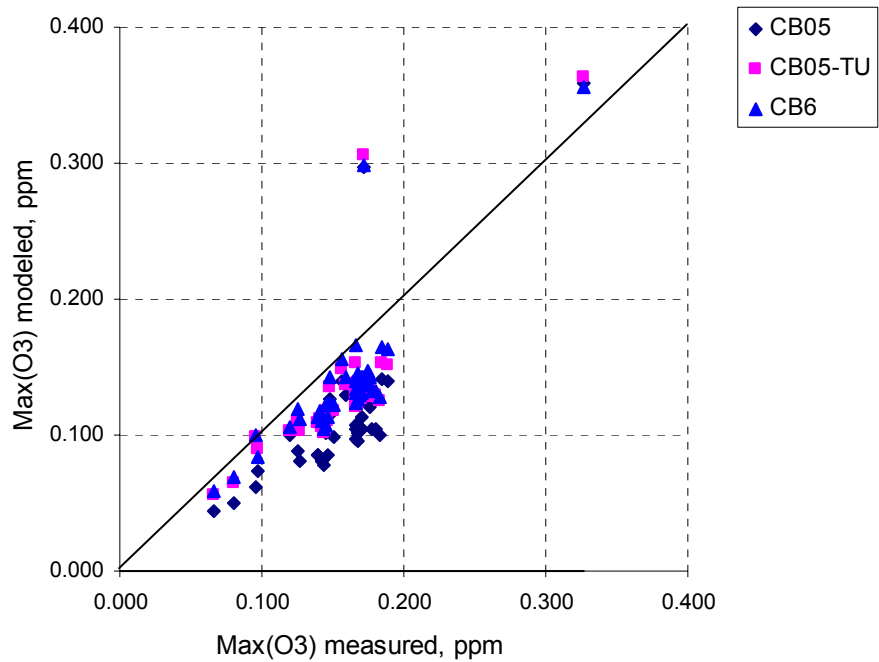
Table 3-24. Summary of model errors for 2 Surg-NA type VOC mixture - NOx experiments.^a

	Max(O ₃) [%]			Max(D(O ₃ -NO) [%])			NOx crossover time [min]		
	CB05	CB05-TU	CB6	CB05	CB05-TU	CB6	CB05	CB05-TU	CB6
Average	3	3	3	1	1	1	-8	-8	4
Std. dev.	16	16	16	13	13	13	4	4	7

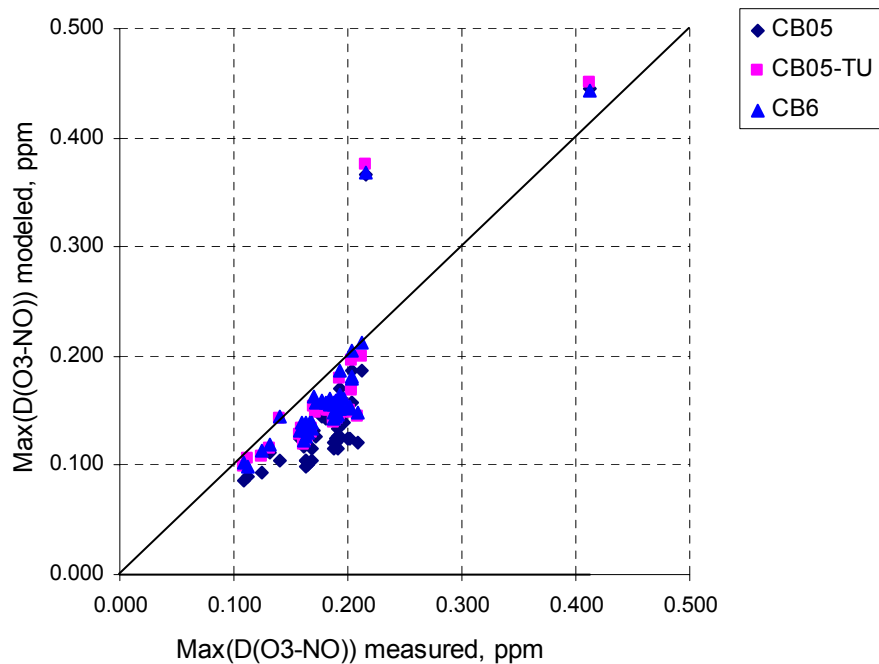
^aSurg-NA: incomplete surrogate mixtures without TOL, XYL and FORM. For details, refer to Table 2-2.

3.3.22b. Incomplete surrogate mixtures including either TOL or XYL: 57 experiments.

(a)



(b)



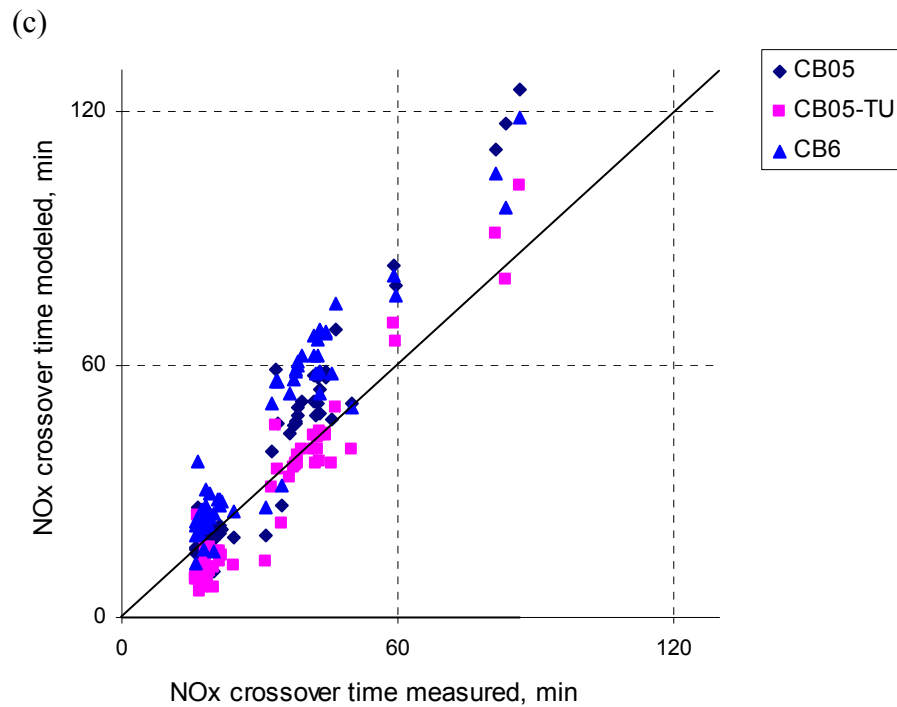


Figure 3-23. Mechanism performance against 57 incomplete surrogate VOC mixture - NOx experiments: (a) Max(O₃), (b) Max(D(O₃-NO)), (c) NOx crossover time.
Note: incomplete surrogate mixtures including either TOL or XYL (refer to Table 3-5 for details).

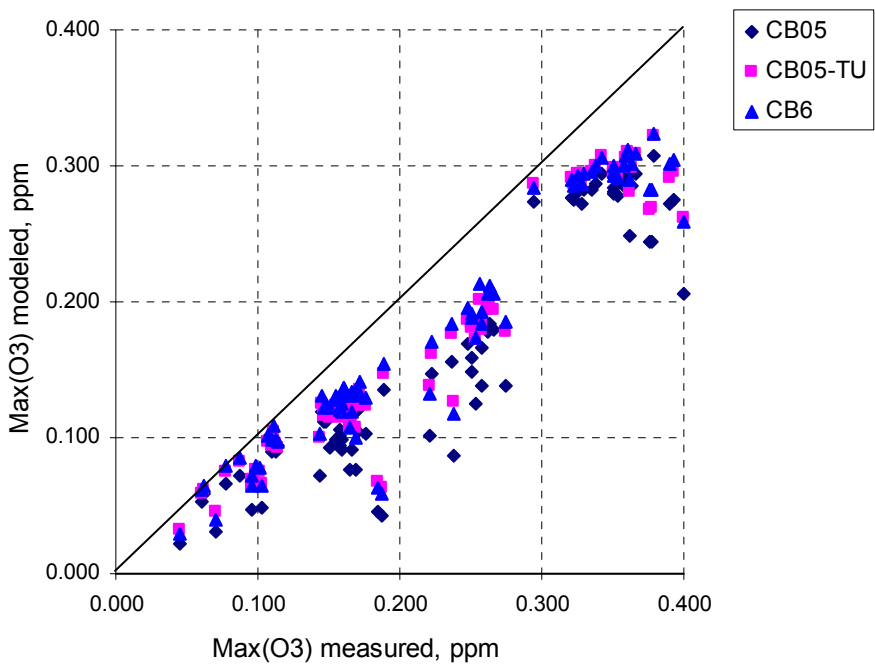
Table 3-25. Summary of model errors for 57 incomplete surrogate VOC mixture - NOx experiments.^a

	Max(O ₃) [%]			Max(D(O ₃ -NO) [%])			NOx crossover time [min]		
	CB05	CB05-TU	CB6	CB05	CB05-TU	CB6	CB05	CB05-TU	CB6
Average	-28	-18	-15	-25	-17	-14	6	-4	12
Std. dev.	17	15	14	16	14	14	11	7	10

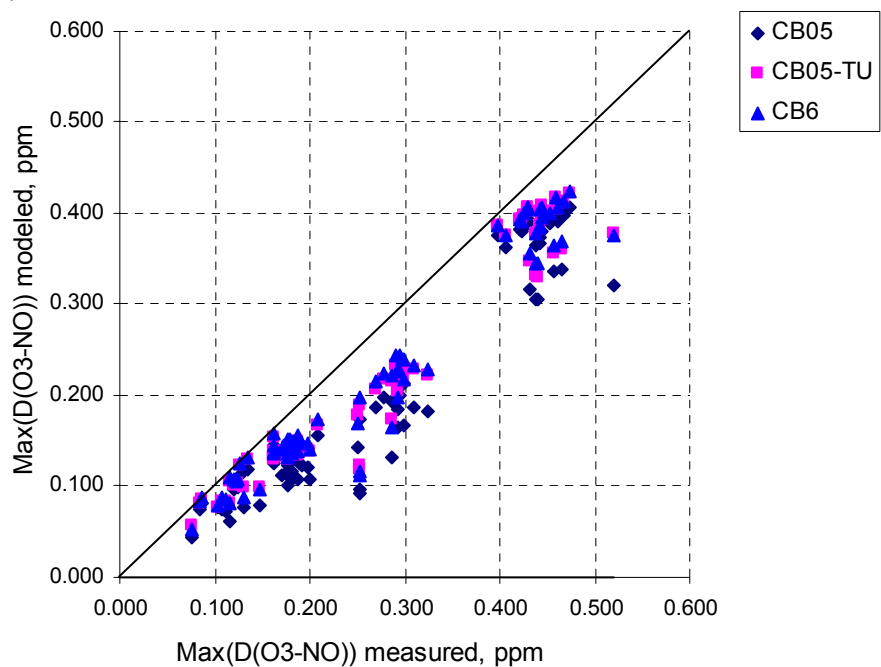
^aIncomplete surrogate mixtures contain at least one of TOL and XYL (refer to Table 3-2 for details).

3.3.22c. Full surrogate mixtures containing ETH, OLE (propene), IOLE (t-2-butene), 2 alkanes (n-butane and n-hexane in most cases), TOL (toluene), XYL (m-xylene) and FORM.

(a)



(b)



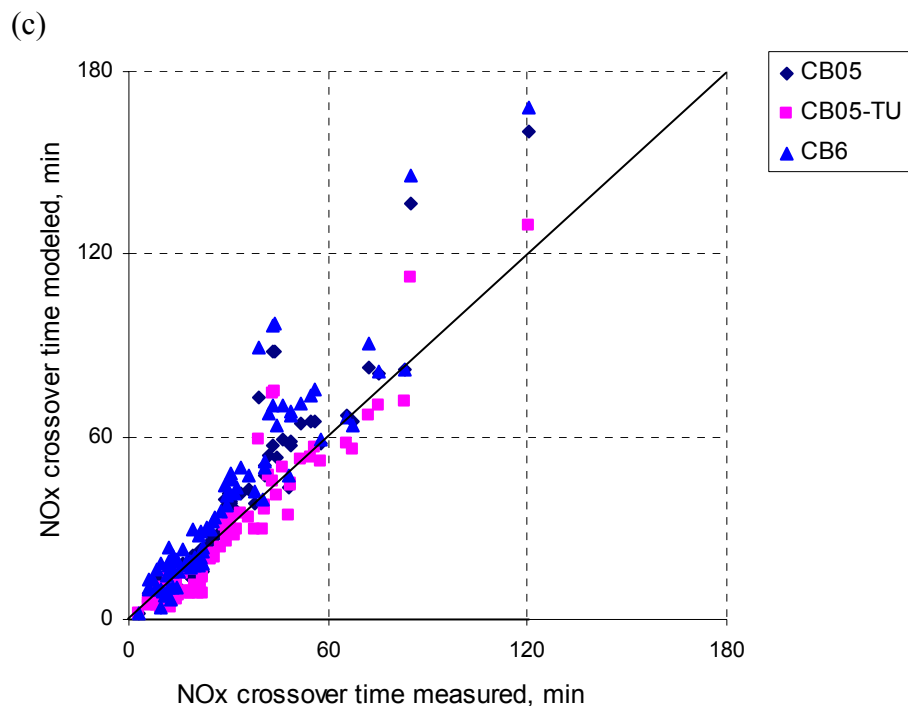


Figure 3-24. Mechanism performance against 81 full surrogate VOC mixture - NO_x experiments: (a) Max(O₃), (b) Max(D(O₃-NO)), (c) NO_x crossover time.

Note: full surrogate mixtures contain ETH, OLE (propene), IOLE (t-2-butene), 2 alkanes (n-butane and n-hexane in most cases), TOL (toluene), XYL (m-xylene) and FORM (refer to Table 3-5 for details).

Table 3-26. Summary of model errors for 81 full surrogate VOCs - NO_x experiments.^a

	Max(O ₃) [%]			Max(D(O ₃ -NO) [%])			NO _x crossover time [min]		
	CB05	CB05-TU	CB6	CB05	CB05-TU	CB6	CB05	CB05-TU	CB6
Average	-31	-23	-21	-27	-20	-18	4	-3	9
Std. dev.	15	11	12	13	10	10	11	8	13

^aFull surrogate: Surrogate mixtures containing ETH, OLE (propene), IOLE (t-2-butene), 2 alkanes (n-butane and n-hexane in most cases), TOL (toluene), XYL (m-xylene) and FORM. For details, refer to Table 3-2.

3.4. SUMMARY

The performance of CB6 in simulating three performance metrics for 339 chamber experiments is summarized graphically in Figures 3-25, 3-26 and 3-27 for Max(O₃), Max(D(O₃-NO)) and the NOx crossover time, respectively and numerically in Table 3-27 for Max(O₃), Max(D(O₃-NO)) and the NOx crossover time. Overall, CB6 performed better than CB05 and CB05-TU.

Following some introductory remarks, this section summarizes mechanism performance for individual compounds beginning with CO and progressing through more complex molecules and then closes with a summary for surrogate mixtures.

The format of Figures 3-25 to 3-27 shows average model errors displayed as bars for CB05, CB05-TU and CB6. Model errors were calculated as $\{(\text{modeled} - \text{experimental})/\text{experimental}\}$ expressed as percentages for Max(O₃) and Max(D(O₃-NO)) but minutes for the NOx crossover time. The composition of surrogate mixtures are as follows: Surg-NA mixtures are incomplete surrogate mixtures without toluene, xylene or formaldehyde; Surg-Inc (Surg-incomplete) mixtures are incomplete surrogate mixtures containing at least one of toluene or xylene; Surg-Full mixtures are full surrogate mixtures that contain at least 8 different VOCs (n-butane, n-octane, ethene, propene, trans-2-butene, toluene, m-xylene, formaldehyde) with NOx. The Surg-NA, Surg-Inc and Surg-Full experiments are Group 1, Group 2 and Group 3 in Table 3-3. Table 3-27 presents the average model errors shown in Figures 3-25 to 3-27 with associated standard deviations.

CB6 performed much better than CB05 or CB05-TU in simulating several species that were added to CB6 but represented by surrogates in CB05, i.e., ACET (acetone), KET (higher ketones), PRPA (propane), BENZ (benzene) and ETHY (ethyne). The evaluation for some compounds, i.e., MEOH (methanol), ETOH (ethanol), ETHA (ethane) and PRPA (propane), suffered from additional uncertainty because only blacklight/mixture experiments were available. Thus, model results are influenced by other compounds within the mixtures (e.g., ethene and m-xylene) and uncertainties in the photolysis data due to use of blacklights as the chamber light source.

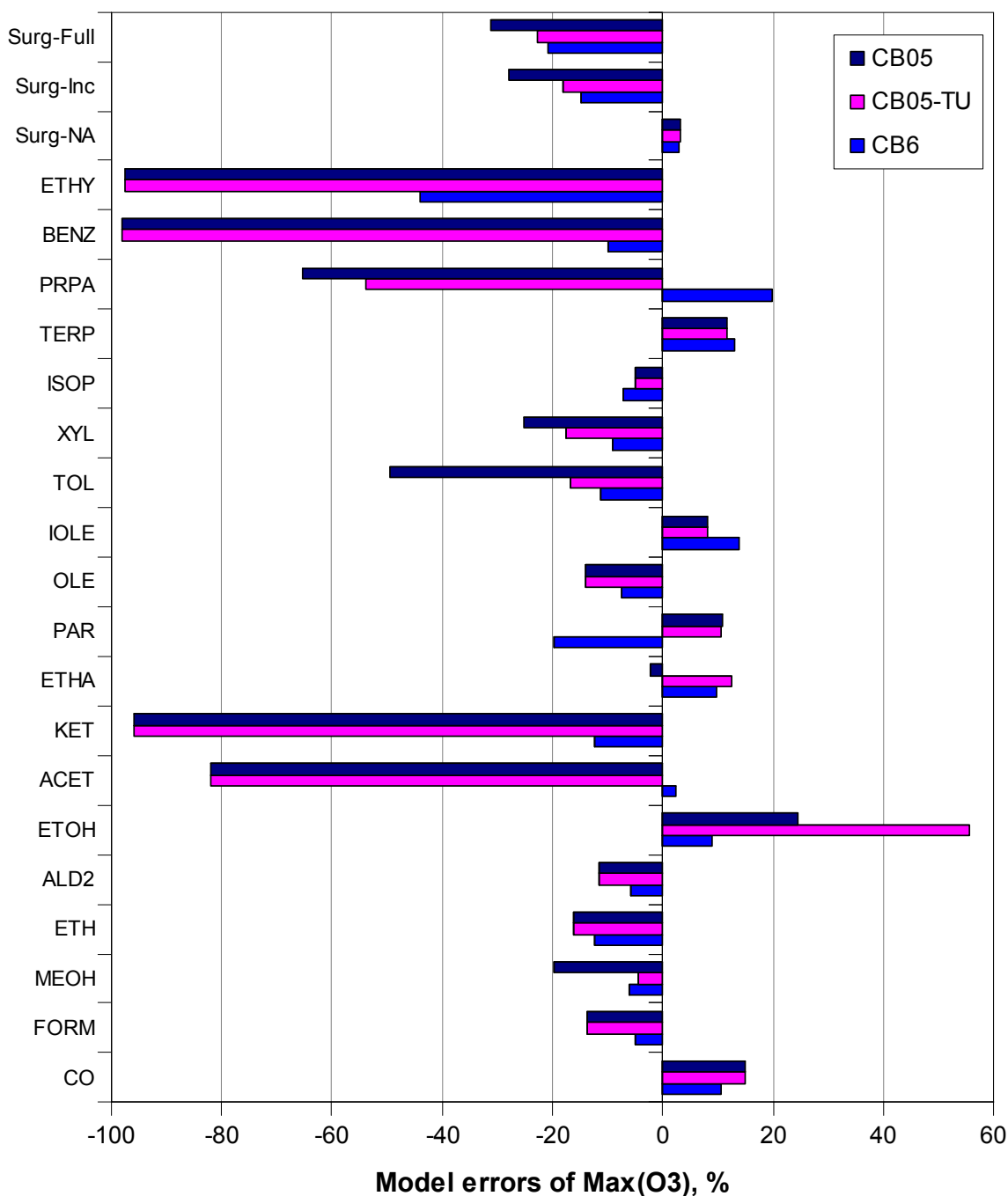


Figure 3-25. Graphical summary of mechanism performance in simulating Max(O₃) against 194 single test compound (or special VOC mixture) - NO_x experiments and 145 surrogate VOC mixture - NO_x experiments.

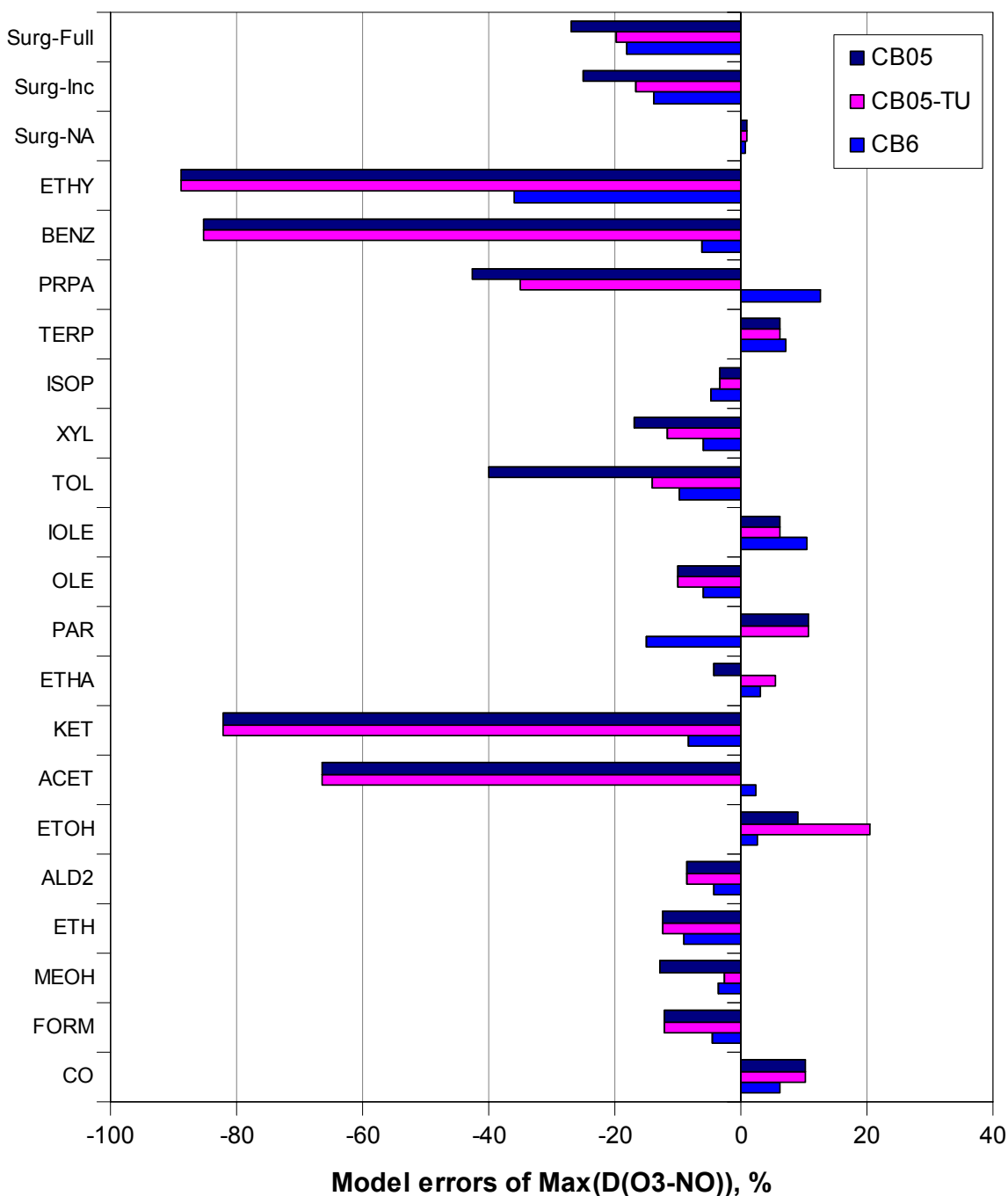


Figure 3-26. Graphical summary of mechanism performance in simulating Max(D(O₃-NO)) against 194 single test compound (or special VOC mixture) - NO_x experiments and 145 surrogate VOC mixture - NO_x experiments.

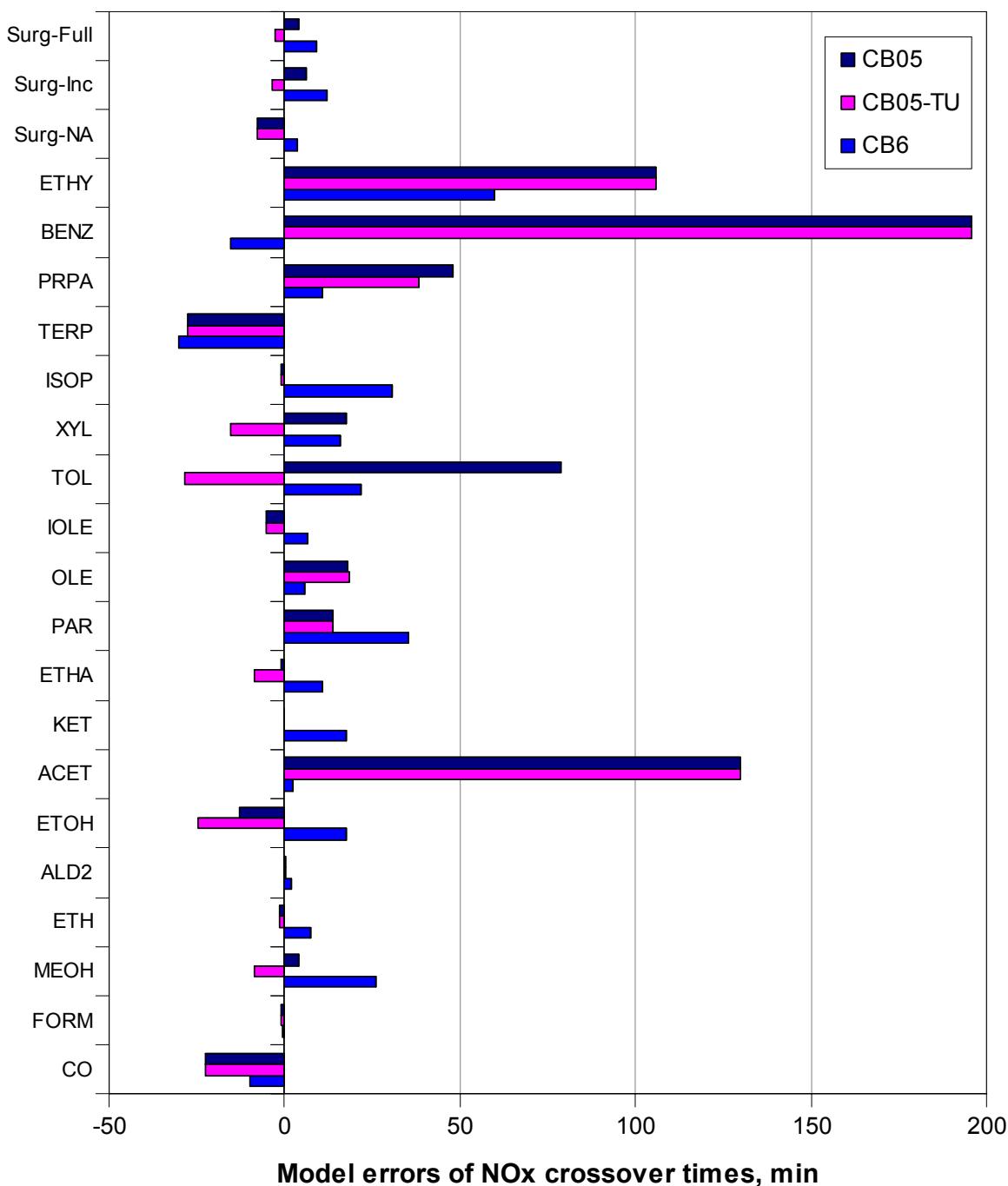


Figure 3-27. Graphical summary of mechanism performance in simulating NO_x crossover times against 194 single test compound (or special VOC mixture) - NO_x experiments and 145 surrogate VOC mixture - NO_x experiments.

Note: CB05 and CB05-TU did not show NO_x crossovers by hour of 6 for experiment CTC178A, one of the two experiments selected for testing KET chemistry. Thus, results for CB05 and CB05-TU are not shown for KET.

Table 3-27. Numerical summary of average model errors of Max(O₃), Max(D(O₃-NO)) and the NO_x crossover time.^a

CB6 species ^b	N ^c	Max(O ₃) [%]			Max(D(O ₃ -NO) [%]			NO _x crossover time [min]		
		CB05	CB05-TU	CB6	CB05	CB05-TU	CB6	CB05	CB05-TU	CB6
CO	33	15 (38)	15 (38)	11 (31)	10 (30)	10 (30)	6 (25)	-23 (27)	-23 (27)	-10 (23)
FORM	9	-14 (4)	-14 (5)	-5 (5)	-12 (5)	-12 (5)	-4 (4)	-1 (3)	-1 (3)	0 (3)
MEOH ^d	2	-20 (7)	-5 (3)	-6 (10)	-13 (4)	-3 (2)	-4 (6)	4 (2)	-9 (3)	26 (1)
ETH	11	-16 (12)	-16 (12)	-12 (16)	-12 (7)	-12 (7)	-9 (10)	-1 (16)	-1 (16)	8 (18)
ALD2	8	-12 (8)	-12 (8)	-6 (9)	-9 (5)	-9 (5)	-4 (6)	0 (7)	0 (7)	2 (6)
ETOH ^d	3	24 (8)	55 (13)	9 (14)	9 (3)	21 (4)	3 (5)	-13 (1)	-25 (2)	17 (4)
ACET	4	-82 (17)	-82 (17)	2 (8)	-66 (14)	-66 (14)	2 (7)	130 (41)	130 (41)	2 (4)
KET	2	-96 (3)	-96 (3)	-12 (14)	-82 (2)	-82 (2)	-8 (8)	^e	^e	18 (15)
ETHA ^d	5	-2 (27)	12 (33)	10 (42)	-4 (21)	5 (23)	3 (29)	-1 (5)	-9 (7)	11 (15)
PAR	5	11 (37)	11 (37)	-20 (37)	11 (30)	11 (30)	-15 (30)	14 (2)	14 (2)	35 (9)
OLE	48	-14 (17)	-14 (17)	-7 (16)	-10 (10)	-10 (10)	-6 (11)	18 (18)	18 (17)	6 (14)
IOLE	3	8 (6)	8 (6)	14 (6)	6 (5)	6 (5)	11 (5)	-5 (8)	-5 (8)	7 (10)
TOL	20	-49 (28)	-17 (16)	-11 (15)	-40 (26)	-14 (14)	-10 (12)	79 (63)	-29 (19)	22 (20)
XYL	27	-25 (14)	-17 (10)	-9 (12)	-17 (11)	-12 (8)	-6 (9)	18 (40)	-15 (36)	16 (39)
ISOP	6	-5 (19)	-5 (19)	-7 (23)	-3 (12)	-3 (12)	-5 (16)	-1 (6)	-1 (6)	31 (15)
TERP	2	12 (38)	12 (38)	13 (37)	6 (23)	6 (23)	7 (22)	-28 (75)	-28 (75)	-30 (74)
PRPA ^d	2	-65 (2)	-54 (2)	20 (24)	-43 (0)	-35 (0)	13 (16)	48 (6)	38 (6)	11 (7)
BENZ	2	-98 (0)	-98 (0)	-10 (2)	-85 (2)	-85 (2)	-6 (1)	196 (20)	196 (20)	-15 (2)
ETHY	2	-97 (1)	-97 (1)	-44 (26)	-89 (2)	-89 (2)	-36 (21)	106 (14)	106 (14)	60 (8)
Surg-NA	2	3 (16)	3 (16)	3 (16)	1 (13)	1 (13)	1 (13)	-8 (4)	-8 (4)	4 (7)
Surg-Inc	57	-28 (17)	-18 (15)	-15 (14)	-25 (16)	-17 (14)	-14 (14)	6 (11)	-4 (7)	12 (10)
Surg-Full	86	-31 (15)	-23 (11)	-21 (12)	-27 (13)	-20 (10)	-18 (10)	4 (11)	-3 (8)	9 (13)

^aStandard deviations are given in parentheses. For graphical representation of average model errors, refer to Figures 4-25 to 4-27.^bSurg-NA, Surg-Inc and Surg-Full at the end of this column are for Surrogate mixtures corresponding to Group 1, Group 2 and Group 3 in Table 4-3.^cThe total number of chamber experiments used for each CB6 species.^dOnly blacklight/mixture experiments were available for testing.^eCB05 and CB05-TU did not show NO_x crossovers by hour of 6 for experiment CTC178A, one of the two experiments selected for testing KET chemistry. Thus, results for CB05 and CB05-TU are not shown for KET.

Performance for chamber characterization experiments using CO (CO – NO_x experiments) is reasonably good (Figures 3-25 to 3-27, Table 3-27; refer to Section 3.3.1 for details). Due to lack of a significant internal radical source the chemical system of CO – NO_x is most sensitive to chamber radical sources which are difficult to characterize. Therefore, these CO experiments test the interaction between the inorganic reactions and the chamber-dependent radical source. The chamber mechanism developed for SAPRC-07 was used with CB6, and CB6 and SAPRC-07 showed similar performance in simulating CO – NO_x experiments (refer to Figure 3-2 and Table 3-4 in Section 3.2.3).

Performance for formaldehyde (FORM) is very good (Figures 3-25 to 3-27, Table 3-27; refer to Section 3.3.2 for details). These FORM - NO_x experiments test the interaction between radical production from formaldehyde photolysis and radical sinks in the inorganic chemistry.

Performance for ethene (ETH) is good when blacklight-used experiments are excluded (Figures 3-25 to 3-27, Table 3-27). These experiments are strongly influenced by formaldehyde and support the good performance found for formaldehyde. The degradation in performance with blacklights is not expected (because UV absorption cross-sections and quantum yields are well characterized for formaldehyde) and we have no clear explanation for the differences in performance: e.g., -13% ($\pm 17\%$) and +28% ($\pm 17\%$) bias in simulating Max(O₃) for non-blacklight experiments and blacklight experiments (refer to Section 3.3.5 for details).

Performance for acetaldehyde is very good (Refer to Figures 3-25 to 3-27 for ALD2 performance; for details, see Section 3.3.6). These experiments are influenced by PAN formation and good performance reveals no problem with the PAN chemistry of CB6.

Performance for methanol, ethanol, ethane and propane experiments shows no apparent problems but suffers uncertainties because blacklights were the chamber light sources and VOC - NO_x mixtures contained other VOC compounds (e.g., ethene and m-xylene) in addition to the main test compound. However, CB6 performs much better for ethanol (ETOH) and propane (PRPA) than CB05 and CB05-TU (Figures 3-25 and 3-27, and Table 3-27).

The ketone experiments (acetone and methyl ethyl ketone) show much better performance for CB6 than CB05 confirming that these mechanism updates are working and improve performance. Performance is better for acetone (ACET) than for higher ketones such as methyl ethyl ketone (MEK) (Refer to performance for ACET and KET in Figures 3-25 to 3-27 and Table 3-27; for details, see Sections 3.3.8 and 3.3.9).

The PAR experiments show fairly good performance for CB6 in simulating maximum ozone but a late bias in the NO_x crossover times (Table 3-27). For three experiments with n-butane, CB6 showed better performance in simulating Max(O₃) and Max(D(O₃-NO)) and worse performance in simulating NO_x crossover times than CB05 (Figure 3-12 and Table 3-14b). Test simulations with CB6 using the chamber mechanism for CB05 resulted in simulation results similar to those produced with CB05 demonstrating that alkane (PAR) simulations are sensitive to the chamber wall mechanism. This sensitivity results from the fact that alkane chemistry has only weak internal radical sources. Therefore, the current evaluation for PAR is not conclusive on determining whether the CB6 PAR chemistry performed worse than CB05. Further investigation is warranted to clearly understand why CB6 performance is degraded from CB05.

Performance is very good for the alkene species (OLE and IOLE) tested against their prototype species: propene and 2-butene (Figures 3-25 to 3-27, Table 3-27; for details, see Sections 3.3.13 and 3.3.14). These experiments rely upon the mechanisms for aldehydes (ALD2 and ALDX) and inorganic species (which perform well together in CB6) in addition to the alkenes. More experiments with larger alkenes (e.g., 1-butene, 1-pentene and 2-pentene) would be valuable to expand the alkene mechanism testing. We chose not to use any blacklight experiments for testing OLE and IOLE because of the unexplained performance differences for ethene mentioned above.

Performance for toluene is good for both peak ozone and crossover times. CB6 performs better than CB05_TU and much better than CB05 (Figures 3-25 to 3-27, Table 3-27; for details, see Section 3.3.15).

Performance for xylenes is good for peak ozone but the crossover times have much scatter (i.e., relatively large standard deviation) (Figures 3-25 to 3-27, Table 3-27; for details, see Section 3.3.16). Scattered performance for crossover times is to be expected because there is a wide range in $k(\text{OH})$ over the species represented by XYL and included in the chamber evaluation database: o-xylene, m-xylene, p-xylene, 1,2,3-trimethylbenzene, 1,2,4-trimethylbenzene and 1,3,5-trimethylbenzene. Consideration may be given to splitting XYL into two species to improve mechanism performance and may be warranted because xylenes and larger aromatics are important contributors to hydrocarbon reactivity and ozone formation in many polluted atmospheres.

Performance for isoprene is good for peak ozone but the crossover time tends to be late (Figures 3-25 to 3-27, Table 3-27; for details, see Section 3.3.17). Further study on causes of these delayed NO_x crossovers is suggested.

Performance for terpenes (TERP) is good for peak ozone but the crossover times have much scatter (Figures 3-25 to 3-27, Table 3-27; for details, see Section 3.3.18). The current TERP chemistry of CB6 performed better against α -pinene experiments than β -pinene experiments (see Section 3.3.18). Scattered performance for crossover times is to be expected because there is a wide range in $k(\text{OH})$ over the species represented by TERP: e.g., α -pinene, β -pinene, 3-carene, d-limonene and sabinene. The scattered performance may be acceptable for terpenes (in contrast to xylenes) because terpene emissions tend to occur in locations where ozone formation is limited by NO_x.

The benzene species added in CB6 (BENZ) appears to be working based on very limited evaluation (Figures 3-25 to 3-27, Table 3-27; for details, see Section 3.3.20).

The acetylene (ethyne) species added in CB6 (ETHY) resulted in better performance with CB6 than with CB05 (Figures 3-25 to 3-27, Table 3-27; for details, see Section 3.3.21). Uncertainties in the chemistry of glyoxal (GLY) seem to contribute to relatively poor performance for ETHY. Further studies on causes of underpredicted peak ozone and delayed NO_x crossovers are suggested.

Surrogate mixture experiments show some bias to low ozone production and late crossovers in complex mixtures (Figures 3-25 to 3-27, Table 3-27; for details, see Section 3.3.22). Additional study is needed to investigate whether performance is poorer than the sum of the parts. However, based on limited tests against surrogate mixture experiments where neither toluene nor xylene was injected, the aromatics chemistries seem to contribute the overall under-predictions of $\text{Max}(\text{O}_3)$ and $\text{Max}(\text{D}(\text{O}_3\text{-NO}))$ (compare results for Surg-NA and other surrogate types in Figures 3-25 to 3-27; for details, see Section 3.3.22). Further studies are warranted to investigate whether this performance deficit can be explained solely by low ozone production from the aromatic compounds or whether some interactions between the aromatics and other components of the mixture contribute. For this investigation, producing and analyzing experimental data on NO_x sinks (e.g., speciated measurements of NO_x oxidation products such as HNO₃ and PAN) in the chemical systems of toluene – NO_x, xylene – NO_x and surrogate VOC mixture – NO_x is recommended.

4. CAMx MODELING

The CB6 mechanism was implemented in the CAMx air quality model (ENVIRON, 2010) in order to test the mechanism and evaluated differences in modeled air quality compared to CB05. Results obtained using two chemistry solvers, LSODE and EBI, were compared to confirm that the mechanism was correctly implemented in CAMx. The LSODE solver is more accurate and easier to implement but too slow for everyday use. The EBI solver is efficient but implementation is more difficult. Results obtained using the EBI solver were similar to results using LSODE and CB6 was found to be working correctly with both solvers.

CAMx simulations were performed for two modeling domains, Los Angeles and Texas. The Los Angeles simulations are useful because the modeled ozone concentrations are sensitive to VOC emissions and therefore reveal differences in the tendency of VOCs to form O₃ under VOC-limited conditions (reactivity). In contrast, the Texas domain simulations cover the entire eastern US where O₃ formation is predominantly NO_x- limited outside of a few urban centers.

4.1 DATA FOR DEPOSITION CALCULATIONS

When chemical mechanisms are implemented in air quality models such as CAMx and CMAQ the model species in the chemical mechanism must be included in the dry- and wet-deposition calculations (ENVIRON, 2010). Data required for deposition calculations include Henry Constants (for gas-aqueous partitioning) and molecular weight (for molecular diffusivity). Data needed to calculate deposition for CB6 model species were compiled and are provided in Table 4-1. Several points are noted:

- Molecular weights shown in Table 4-1 are for representative molecules to be considered in deposition calculations which may differ from the assumptions for carbon balance in the mechanism. For example, PAR is a 1-carbon species but for purposes of deposition calculations PAR is modeled on butane.
- Henry constant data are from the compilation by Sander (<http://www.mpch-mainz.mpg.de/~sander/res/henry.html>) and, where the compilation reported several values, we favored recent data and experiments over computations.
- Where no temperature dependence is reported for the Henry Constant we assumed a default value of -4000 K.

Temperature dependent Henry Constants (H_T) are defined by the expression:

$$H_T = H_{298} \exp \left[A \left(\frac{1}{298} - \frac{1}{T} \right) \right]$$

where A is the temperature dependence factor.

Table 4-1. Data for use in deposition calculations.

CB6 Name	Description	Formula					M Wt	Henry Constant		Comments
		C	H	O	N	S		H ₂₉₈	T factor	
AACD	Acetic acid	2	4	2			60.0	5.50E+03	-6300	
ACET	Acetone	3	6	1			58.1	3.00E+01	-4600	
ALD2	Acetaldehyde	2	4	1			44.0	1.40E+01	-5600	
ALDX	Propionaldehyde and higher aldehydes	3	6	1			58.1	5.30E+00	-5600	
BENZ	Benzene	6	6				78.1	1.80E-01	-4000	
CAT1	Methyl-catechols	7	8	2			124.1	4.60E+03	-4000 (a)	pyrocatechol
CO	Carbon monoxide	1		1			28.0	9.90E-04	-1300	
CRES	Cresols	7	8	1			108.1	1.70E+03	-4000 (a)	average of cresol isomers
CRON	Nitro-cresols	7	7	3	1		153.1	4.60E+03	-4000 (a)	dinitro-o-cresol
CRPX	Nitro-cresol hydroperoxides	7	7	4	1		169.1	4.60E+03	-4000 (a)	dinitro-o-cresol
EPOX	Epoxide formed from ISPX reaction with OH	5	10	3			118.1	7.20E+00	-5800	methyl ethyl ketone
ETH	Ethene	2	4				28.0	4.80E-03	-4000 (a)	
ETHA	Ethane	2	6				30.1	2.00E-03	-4000 (a)	
ETHY	Ethyne	2	2				26.0	3.90E-02	-4000 (a)	
ETOH	Ethanol	2	6	1			46.1	2.00E+02	-4000 (a)	
FACD	Formic acid	1	2	2			46.0	5.40E+03	-5700	
FORM	Formaldehyde	1	2	1			30.0	3.20E+03	-6800	
GLY	Glyoxal	2	2	2			58.0	3.60E+05	-4000 (a)	
GLYD	Glycolaldehyde	2	4	2			60.0	3.60E+05	-4000 (a)	glyoxal
H2O2	Hydrogen peroxide		2	2			34.0	8.60E+04	-6500	
HNO3	Nitric acid		1	3	1		63.0	2.10E+05	-8700	
HONO	Nitrous acid		1	2	1		47.0	5.00E+01	-4900	
INTR	Organic nitrates from ISO2 reaction with NO	5	9	4	1		147.1	6.00E+03	-4000 (a)	2-nitrooxy-1-butanol
IOLE	Internal olefin carbon bond (R-C=C-R)	4	8				56.1	4.40E-03	-4000 (a)	cis-2-butene and trans-2-butene
ISOP	Isoprene	5	8				68.1	1.30E-02	-4000 (a)	
ISPD	Isoprene products (methacrolein, methyl vinyl ketone, etc.)	4	6	1			70.1	6.50E+00	-4000 (a)	methacrolein
ISPX	Hydroperoxides from ISO2 reaction with HO2	5	10	3			118.1	6.50E+00	-4000 (a)	methacrolein
KET	Ketone carbon bond (C=O)	4	8	1			72.1	7.20E+00	-5800	methyl ethyl ketone
MEOH	Methanol	1	4	1			32.0	2.20E+02	-4000 (a)	
MEPX	Methylhydroperoxide	1	4	2			48.0	3.10E+02	-5200	
MGLY	Methylglyoxal	3	4	2			72.0	3.20E+04	-4000 (a)	
N2O5	Dinitrogen pentoxide			5	2		108.0	1.00E+05	-4000 (a)	
NO	Nitric oxide			1	1		30.0	1.90E-03	-1400	
NO2	Nitrogen dioxide			1	2		44.0	1.20E-02	-2500	
NO3	Nitrate radical			3	1		62.0	1.80E+00	-4000 (a)	
NTR	Organic nitrates	4	9	3	1		119.1	6.50E-01	-4000 (a)	1-butyl nitrate and 2-butyl nitrate
O3	Ozone			3			48.0	8.90E-03	-2900	
OLE	Terminal olefin carbon bond (R-C=C)	3	6				42.1	4.80E-03	-4000 (a)	propene

CB6 Name	Description	Formula					M Wt	Henry Constant		Comments
		C	H	O	N	S		H ₂₉₈	T factor	
OPAN	Peroxyacyl nitrate (PAN compound) from OPO3	4	3	6	1		161.0	1.70E+00	-4000 (a)	peroxymethacryloyl nitrate
OPEN	Aromatic ring opening product (unsaturated aldehyde)	4	4	2			84.0	6.50E+00	-4000 (a)	methacrolein
PACD	Peroxyacetic and higher peroxydicarboxylic acids	2	4	3			76.0	8.40E+02	-5300	
PAN	Peroxyacetyl Nitrate	2	3	5	1		121.0	4.10E+00	-4000 (a)	
PANX	C3 and higher peroxyacyl nitrate	3	5	5	1		135.0	2.90E+00	-4000 (a)	peroxypropionyl nitrate
PAR	Paraffin carbon bond (C-C)	4	8				56.1	1.10E-03	-4000 (a)	butane
PNA	Peroxyntiric acid		1	4	1		79.0	2.10E+05	-8700	nitric acid
PRPA	Propane	3	8				44.1	1.40E-03	-4000 (a)	
ROOH	Higher organic peroxide	4	9	2			89.1	3.40E+02	-6000	ethyl hydroperoxide
SO2	Sulfur dioxide			2		1	64.0	1.30E+00	-1800	
SULF	Sulfuric acid (gaseous)		2	4		1	98.0	1.00E+10	0	high solubility, low volatility
TERP	Monoterpenes	10	16				136.2	4.90E-02	-4000 (a)	pinene
TOL	Toluene and other monoalkyl aromatics	7	8				92.1	1.60E-01	-4000 (a)	
XOPN	Aromatic ring opening product (unsaturated ketone)	6	8	2			112.1	7.20E+00	-5800	methyl ethyl ketone
XYL	Xylene and other polyalkyl aromatics	8	10				106.2	1.57E-01	-5633	average of xylene isomers

Table notes:

H₂₉₈ is the Henry Constant at 298 K and T factor is the temperature dependence (K)

Henry constant data from <http://www.mpch-mainz.mpg.de/~sander/res/henry.html>

Henry constants are for the exact compound unless noted otherwise under comments

(a) Default temperature dependence of 4000 K

4.2 EMISSION INVENTORY PREPARATION

Emission inventory preparation for VOCs includes a step called chemical speciation where the VOC species included in the inventory are assigned to the model species included in the chemical mechanism. There are 5 new VOC model species in CB6 that should be considered in emissions processing:

- PRPA representing propane (1.5 PAR + 1.5 NR in CB05)
- BENZ representing benzene (1 PAR + 5 NR in CB05)
- ETHY representing ethyne (ALDX in CB05)
- ACET representing acetone (3 PAR in CB05)
- KET representing ketone groups (PAR in CB05)

The usage of the KET species is illustrated by methylethylketone (CH₃C(O)CH₂CH₃) which is represented as 3 PAR + KET in CB6 and 4 PAR in CB05.

Other new VOC species in CB6 such as glyoxal (GLY) and glycolaldehyde (GLYD) have negligible emissions and need not be added to emission inventories. Continue to use surrogate representations for any glyoxal and glycolaldehyde emissions.

CB6 is backward compatible with CB05 and CB4 and can be used with emission inventories (or other model inputs such as boundary conditions) that were prepared for CB05 or CB4. However, updating model inputs to CB6 is preferable to take full advantage of mechanism improvements.

4.3 LOS ANGELES MODELING

The Los Angeles (LA) modeling episode is for August 3–7, 1997 from the Southern California Ozone Study (SCOS). The modeling domain covered 65 by 40, 5-km grid cells as shown in Figure 4-1 (Yarwood et al., 2003 and 2008). CAMx was configured with 10 layers extending between a surface layer of 60 m and a model top at 4 km. Meteorological input data for CAMx were developed using MM5 with data assimilation of SCOS observation data (i.e., radar wind profiler upper-air data and surface site data) and analysis fields from the Eta Data Analysis System of the National Centers for Environmental Prediction (NCEP). The emission inventories were developed by the California Air Resources Board and speciated for the CB4 mechanism. The CB4 speciated inventory was used with the CB4, CB05 and CB6 mechanisms which makes model results directly comparable but doesn't take full advantage of new model species added in CB05 (IOLE, TERP and ALDX) and CB6 (ETHY, PRPA, ACET, KET and BENZ).

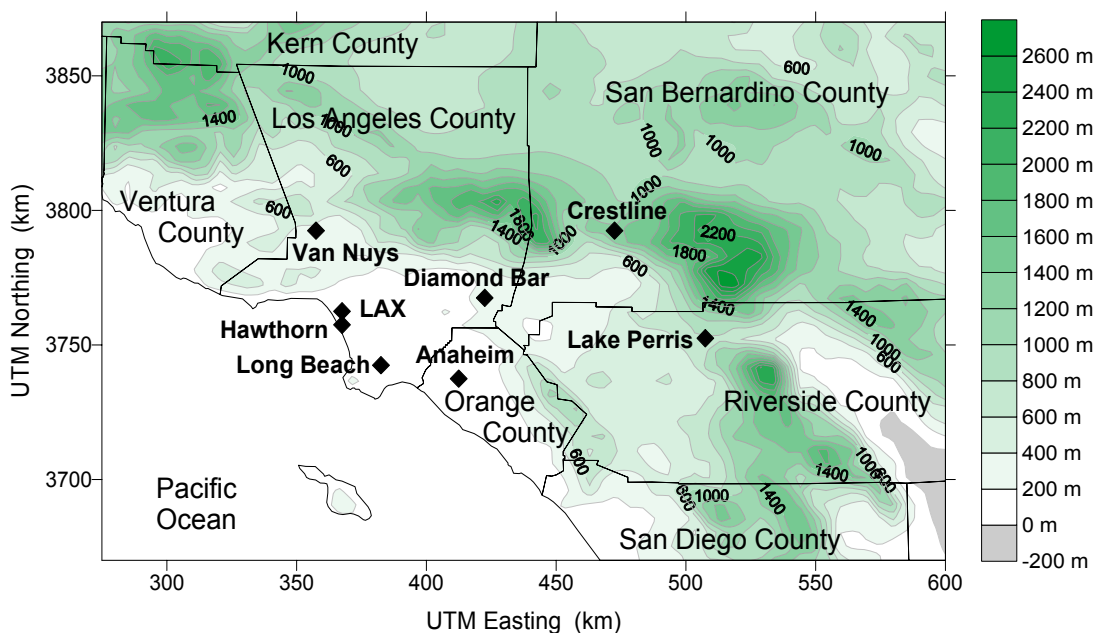


Figure 4-1. Modeling domain for the Los Angeles modeling scenario used to test Chemical Process Analysis.

Daily maximum 8-hr O₃ results are shown in Figure 4-2 for August 5, 1997, which was the episode day with the highest observed O₃. The meteorology on this day trapped O₃ formed from emissions in the Los Angeles basin within the surrounding mountains (Figure 4-1). CB6 increases O₃ compared to both CB05 and CB4. The peak 8-hr O₃ with CB6 (145 ppb) is 23% higher than with CB4 (118 ppb). There is greater O₃ increase from CB4 to CB6 (up to 36 ppb increase) than from CB4 to CB05 (up to 12 ppb increase).

The O₃ changes shown in Figure 4-2 would impact model performance as determined by comparisons between models predicted and observed O₃. However, previous modeling has demonstrated that chemistry and meteorology can exert opposite influences on ozone for Los Angeles (i.e., more ozone productive chemistry gives good model performance in combination with more dispersive meteorology, and vice-versa). It would be inappropriate to use model performance as the basis for conclusions upon the accuracy of ozone formation in particular mechanisms.

Ozone formation is VOC-limited in this 1997 model for Los Angeles (Yarwood et al., 2008) and the modeling results indicate that VOCs have a greater tendency to form O₃ in CB6 than CB05 or CB4. A reactivity analysis was performed to evaluate changes in O₃ reactivity for individual model VOC species.

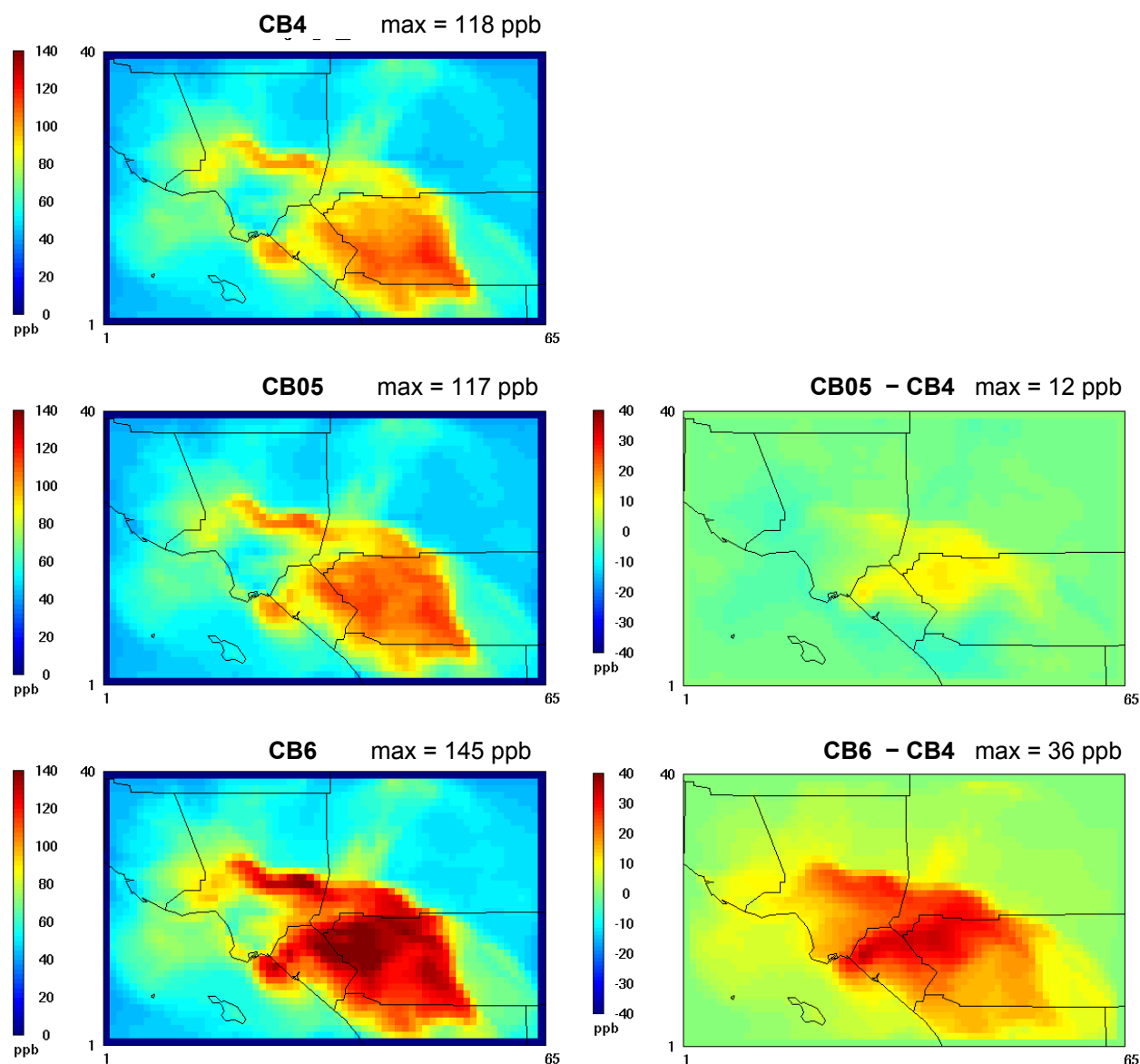


Figure 4-2. Daily maximum 8-hour ozone (ppb) for the Los Angeles domain on August 5, 1997.

4.2.1 VOC Reactivity Analysis

The decoupled direct method (DDM) implemented in CAMx (ENVIRON, 2010) can be used to evaluate the O₃ forming tendency (reactivity) of VOCs as described by Carter et al. (2003). Briefly, DDM is used to compute the sensitivity of O₃ to emitted species. First, sensitivity to emitted NO_x (dO₃/dNO_x) and anthropogenic VOC (dO₃/dVOC) is calculated to determine where and when modeled O₃ is more sensitive to VOC than NO_x. Grid cells where dO₃/dVOC > dO₃/dNO_x are classified as VOC-limited. Then, O₃ sensitivities are calculated to emissions of specific VOC model species (dO₃/dVOC_i) and evaluate for the VOC-limited grid cells. To prevent differences in the spatial/temporal distributions of VOC model species emissions from influencing the evaluation, the O₃ sensitivities (dO₃/dVOC_i) are calculated with respect to VOC_i emissions with the same spatial/temporal distribution as the total anthropogenic VOC emissions (Carter et al., 2003).

Results of the VOC reactivity analysis for CB6 are shown in Figure 4-3. The O₃ sensitivities for individual model species (dO₃/dVOC_i) are compared to ethane (dO₃/dETHA) for the VOC-limited grid cells at 3 pm on August 5, 1997. The O₃ sensitivities are well-correlated between model VOC species and regression analysis was used to characterize the reactivity for each model VOC compared to an ethane reactivity of 0.135 mole O₃/mole VOC (Table 4-2). The same calculations were repeated for CB05 in order to compare mechanisms.

Table 4-2. Comparison of CB05 and CB6 incremental reactivity factors (mole O₃/mole VOC).

CB6 Species	CB05	CB6	Change
ETHA	0.135 (a)	0.135 (a)	0%
PRPA	0.504 (b)	0.541	7%
PAR	0.336	0.509	51%
ACET	1.01 (b)	0.564	-44%
KET	0.336 (b)	1.39	314%
ETHY	7.22	0.487	-93%
ETH	4.26	4.95	16%
OLE	8.02	9.66	20%
IOL	13.7	16.0	17%
ISOP	12.1	12.7	5%
TERP	8.5	9.91	17%
BENZ	0.336 (b)	1.39	314%
TOL	2.15	7.39	244%
XYL	14.2	20.5	44%
FORM	4.32	4.87	13%
ALD2	4.68	5.80	24%
ALDX	7.22	8.35	16%
MEOH	0.354	0.480	36%
ETOH	1.11	1.53	38%

Notes

- (a) The reactivity of ethane (ETHA) was held constant at 0.135
- (b) PRPA, ACET, KET, ETHY and BENZ are not model species in CB05 and therefore are represented by surrogate species

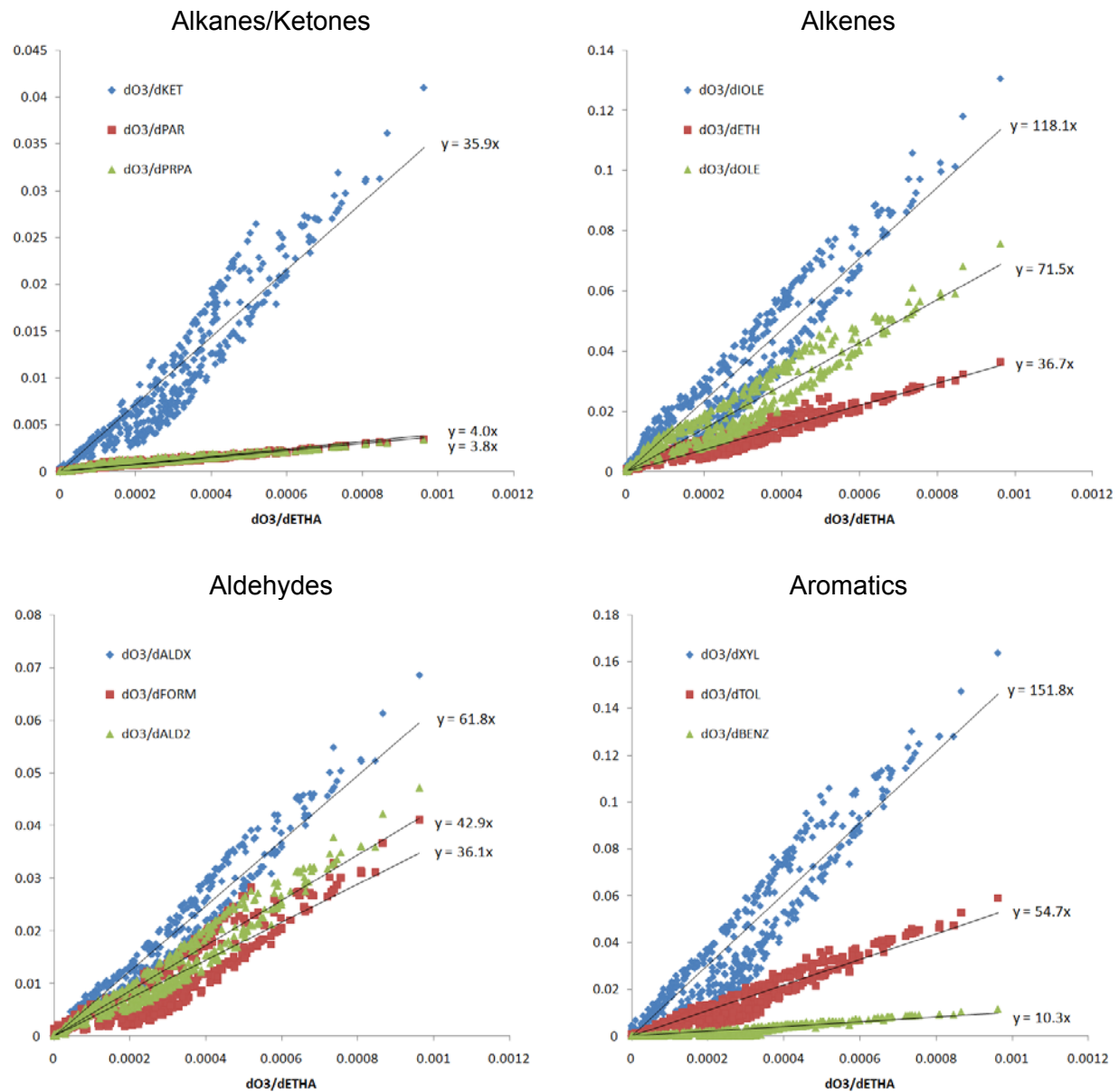


Figure 4-3. CB6 ozone sensitivities to VOC emissions ($dO_3/dVOC$) compared to $dO_3/dETHA$ for Los Angeles.

Comparing VOC reactivity factors for CB6 and CB05 (Table 4-2) shows increased reactivity for almost all species in CB6. Exceptions are ethyne (ETHY) and acetone (ACET) which are not CB05 model species and therefore are represented by surrogates in CB05. The reactivity of aldehyde species (FORM, ALD2, ALDX) increased by 13% to 24% and anthropogenic alkene (ETH, OLE, IOLE) reactivity increased by 16% to 20%; these increases are in part due to more rapid photolysis of formaldehyde to radical products in CB6 (27% increase, see section 2) and also reflect changes to the inorganic rate constants and the mechanism design.

The greatest increases in VOC reactivity from CB05 to CB6 are for aromatic hydrocarbons (BENZ, TOL, XYL). Benzene is not a model species in CB05 and so the 314% reactivity increase for benzene reflects a change from using a surrogate representation to an explicit model species. The reactivity increases for toluene (244%) and xylene (44%) reflect complete redesign of the aromatics mechanisms in CB6. Evaluating the aromatics mechanisms against chamber data (section 3) showed improved performance for CB6 compared to CB05.

The way that the model species PAR is used in CB6 is changed by the addition of new model species for propane (PRPA), acetone (ACET) and higher ketones (KET) all of which were represented by PAR in CB05. For ketones, CB6 has 44% lower reactivity for acetone but 314% greater reactivity for higher ketones. The reactivity of PAR is 51% higher in CB6 in part because PAR is a precursor to KET (which is more reactive in CB6) and FORM (which has more rapid photolysis in CB6). The reactivity of propane (PRPA) is almost the same in CB05 and CB6.

4.4 TEXAS MODELING FOR THE EASTERN US

CAMx modeling was performed for a June 3-15, 2006 ozone episode developed by the TCEQ for Houston/Galveston/Brazoria (HGB) 8-hour ozone State Implementation Plan (SIP). The modeling domain covers the eastern US using nested grids with 36-km, 12-km and 4-km resolution as shown in Figure 4-4. Meteorological input data for CAMx were developed using MM5 and emission inventories were developed by the TCEQ for the CB05 mechanism.

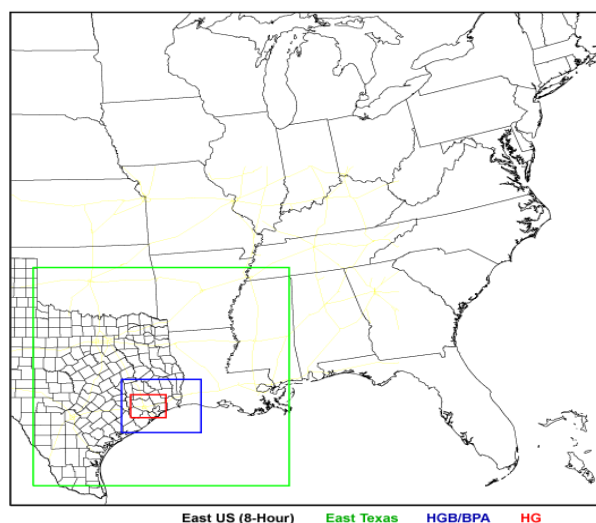


Figure 4-4. Modeling domain for HGB with 36-km (Eastern US), 12-km (East Texas) and 4-km (HGB/BPA) resolution nested grids.

The daily maximum 8-hr O₃ with CB6 and CB05 is compared in Figure 4-5 for the 36-km grid, averaged over the days June 3-15, 2006. There were three model spin-up days prior to the days shown in Figure 4-5. CB6 increased O₃ throughout the domain with a maximum increase of 11 ppb occurring over the Gulf of Mexico and widespread increases exceeding 5 ppb over land. The increases in O₃ from CB05 to CB6 are in the range 10% to 15% over wide areas. The same comparison of O₃ differences is shown in Figure 4-6 for the 12-km and 4-km domains. The increases in O₃ with CB6 are regional in character and do not show plumes of difference downwind of large urban areas such as Houston and Dallas. The pattern of O₃ increases with CB6 suggests that they mostly result from changes in the efficiency of O₃ production from NO_x rather than changes in VOC reactivity documented above for the VOC-limited Los Angeles domain. Additional study is needed to determine what factors cause higher O₃ concentrations with CB6 for the generally NO_x-limited conditions of the eastern US. Potential explanations are increased recycling of NO_x from organic nitrates (NTR and INTR in CB6) and decreased conversion of NO_x to nitric acid at night via reactions of N₂O₅.

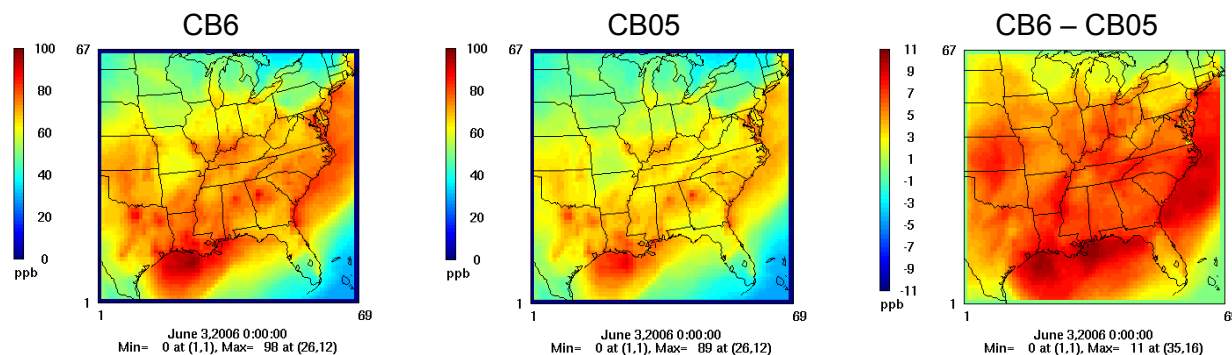


Figure 4-5. Average daily maximum 8-hr O₃ (ppb) for June 3-15, 2006, with CB6 and CB05

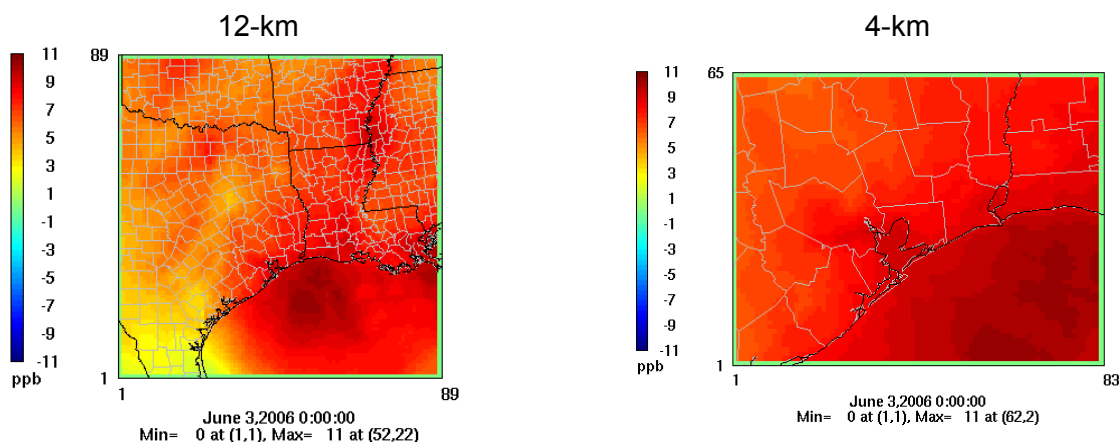


Figure 4-6. Difference (CB6 – CB05) in average daily maximum 8-hr O₃ (ppb) for June 3-15, 2006, for the 12-km and 4-km grids.

The OH concentration at 13:00-14:00 CST is compared in Figure 4-7, averaged over the days June 3-15, 2006. CB6 predicts substantially higher OH concentrations throughout the 36-km grid with the increases being in the range 25% to 50% over wide areas. Several factors contribute to higher OH concentrations with CB6 including changes to the isoprene mechanism to produce more OH (reactions 151, 154 and 163), more rapid photolysis of formaldehyde to HO₂ (which can be converted to OH) and OH formation from reactions between peroxyacyl radicals and HO₂ (reactions 57, 65 and 216).

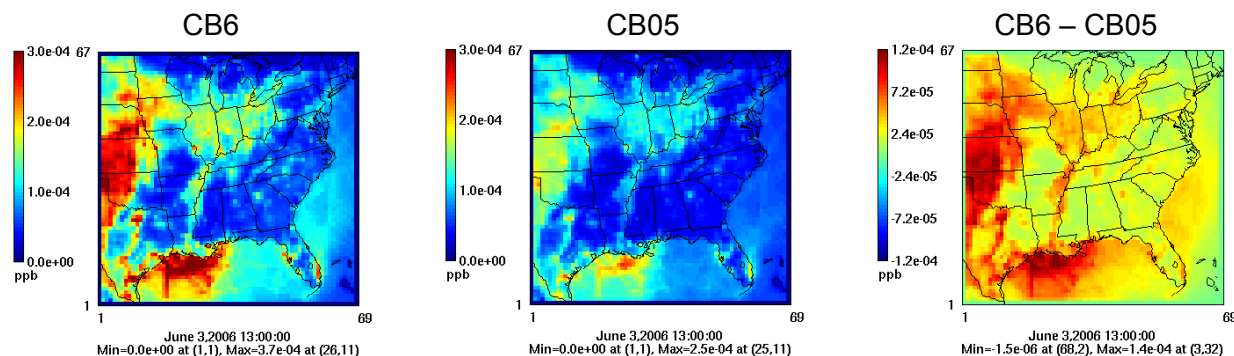


Figure 4-7. Average OH (ppb) at 13:00-14:00 CST for June 3-15, 2006, with CB6 and CB05.

The daily maximum 8-hr concentrations of isoprene with CB6 and CB05 are compared in Figure 4-8, averaged over the days June 3-15, 2006. Isoprene concentrations are lower with CB6 due to more rapid isoprene consumption by reaction with higher OH concentrations. An important product of isoprene reaction is ISPD and its concentrations are compared in Figure 4-9. ISPD concentrations are lower with CB6 partly because of more rapid removal by reaction with OH but also because ISPD yields are lower in CB6 than CB05. Isoprene forms additional products in CB6 (ISPX, EPOX, GLYD and GLY) that are not formed in CB05. Isoprene also is a precursor to formaldehyde (FORM) which is compared in Figure 4-10. FORM concentrations are lower with CB6 than CB05 due to more rapid removal by higher OH concentrations and more rapid photolysis.

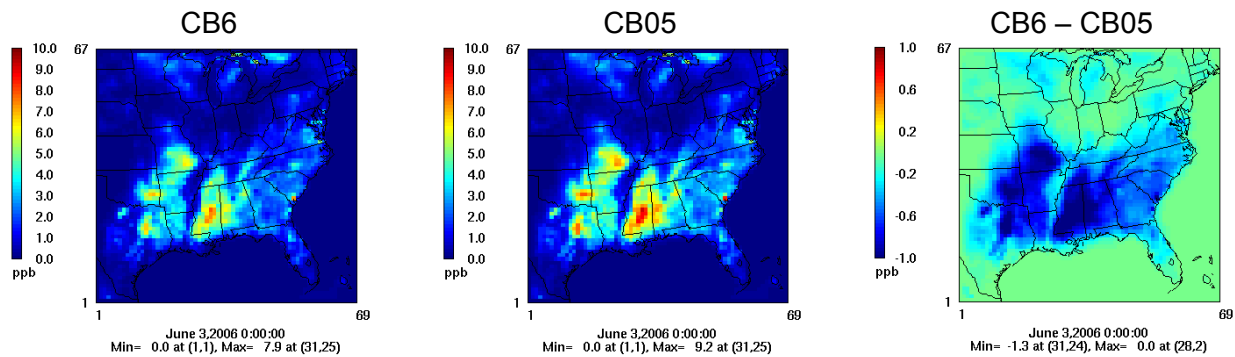


Figure 4-8. Average daily maximum 8-hr isoprene (ISOP; ppb) for June 3-15, 2006, with CB6 and CB05.

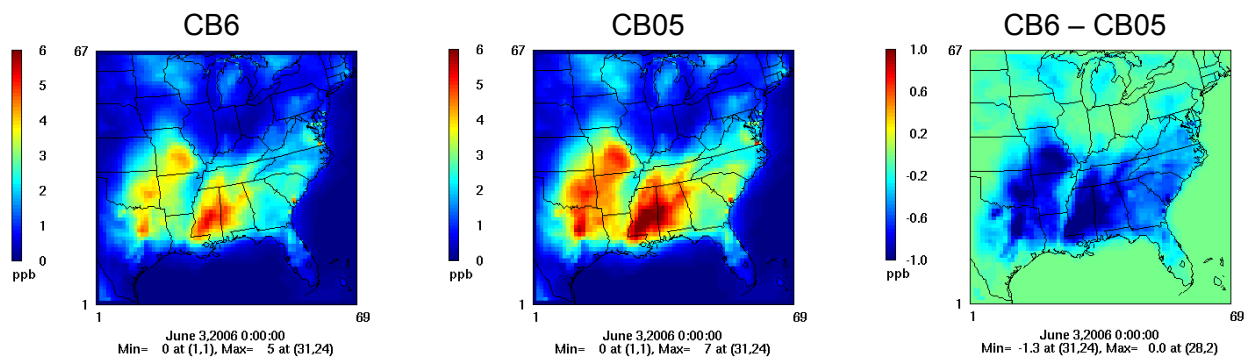


Figure 4-9. Average daily maximum 8-hr isoprene product (ISPD; ppb) for June 3-15, 2006, with CB6 and CB05.

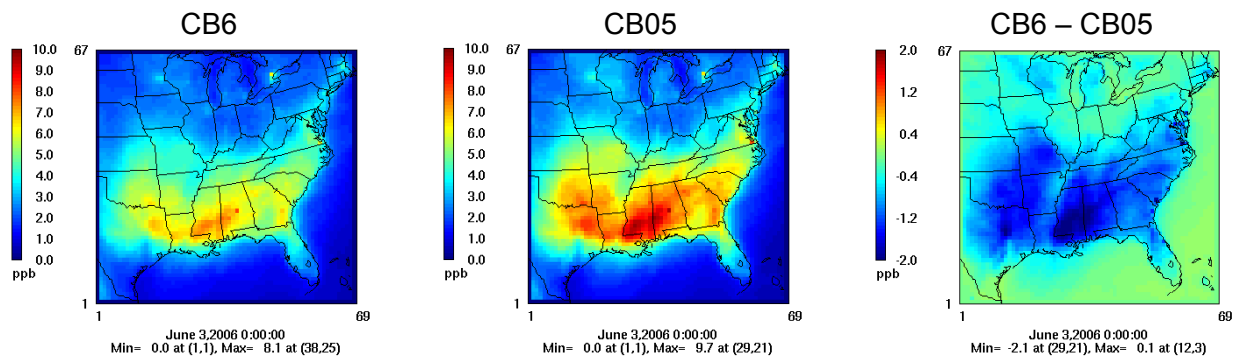


Figure 4-10. Average daily maximum 8-hr formaldehyde (FORM; ppb) for June 3-15, 2006, with CB6 and CB05.

Although PM was not modeled in the Texas domain simulation, hydrogen peroxide (H_2O_2) and nitric acid (HNO_3) formed by gas-phase chemistry are important to PM chemistry. H_2O_2 is important to sulfate formation because it oxidizes SO_2 to sulfate. Figure 4-11 shows that maximum H_2O_2 concentrations are lower with CB6 than CB05 which will cause slower sulfate formation with CB6 than CB05. Lower H_2O_2 with CB6 is attributed to a change in RO_2 radical chemistry (introduction of the species XO_2H) which more accurately represents H_2O_2 production under low- NO_x conditions. HNO_3 is the precursor to PM nitrate and Figure 4-12 shows both increases and decreases in maximum HNO_3 concentrations with CB6 compared to CB05. PM modeling would be required to evaluate how changing from CB05 to CB6 impacts PM nitrate formation.

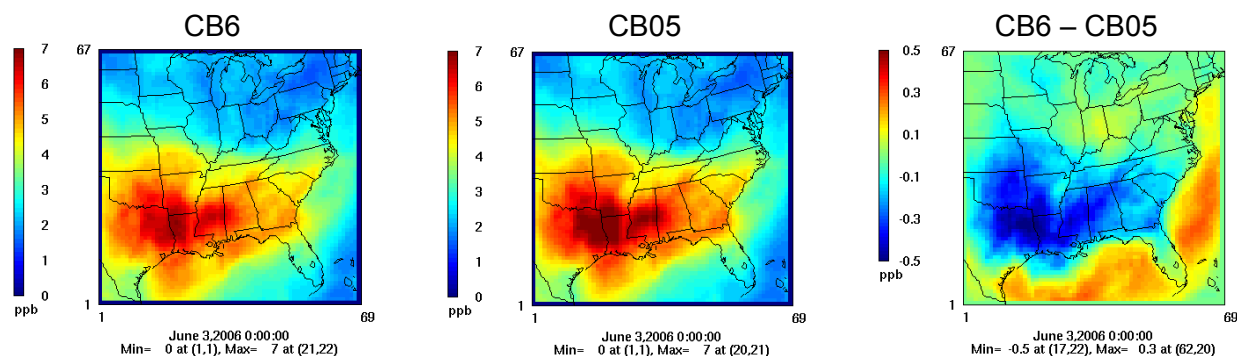


Figure 4-11. Average daily maximum 8-hr H_2O_2 (ppb) for June 3-15, 2006, with CB6 and CB05.

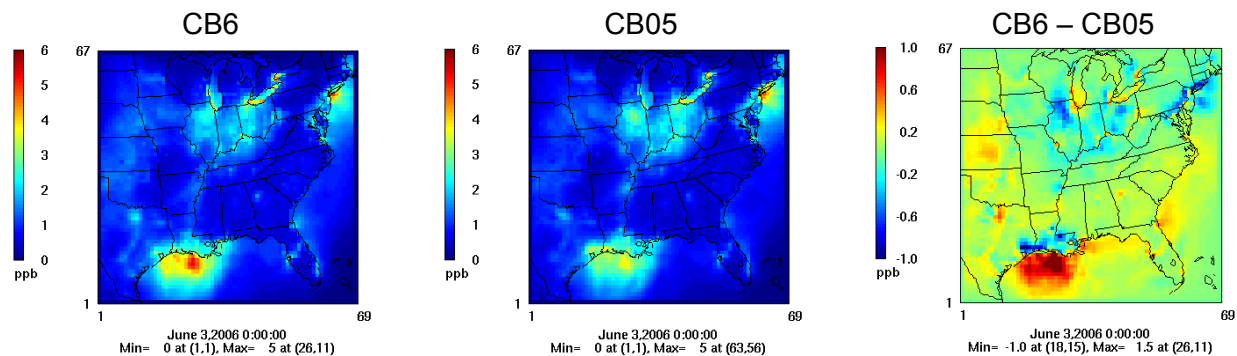


Figure 4-12. Average daily maximum 8-hr HNO_3 (ppb) for June 3-15, 2006, with CB6 and CB05.

5. SUMMARY AND CONCLUSIONS

A new version of the Carbon Bond (CB) chemical mechanism has been developed (CB6) as an update to the previous version (CB05; Yarwood et al., 2005). CB6 is a condensed chemical mechanism for tropospheric oxidants that is suitable for use in photochemical grid models such as CAMx (ENVIRON, 2010). CB6 is intended for modeling ozone, particulate matter (PM), acid deposition and air toxics. Compared to CB05, CB6 increases the number of model species from 51 to 77 and the number of reactions from 156 to 218.

Several organic compounds that are long-lived and relatively abundant, namely propane, acetone, benzene and ethyne (acetylene), are added explicitly in CB6 so as to improve oxidant formation from these compounds as they are oxidized slowly at the regional scale. Alpha-dicarbonyl compounds (glyoxal and analogues) which can form secondary organic aerosol (SOA) via aqueous-phase reactions (Carlton et al., 2007) are added in CB6 to improve support for SOA modeling. Precursors to alpha-dicarbonyls in CB6 are aromatics, alkenes and ethyne. CB6 includes several updates to peroxy radical chemistry that will improve formation of hydrogen peroxide (H_2O_2) and therefore sulfate aerosol formation. The gas-phase reaction of dinitrogen pentoxide (N_2O_5) with water vapor is slower in CB5 which will reduce nighttime formation of nitric acid although heterogeneous reactions on aerosol surfaces may dominate nitric acid formation at night (Brown et al., 2006). When CB6 is used in atmospheric models the heterogeneous reaction between N_2O_5 and water vapor should be accounted for.

The CB05 mechanism was completely reviewed and updated to develop CB6. The core inorganic chemistry mechanism for CB6 is based on evaluated data from the IUPAC tropospheric chemistry panel as of January, 2010 (Atkinson et al., 2010). IUPAC also is the primary source for photolysis data in CB6 with some data being from the 2006 NASA/JPL data evaluation (Sander et al., 2006) or other sources for photolysis of some organic compounds. There are changes to the organic chemistry for alkanes, alkenes, aromatics and oxygenates. The most extensive changes are for aromatics and isoprene. Chemistry updates for aromatics were based on the updated toluene mechanism (CB05-TU) developed by Whitten et al. (2009) extended to benzene and xylenes. The isoprene mechanism was revised based on several recently published studies.

CB6 was evaluated using data from environmental chamber studies where VOCs and NO_x were irradiated in enclosed chambers to form ozone. Experiments were selected by focusing, where possible, on experiments that used low initial NO_x (less than 100 ppb) and broad spectrum illumination rather than UV illumination by blacklights. A total of 339 experiments from several chambers at the University of California at Riverside and the Tennessee Valley Authority were used to evaluate CB6.

The performance of CB6 and CB05 in simulating chamber studies was comparable for alkanes, alkenes, alcohols and aldehydes with both CB6 and CB05 performing well and exhibiting 20% or less bias for maximum ozone. For species that were explicitly added in CB6 (ethyne, benzene and ketones) CB6 performed much better than CB05. For aromatics, CB6 improved upon CB05 by reducing under prediction bias in maximum ozone to about 10% for benzene, toluene and xylene. For isoprene, both CB05 and CB6 show little bias for maximum ozone (less than 5%) but CB6 tended to form ozone too slowly. Additional research is recommended to improve the isoprene mechanism in CB6. CB6 improved upon CB05 for simulating mixtures of VOCs. For mixtures without aromatics, both CB05 and CB6 showed minimal bias for maximum ozone. For mixtures including aromatics, both CB05 and CB6 under predicted maximum ozone but bias was reduced from about 30% for CB05 to about 20% for CB6. Additional research is needed to understand results for mixtures containing aromatics.

Impacts of CB6 on modeled air quality were evaluated using CAMx simulations for Los Angeles LA and Texas (eastern US) modeling domains. CB6 produced higher ozone than CB05 in both domains but for different reasons. In general, modeled ozone is more VOC-limited for the Los Angeles domain and more NO_x-limited for the Texas domain. For the Los Angeles domain, increased ozone with CB6 is primarily attributed to higher VOC reactivity for almost all model species. The greatest reactivity increases were for aromatics which is consistent with results of the CB6 mechanism evaluation against chamber data.

For the eastern US modeling domain daily maximum 8-hr ozone increased by about 10% to 15% over wide regions of the domain. The pattern of ozone increases with CB6 suggests that they mostly result from changes in the efficiency of ozone production from NO_x rather than changes in VOC reactivity as seen for the VOC-limited Los Angeles domain. Additional study is needed to determine what factors cause higher ozone concentrations with CB6 for the generally NO_x-limited conditions of the eastern US. Potential explanations are increased recycling of NO_x from organic nitrates (NTR and INTR in CB6) and decreased conversion of NO_x to nitric acid at night via reactions of N₂O₅.

Higher ozone concentrations with CB6 in the eastern US were accompanied by higher concentrations of OH radical (25% to 50% higher at mid-day over wide areas). Several factors contribute to higher OH concentrations with CB6 including changes to the isoprene mechanism to produce more OH, more rapid photolysis of formaldehyde and OH formation from reactions between peroxyacyl radicals and HO₂. Higher OH concentrations with CB6 resulted in lower concentrations of VOCs including isoprene and formaldehyde.

Although PM was not modeled in this study, model results for hydrogen peroxide (H₂O₂) and nitric acid (HNO₃) were evaluated. H₂O₂ concentrations are lower with CB6 than CB05 which will cause slower sulfate formation with CB6 than CB05. Lower H₂O₂ with CB6 is attributed to a change in RO₂ radical chemistry which more accurately represents H₂O₂ production under low-NO_x conditions. HNO₃ both increased and decreased with CB6 compared to CB05. PM modeling would be required to evaluate how changing from CB05 to CB6 impacts PM nitrate formation.

6. REFERENCES

- Archibald, A. T., Cooke, M. C., Utembe, S. R., Shallcross, D. E., Derwent, R. G., and Jenkin, M. E., 2010. Impacts of mechanistic changes on HOx formation and recycling in the oxidation of isoprene, *Atmos. Chem. Phys.*, 10, 8097-8118, doi:10.5194/acp-10-8097-2010.
- Atkinson, R.A., D.L. Baulch, R.A. Cox, J.N. Crowley, R.F. Hampson, R.G. Hynes, M.E. Jenkin, J.A. Kerr, M.J. Rossi, and J. Troe (2010). "Evaluated kinetic and photochemical data for atmospheric chemistry - IUPAC subcommittee on gas kinetic data evaluation for atmospheric chemistry." January 3, 2010 web version available at <http://www.iupac-kinetic.ch.cam.ac.uk/index.html>.
- Bertram, T.H., J.A. Thornton, 2009. Toward a general parameterization of N₂O₅ reactivity on aqueous particles: the competing effects of particle liquid water, nitrate and chloride *Atmos. Chem. Phys.*, 9, 8351–8363.
- Bloss, C., Wagner, V., Jenkin, M.E., Volkamer, R., Bloss, W.J., Lee, J.D., Heard, D.E., Wirtz, K., Martin-Reviejo, M., Rea, G., Wenger, J.C., Pilling, M.J., 2005. Development of a detailed chemical mechanism (MCMv3.1) for the atmospheric oxidation of aromatic hydrocarbons. *Atmospheric Chemistry and Physics* 5, 641–644.
- Brown, S. S., Ryerson, T. B., Wollny, A. G., Brock, C. A., Peltier, R., Sullivan, A. P., Weber, R. J., Dube, W. P., Trainer, M., Meagher, J. F., Fehsenfeld, F. C. and Ravishankara, A. R., 2006. Variability in Nocturnal Nitrogen Oxide Processing and Its Role in Regional Air Quality. *Science* 311, 67-70,
- Calvert, J.G., R. Atkinson, J.A. Kerr, S. Madronich, G.K. Moortgat, T.J. Wallington, G. Yarwood. 2000. The mechanisms of atmospheric oxidation of the alkenes. Oxford University Press.
- Calvert, J.G., R. Atkinson, K.H. Becker, J.H. Seinfeld, R.M. Kamens, T.J. Wallington, G. Yarwood. 2002. The mechanisms of atmospheric oxidation of the alkenes. Oxford University Press.
- Carlton, A.G., Turpin, B.J., Altieri, K.E., Seitzinger, S., Reff, A., Lim, H.-J., Ervens, B. 2007. Atmospheric oxalic acid and SOA production from glyoxal: Results of aqueous photooxidation experiments. *Atmospheric Environment* 41, 7588-7602.
- Carr, S., D. E. Heard, M. A. Blitz (2009). "Comment on: Atmospheric Hydroxyl Radical Production from Electronically Excited NO₂ and H₂O." *Science*, 324:336 doi: 10.1126/science.1166669
- Carter, W.P.L. 2010. "Development of the SAPRC-07 chemical mechanism." *Atmospheric Environment*, in press, doi:10.1016/j.atmosenv.2010.01.026

- Carter, W.P.L. 1996. "Condensed Atmospheric Photooxidation Mechanisms for Isoprene." *Atmospheric Environment*, Vol. 30, pp 4275-4290.
- Carter, W.P.L., and R. Atkinson 1996. "Development and Evaluation of a Detailed Mechanism for the Atmospheric Reactions of Isoprene and NO_x." *International Journal of Chemical Kinetics*, Vol. 28, pp 497-530.
- Carter, W.P.L. 2000. Programs and Files Implementing the SAPRC-99 Mechanism and its Associates Emissions Processing Procedures for Models-3 and Other Regional Models. January 31, 2000. Available at <http://www.engr.ucr.edu/~carter/SAPRC99.htm>.
- Carter, W.P.L., Cocker, D.R., Fitz, D.R., Malkina, I.L., Bumiller, K., Sauer, C.G., Pisano, J.T., Bufalino, C., and Song, C., 2005. A new environmental chamber for evaluation of gas-phase chemical mechanisms and secondary aerosol formation. *Atmospheric Environment*, 39, 7768-7788.
- Carter W.P.L., G.S. Tonnesen and G. Yarwood. 2003. "Investigation of VOC Reactivity Effects using Existing Air Quality Models." Final report prepared for the NARSTO Reactivity Research Working Group under contract to the American Chemistry Council (dated April 17, 2003). Available at <http://www.engr.ucr.edu/~carter/RRWG/ddmrept1.pdf>.
- Crowley, J. N. and S. A. Carl (1997). "OH Formation in the Photoexcitation of NO₂ beyond the Dissociation Threshold in the Presence of Water Vapor" *J. Phys. Chem. A* 101:4178 doi: 10.1021/jp970319e
- Dodge, M.C. (2000). "Chemical oxidant mechanisms for air quality modeling: critical review." *Atmospheric Environment* 34, 2103-2130.
- ENVIRON (2009). "Atmospheric Chemical Mechanism Development and Testing." Final Report to the Texas Commission on Environmental Quality for Work Order No. 582-7-84005-FY08-11.
- ENVIRON (2010). "User's Guide to the Comprehensive Air quality Model with extensions." Available at: http://www.camx.com/files/CAMxUserGuide_v5.10.pdf.
- EPA (2010). "Proposed Rule: National Ambient Air Quality Standards for Ozone." *Federal Register*, Vol. 75, No. 11. January 19, 2010. Available at: <http://www.epa.gov/glo/fr/20100119.pdf>.
- Gery, M.W., G.Z. Whitten and J.P. Killus. 1988. "Development and Testing of the CBM-IV for Urban and Regional Modeling." Report to Marcia C. Dodge, US EPA Atmospheric Sciences Research Laboratory.
- Gery, M.W., G.Z. Whitten, J.P. Killus, and M.C. Dodge. 1989. "A Photochemical Kinetics Mechanism for Urban and Regional Scale Computer Modeling." *J. Geophys. Res.*, 94, 925-956.
- Giguère, P. A. and A. W. Olmos. 1956. "Sur le spectre ultraviolet de l'acide peracétique et l'hydrolyse des peracétates" *Can. J. Chem.*, 34, 689-691.

- Heo, G., 2009. Condensed chemical mechanisms and their impact on radical sources and sinks in Houston. Ph.D. dissertation, University of Texas at Austin, August 2009.
- Heo, G., Kimura, Y., McDonald-Buller, E., Carter, W.P.L., Yarwood, G. A, Allen, D.T. (2009). "Modeling alkene chemistry using condensed mechanisms for conditions relevant to southeast Texas, USA." *Atmospheric Environment*, doi:10.1016/j.atmosenv.2009.10.001.
- Hochhauser, A.M. 2009. Hydrocarbon Composition and Fuel Property Characteristics Of Commercial Gasolines. Prepared for the American Petroleum Institute. Available at <http://www.ip.com/pubview/IPCOM000186443D>
- Horowitz, L.W., A.M. Fiore, G.P. Milly, R.C. Cohen, A. Perring, P.J. Wooldridge, P.G. Hess, L.K. Emmons, and J.F. Lamarque (2007) "Observational constraints on the chemistry of isoprene nitrates over the eastern United States." *Journal of Geophysical Research*, Vol. 112, D12S08.
- Hu, D., Tolocka, M., Li, Q., Kamens, R.M., 2007. A kinetic mechanism for predicting secondary organic aerosol formation from toluene oxidation in the presence of NO_x and natural sunlight. *Atmospheric Environment* 41, 6478–6496
- Jenkin, M.E., Saunders, S.M., Pilling, M.J., 1997. The tropospheric degradation of volatile organic compounds: a protocol for mechanism development. *Atmospheric Environment*, 31, 81–104.
- Karl, T., Guenther, A., Turnipseed, A., Tyndall, G., Artaxo, P. and Martin, S., 2009, Rapid formation of isoprene photo-oxidation products observed in Amazonia, *Atmos. Chem. Phys.*, 9, 7753–7767.
- Kwok, E.S.C., J. Arey, R. Atkinson, 1996. Alkoxy Radical Isomerization in the OH Radical-Initiated Reactions of C₄– C₈ n-Alkanes. *J. Phys. Chem*, 100, 214–219, doi: 10.1021/jp952036x
- Lane, T., Donahue, N.M., Pandis, S.N., 2008a. Simulating secondary organic aerosol formation using the volatility basis-set approach in a chemical transport model. *Environmental Science & Technology* 42, 7439–7451.
- Lane, T., Donahue, N.M., Pandis, S.N., 2008b. Effect of NO_x on Secondary Organic Aerosol Concentrations. *Atmospheric Environment* 42, 6022–6027.
- Lelieveld, J., T. M. Butler, J. N. Crowley, T. J. Dillon, H. Fischer, L. Ganzeveld, H. Harder, M. G. Lawrence, M. Martinez, D. Taraborrelli, J. Williams. (2008) "Atmospheric Oxidation Capacity Sustained by a Tropical Forest." *Nature* 452, 737 – 740, doi: 10.1038/nature06870
- Li S., J. Matthews, A. Sinha. (2008) "Atmospheric Hydroxyl Radical Production from Electronically Excited NO₂ and H₂O." *Science*, 319:1657-1660 doi: 10.1126/science.1151443

- Li S., J. Matthews, A. Sinha. (2009) "Response to Comment on Atmospheric Hydroxyl Radical Production from Electronically Excited NO₂ and H₂O." *Science*, 324:366 doi: 10.1126/science.1166877
- Lim, H.J., A.G. Carlton, B.J. Turpin (2005) "Isoprene Forms Secondary Organic Aerosol through Cloud Processing: Model Simulations." *Environmental Science & Technology*, 39:4441-6.
- NIST web database: NIST (2009). "Chemical Kinetics Database, Standard Reference Database 17, Version 7.0 (Web Version), Release 1.4.3, Data Version 2009.01." Available at: <http://kinetics.nist.gov/kinetics/index.jsp>.
- Ng, N.L., Kroll, J.H., Chan, A.W.H., Chhabra, P.S., Flagan, R.C., Seinfeld, J.H., 2007. Secondary organic aerosol formation from m-xylene, toluene, and benzene. *Atmospheric Chemistry and Physics* 7, 3909-3922. (www.atmos-chem-phys.net/7/3909/2007/)
- Osthoff H. D., J. M. Roberts, A. R. Ravishankara, E. J. Williams, B. M. Lerner, R. Sommariva, T. S. Bates, D. Coffman, P. K. Quinn, J. E. Dibb, H. Stark, J. B. Burkholder, R. K. Talukdar, J. Meagher, F. C. Fehsenfeld and S. S. Brown (2008) "High levels of nitryl chloride in the polluted subtropical marine boundary layer." *Nature Geoscience*, 1: 324-328 doi:10.1038/ngeo177
- Paulot, F., J.D. Crounse, H.G. Kjaergaard, J.H. Kroll, J.H. Seinfeld, and P.O. Wennberg (2009a) "Isoprene photooxidation: new insights into the production of acids and organic nitrates." *Atmospheric Chemistry and Physics*, Vol. 9, pp 1479-1501.
- Paulot, F., J.D. Crounse, H.G. Kjaergaard, A. Kurten, J.M. St.Clair, J.H. Seinfeld, and P.O. Wennberg (2009b) "Unexpected Epoxide Formation in the Gas-Phase Photooxidation of Isoprene." *Science*, Vol. 325, pp 730-733.
- Peeters, J., Nguyen, T.L., Vereecken, L., 2009. HO_x radical regeneration in the oxidation of isoprene. *Physical Chemistry and Chemical Physics* 11, 5935-5939
- Perring, A.E., A. Wisthaler, M. Graus, P.J. Wooldridge, A.L. Lockwood, L.H. Mielke, P.B. Shepson, A. Hanset, and R.C. Cohen (2009) "A product study of the isoprene+NO₃ reaction." *Atmospheric Chemistry and Physics*, 9, 4945-4956.
- Pugh, T. A. M., MacKenzie, A. R., Hewitt, C. N., Langford, B., Edwards, P. M., Furneaux, K. L., Heard, D. E., Hopkins, J. R., Jones, C. E., Karunaharan, A., Lee, J., Mills, G., Misztal, P., Moller, S., Monks, P. S., and Whalley, L. K., 2010. Simulating atmospheric composition over a South-East Asian tropical rainforest: performance of a chemistry box model, *Atmos. Chem. Phys.*, 10, 279-298, doi:10.5194/acp-10-279-2010.
- Robinson, A.L., Donahue, N.M., Shrivastava, M.K., Weitkamp, E.A., Sage, A.M., Grieshop, A.P., Lane, T.E., Pierce, J.R., Pandis, S.N., 2007. Rethinking organic aerosols: semivolatile emissions and photochemical aging. *Science* 315, 1259-1262.

- Sander, S.P., R.R. Friedl, D. M. Golden, M. J. Kurylo, G. K. Moortgat, P. H. Wine, A. R. Ravishankara, C. E. Kolb, M. J. Molina, B. J. Finlayson-Pitts, R. E. Huie and V. L. Orkin (2006). "Chemical Kinetics and Photochemical Data for use in Atmospheric Studies, Evaluation Number 15. NASA Jet Propulsion Laboratory." July 2006, Available from: <http://jpldataeval.jpl.nasa.gov/download.html>.
- Sarwar, G., D. Luecken, G. Yarwood. (2007) "Developing and implementing an updated chlorine chemistry into the community multiscale air quality model." Air Pollution Modeling and Its Application XVIII, Developments in Environmental Science, Volume 6, C. Borrego and E. Renner (Editors), Elsevier.
- Shepson, P.B., E.O. Edney, T.E. Kleindienst, J.H. Pittman, G.R. Namie, 1985, Production of organic nitrates from hydroxyl and nitrate radical reaction with propylene, Environ. Sci. Technol., 19, 849–854, doi: 10.1021/es00139a014
- Wennberg, P. O. and D. Dabdub (2008) "Atmospheric Chemistry: Rethinking Ozone Production." Science, 319, 1624-1625 doi 10.1126/science.1155747
- Whitten, G.Z., Heo, G., Kimura, Y., McDonald-Buller, E., Allen, D.T., Carter, W.P.L., Yarwood, G. (2010). "A New Condensed Toluene Mechanism for Carbon Bond: CB05-TU." Atmospheric Environment, doi: 10.1016/j.atmosenv.2009.12.029.
- Whitten, G. Z., 1983. The chemistry of smog formation: A review of current knowledge. Environmental International 9, 447-463.
- Yarwood, G., S. Rao, M. Yocke, and G.Z. Whitten (2005) "Updates to the Carbon Bond Mechanism: CB05." Final Report to the U.S. EPA. Available at http://www.camx.com/publ/pdfs/CB05_Final_Report_120805.pdf.
- Yarwood, G., T.E. Stoeckenius, J.G. Heiken, A.M. Dunker. 2003. "Modeling Weekday/Weekend Ozone Differences in the Los Angeles Region for 1997." J. Air & Waste Manage. Assoc. 53, 864.
- Yarwood, G., J. Grant, B. Koo, A.M. Dunker. 2008. Modeling weekday to weekend changes in emissions and ozone in the Los Angeles basin for 1997 and 2010. Atmospheric Environment, 42, 3765-3779.

APPENDIX A.

Chamber Experiments Used to Evaluate CB6

CHAMBER EXPERIMENTS USED TO EVALUATE CB6

Table A-1. List of 194 UCR and TVA chamber experiments of single test compounds and special mixtures used for evaluating CB6.^a

CB6 model species		Test compound	Experiment ID	Date (mm/dd/yy)	Light ^a	Initial NO (ppm)	Initial NOx (ppm)
CO	1	CO	EPA070A	2/12/03	A	0.025	0.027
	2	CO	EPA070B	2/12/03	A	0.026	0.027
	3	CO	EPA103A	4/25/03	A	0.016	0.026
	4	CO	EPA103B	4/25/03	A	0.018	0.027
	5	CO	EPA140A	7/16/03	A	0.014	0.023
	6	CO	EPA140B	7/16/03	A	0.014	0.023
	7	CO	EPA174A	9/13/03	A	0.014	0.023
	8	CO	EPA174B	9/13/03	A	0.014	0.023
	9	CO	EPA214A	10/27/03	A	0.015	0.023
	10	CO	EPA214B	10/27/03	A	0.015	0.023
	11	CO	EPA228A	12/15/03	A	0.016	0.025
	12	CO	EPA228B	12/15/03	A	0.015	0.025
	13	CO	EPA234A	1/7/04	A	0.017	0.025
	14	CO	EPA234B	1/7/04	A	0.017	0.026
	15	CO	EPA326A	6/30/04	A	0.015	0.025
	16	CO	EPA326B	6/30/04	A	0.018	0.030
	17	CO	EPA345A	8/26/04	A	0.017	0.027
	18	CO	EPA345B	8/26/04	A	0.017	0.028
	19	CO	EPA346A	8/27/04	A	0.017	0.027
	20	CO	EPA346B	8/27/04	A	0.017	0.027
	21	CO	EPA362A	9/23/04	A	0.013	0.021
	22	CO	EPA362B	9/23/04	A	0.013	0.021
	23	CO	EPA437A	3/14/05	A	0.018	0.028
	24	CO	EPA437B	3/14/05	A	0.018	0.029
	25	CO	EPA585A	5/23/06	A	0.016	0.024
	26	CO	EPA585B	5/23/06	A	0.016	0.025
	27	CO	TVA002	8/7/93	Bs	0.044	0.053
	28	CO	TVA012	9/24/93	Bs	0.043	0.051
	29	CO	TVA018	10/16/93	Bs	0.043	0.051
	30	CO	TVA041	6/17/94	Bs	0.049	0.054
	31	CO	TVA055	12/1/95	Bs	0.046	0.051
	32	CO	TVA070	3/28/96	Bs	0.046	0.051
	33	CO	TVA083	5/29/96	Bs	0.047	0.052
FORM	1	FORM	CTC016	10/14/94	A	0.185	0.241
	2	FORM	EPA068A	2/10/03	A	0.020	0.021
	3	FORM	EPA068B	2/10/03	A	0.016	0.016
	4	FORM	EPA176A	9/15/03	A	0.013	0.022
	5	FORM	EPA176B	9/15/03	A	0.013	0.022
	6	FORM	EPA202A	10/15/03	A	0.015	0.024
	7	FORM	EPA202B	10/15/03	A	0.015	0.024
	8	FORM	TVA005	8/20/93	Bs	0.033	0.040
	9	FORM	XTC086	8/30/93	A	0.123	0.161
MEOH	1	MEOH	ETC285	10/1/91	BI	0.397	0.517
	2	MEOH	ETC289	10/9/91	BI	0.375	0.505
ETH	1	ETH	EC142	4/1/76	A	0.329	0.489
	2	ETH	EC156	5/4/76	A	0.371	0.472
	3	ETH	EPA073A	2/21/03	A	0.024	0.025
	4	ETH	EPA073B	2/21/03	A	0.010	0.010
	5	ETH	OTC278B	6/29/93	S	0.298	0.465
	6	ETH	OTC297B	8/16/93	S	0.220	0.277
	7	ETH	OTC304B	9/2/93	S	0.211	0.232
	8	ETH	TVA008	9/10/93	Bs	0.042	0.052
	9	ETH	TVA009	9/15/93	Bs	0.022	0.025
	10	ETH	TVA011	9/21/93	Bs	0.043	0.049

CB6 model species		Test compound	Experiment ID	Date (mm/dd/yy)	Light ^a	Initial NO (ppm)	Initial NOx (ppm)
	11	ETH	XTC105	10/14/93	A	0.211	0.241
ALD2	1	ALD2	EC254	11/22/77	A	0.080	0.107
	2	ALD2	EPA075A	2/26/03	A	0.010	0.010
	3	ALD2	OTC273B	6/18/93	S	0.231	0.299
	4	ALD2	OTC274A	6/21/93	S	0.210	0.276
	5	ALD2	OTC305A	9/3/93	S	0.216	0.282
	6	ALD2	OTC317B	10/21/93	S	0.214	0.255
	7	ALD2	XTC083	8/25/93	A	0.204	0.246
	8	ALD2	XTC092	9/15/93	A	0.183	0.249
ETOH	1	ETOH	ETC131	7/17/90	BI	0.402	0.538
	2	ETOH	ETC133	7/19/90	BI	0.397	0.534
	3	ETOH	ETC138	7/27/90	BI	0.396	0.536
ACET	1	ACET	OTC273A	6/18/93	S	0.235	0.301
	2	ACET	OTC274B	6/21/93	S	0.204	0.269
	3	ACET	XTC084	8/26/93	A	0.174	0.241
	4	ACET	XTC090	9/10/93	A	0.142	0.195
KET	1	MEK	CTC178A	12/3/96	A	0.197	0.241
	2	MEK	CTC178B	12/3/96	A	0.070	0.091
ETHA	1	ETHA	DTC242A	8/9/95	BI	0.239	0.320
	2	ETHA	EPA292A	5/4/04	BI	0.029	0.047
	3	ETHA	EPA297B	5/11/04	BI	0.011	0.019
	4	ETHA	ETC235	7/11/91	BI	0.378	0.491
	5	ETHA	ETC506	2/17/93	BI	0.290	0.412
PAR	1	N-Butane	EC178	7/13/76	A	0.085	0.099
	2	N-Butane	EC305	7/26/78	A	0.084	0.108
	3	N-Butane	EC307	7/28/78	A	0.090	0.114
	4	Alkanes	EC166	5/24/76	A	0.093	0.106
	5	Alkanes	EC172	6/10/76	A	0.084	0.102
OLE	1	Propene	CTC012	10/5/94	A	0.317	0.419
	2	Propene	CTC018	10/10/94	A	0.345	0.472
	3	Propene	CTC023	10/25/94	A	0.359	0.497
	4	Propene	CTC049	12/14/94	A	0.364	0.497
	5	Propene	CTC059	1/11/95	A	0.376	0.488
	6	Propene	CTC078	2/16/95	A	0.358	0.470
	7	Propene	CTC086A	3/7/95	A	0.337	0.445
	8	Propene	CTC086B	3/7/95	A	0.336	0.440
	9	Propene	CTC102A	4/5/95	A	0.374	0.486
	10	Propene	CTC102B	4/5/95	A	0.374	0.485
	11	Propene	CTC115A	5/4/95	A	0.358	0.465
	12	Propene	CTC115B	5/4/95	A	0.358	0.473
	13	Propene	CTC132A	6/8/95	A	0.372	0.489
	14	Propene	CTC132B	6/8/95	A	0.372	0.488
	15	Propene	CTC163B	3/13/96	A	0.372	0.500
	16	Propene	CTC191A	1/7/97	A	0.343	0.477
	17	Propene	CTC191B	1/7/97	A	0.340	0.472
	18	Propene	CTC203A	1/31/97	A	0.348	0.479
	19	Propene	CTC203B	1/31/97	A	0.344	0.474
	20	Propene	CTC219A	4/11/97	A	0.354	0.488
	21	Propene	CTC219B	4/11/97	A	0.339	0.484
	22	Propene	CTC245A	9/15/98	A	0.403	0.492
	23	Propene	CTC245B	9/15/98	A	0.399	0.492
	24	Propene	CTC264B	10/15/98	A	0.408	0.498
	25	Propene	EC277	3/30/78	A	0.098	0.114
	26	Propene	EC278	3/31/78	A	0.368	0.498
	27	Propene	EC687	6/9/82	A	0.396	0.470
	28	Propene	EC691	6/23/82	A	0.405	0.490
	29	Propene	EPA065A	2/3/03	A	0.023	0.024
	30	Propene	EPA177A	9/16/03	A	0.006	0.010
	31	Propene	EPA177B	9/16/03	A	0.013	0.020
	32	Propene	EPA255A	3/9/04	A	0.017	0.027

CB6 model species		Test compound	Experiment ID	Date (mm/dd/yy)	Light ^a	Initial NO (ppm)	Initial NOx (ppm)
	33	Propene	EPA255B	3/9/04	A	0.017	0.027
	34	Propene	EPA260A	3/17/04	A	0.018	0.029
	35	Propene	EPA260B	3/17/04	A	0.018	0.028
	36	Propene	EPA262A	3/19/04	A	0.017	0.027
	37	Propene	EPA329A	7/7/04	A	0.014	0.021
	38	Propene	EPA329B	7/7/04	A	0.017	0.027
	39	Propene	EPA341A	8/19/04	A	0.008	0.013
	40	Propene	EPA341B	8/19/04	A	0.008	0.013
	41	Propene	EPA348A	8/31/04	A	0.017	0.028
	42	Propene	EPA417A	2/10/05	A	0.017	0.028
	43	Propene	EPA417B	2/10/05	A	0.016	0.027
	44	Propene	TVA013	9/28/93	Bs	0.017	0.022
	45	Propene	TVA014	10/1/93	Bs	0.043	0.053
	46	Propene	TVA015	10/5/93	Bs	0.044	0.054
	47	Propene	TVA016	10/8/93	Bs	0.044	0.054
	48	1-butene	EC123	3/1/76	A	0.401	0.510
	1	T-2-butene	TVA063	2/21/96	Bs	0.018	0.020
	2	T-2-butene	TVA064	2/27/96	Bs	0.036	0.040
	3	T-2-butene	TVA065	3/4/96	Bs	0.037	0.041
	1	toluene	CTC026	10/28/94	A	0.212	0.270
	2	toluene	CTC048	12/13/94	A	0.196	0.248
	3	toluene	EC271	3/21/78	A	0.185	0.215
	4	toluene	EC273	3/23/78	A	0.096	0.112
	5	toluene	EPA072A	2/19/03	A	0.014	0.014
	6	toluene	EPA072B	2/19/03	A	0.015	0.015
	7	toluene	EPA074A	2/25/03	A	0.024	0.024
	8	toluene	EPA074B	2/25/03	A	0.026	0.027
	9	toluene	EPA077A	2/28/03	A	0.022	0.023
	10	toluene	EPA077B	2/28/03	A	0.026	0.026
	11	toluene	EPA210A	10/23/03	A	0.027	0.042
	12	toluene	EPA210B	10/23/03	A	0.066	0.093
	13	toluene	EPA443A	3/21/05	A	0.030	0.031
	14	toluene	EPA443B	3/21/05	A	0.066	0.099
	15	toluene	OTC300B	8/20/93	S	0.186	0.224
	16	toluene	TVA071	4/2/96	Bs	0.238	0.266
	17	toluene	TVA080	5/13/96	Bs	0.050	0.054
	18	toluene	XTC106	10/15/93	A	0.217	0.245
	19	ethylbenzene	CTC057	1/6/95	A	0.205	0.272
	20	ethylbenzene	CTC092B	3/17/95	A	0.215	0.270
	1	o-XYL	CTC038	11/22/94	A	0.199	0.253
	2	o-XYL	CTC068	1/27/95	A	0.208	0.262
	3	o-XYL	CTC081	2/22/95	A	0.215	0.260
	4	o-XYL	CTC091A	3/16/95	A	0.225	0.281
	5	m-XYL	EPA149A	11/8/94	A	0.219	0.271
	6	m-XYL	EPA149B	11/17/94	A	0.211	0.276
	7	m-XYL	EPA178A	8/1/03	A	0.052	0.056
	8	m-XYL	EPA178B	8/1/03	A	0.051	0.054
	9	m-XYL	EPA186B	9/17/03	A	0.007	0.011
	10	m-XYL	EPA365A	9/17/03	A	0.007	0.011
	11	m-XYL	EPA365B	9/27/03	A	0.057	0.093
	12	m-XYL	EPA441A	9/28/04	A	0.021	0.022
	13	m-XYL	EPA441B	9/28/04	A	0.065	0.070
	14	m-XYL	EPA556A	3/18/05	A	0.024	0.025
	15	m-XYL	EPA556B	3/18/05	A	0.075	0.080
	16	m-XYL	CTC029	4/19/06	A	0.078	0.078
	17	m-XYL	CTC035	4/19/06	A	0.078	0.079
	18	m-XYL	TVA048	5/19/95	Bs	0.090	0.100
	19	m-XYL	TVA049	6/2/95	Bs	0.089	0.098
	20	p-XYL	CTC047	12/12/94	A	0.223	0.276
	21	p-XYL	CTC069	1/31/95	A	0.215	0.242

CB6 model species		Test compound	Experiment ID	Date (mm/dd/yy)	Light ^a	Initial NO (ppm)	Initial NOx (ppm)
	22	123-TMB	CTC054	12/21/94	A	0.203	0.229
	23	123-TMB	CTC076	2/10/95	A	0.219	0.258
	24	124-TMB	CTC056	1/5/95	A	0.207	0.254
	25	124-TMB	CTC091B	3/16/95	A	0.226	0.281
	26	135-TMB	CTC050	12/15/94	A	0.220	0.271
	27	135-TMB	CTC073	2/7/95	A	0.221	0.257
ISOP	1	ISOP	EC520	4/14/81	A	0.381	0.492
	2	ISOP	OTC309A	9/28/93	S	0.169	0.213
	3	ISOP	OTC309B	9/28/93	S	0.296	0.375
	4	ISOP	OTC316A	10/20/93	S	0.339	0.424
	5	ISOP	OTC316B	10/20/93	S	0.338	0.422
	6	ISOP	XTC093	9/16/93	A	0.119	0.165
TERP	1	A-PINENE	XTC095	9/21/93	A	0.183	0.242
	2	B-PINENE	XTC099	9/27/93	A	0.181	0.233
PRPA	1	Propane (IR)	ETC230	6/21/91	Bl	0.404	0.513
	2	Propane (IR)	ETC305	10/31/91	Bl	0.387	0.544
BENZ	1	benzene	CTC159A	1/12/96	A	0.182	0.263
	2	benzene	CTC159B	1/12/96	A	0.181	0.260
ETHY	1	ethyne	CTC188A	12/20/96	A	0.089	0.134
	2	ethyne	CTC188B	12/20/96	A	0.089	0.133

^aA = arc; Bl = blacklights; S = natural sunlight; Bs = combination of blacklights and sunlight-simulators.

Table A-2. List of 145 non-blacklight surrogate mixture experiments used for evaluating CB6.

Surrogate type ^a	No.	Experiment ID	Date (mm/dd/yy)	Light ^b	Initial NO (ppm)	Initial NOx (ppm)
Incomplete surrogate without aromatics (Surg-NA)	1	EPA427A	2/24/05	A	0.030	0.047
	2	EPA427B	2/24/05	A	0.011	0.017
Incomplete surrogate but with TOL or XYL	1	EC233	8/12/77	A	0.087	0.094
	2	EC676	5/12/82	A	0.070	0.090
	3	EPA226A	12/11/03	A	0.020	0.031
	4	EPA226B	12/11/03	A	0.020	0.031
	5	EPA227A	12/12/03	A	0.015	0.025
	6	EPA227B	12/12/03	A	0.015	0.025
	7	EPA229B	12/16/03	A	0.020	0.032
	8	EPA230A	12/17/03	A	0.021	0.033
	9	EPA231A	12/18/03	A	0.017	0.027
	10	EPA232B	12/19/03	A	0.017	0.027
	11	EPA233A	12/23/03	A	0.018	0.027
	12	EPA233B	12/23/03	A	0.018	0.027
	13	EPA235A	1/8/04	A	0.021	0.032
	14	EPA235B	1/8/04	A	0.021	0.032
	15	EPA237A	1/13/04	A	0.017	0.026
	16	EPA238B	1/14/04	A	0.020	0.033
	17	EPA239B	1/15/04	A	0.017	0.027
	18	EPA240B	1/16/04	A	0.017	0.027
	19	EPA242A	1/27/04	A	0.017	0.026
	20	EPA243A	1/28/04	A	0.017	0.027
	21	EPA244A	1/29/04	A	0.019	0.032
	22	EPA245A	1/30/04	A	0.017	0.027
	23	EPA250A	2/11/04	A	0.017	0.027
	24	EPA252B	2/13/04	A	0.017	0.027
	25	EPA253B	2/20/04	A	0.017	0.027
	26	EPA257A	3/11/04	A	0.018	0.033
	27	EPA277B	4/15/04	A	0.020	0.032
	28	EPA278A	4/16/04	A	0.020	0.032
	29	EPA319B	6/21/04	A	0.019	0.031
	30	EPA320A	6/22/04	A	0.013	0.021
	31	EPA323A	6/25/04	A	0.016	0.027
	32	EPA334A	7/14/04	A	0.017	0.028
	33	EPA334B	7/14/04	A	0.017	0.028
	34	EPA335B	7/16/04	A	0.017	0.028
	35	EPA349A	9/1/04	A	0.020	0.033
	36	EPA352A	9/9/04	A	0.019	0.031
	37	EPA353A	9/10/04	A	0.016	0.026
	38	EPA550B	4/13/06	A	0.021	0.028
	39	EPA554A	4/17/06	A	0.015	0.022
	40	EPA581B	5/17/06	A	0.020	0.030
	41	EPA583A	5/19/06	A	0.016	0.025
	42	EPA584A	5/22/06	A	0.017	0.025
	43	EPA586B	5/24/06	A	0.021	0.032
	44	EPA587B	5/26/06	A	0.021	0.030
	45	EPA588A	5/31/06	A	0.020	0.030
	46	EPA589B	6/1/06	A	0.017	0.025
	47	EPA590A	6/5/06	A	0.016	0.023
	48	EPA591B	6/6/06	A	0.020	0.030
	49	EPA592A	6/7/06	A	0.017	0.025
	50	TVA060	1/25/96	Bs	0.045	0.050
	51	TVA072	4/12/96	Bs	0.045	0.050
	52	TVA073	4/18/96	Bs	0.045	0.050
	53	TVA074	4/22/96	Bs	0.045	0.050
	54	TVA076	4/29/96	Bs	0.049	0.054
	55	TVA077	5/2/96	Bs	0.045	0.050
	56	TVA078	5/6/96	Bs	0.046	0.051

Surrogate type ^a	No.	Experiment ID	Date (mm/dd/yy)	Light ^b	Initial NO (ppm)	Initial NOx (ppm)
Full surrogate	57	TVA079	5/9/96	Bs	0.046	0.051
	1	CTC187B	12/19/96	A	0.088	0.148
	2	CTC194B	1/14/97	A	0.088	0.148
	3	CTC195A	1/15/97	A	0.087	0.142
	4	CTC199A	1/23/97	A	0.097	0.158
	5	CTC205A	2/5/97	A	0.104	0.166
	6	CTC210B	2/13/97	A	0.096	0.158
	7	CTC215B	4/7/97	A	0.100	0.179
	8	CTC220A	4/15/97	A	0.106	0.164
	9	CTC223B	4/18/97	A	0.106	0.167
	10	CTC233B	12/18/97	A	0.099	0.167
	11	CTC235B	12/22/97	A	0.091	0.152
	12	CTC238B	1/7/98	A	0.103	0.163
	13	CTC240B	1/9/98	A	0.103	0.164
	14	CTC249B	9/22/98	A	0.103	0.157
	15	CTC253A	9/29/98	A	0.108	0.165
	16	CTC258A	10/7/98	A	0.113	0.170
	17	CTC259B	10/8/98	A	0.113	0.169
	18	CTC263A	10/14/98	A	0.108	0.161
	19	CTC267A	12/4/98	A	0.102	0.163
	20	EPA080A	3/13/03	A	0.063	0.092
	21	EPA080B	3/13/03	A	0.063	0.092
	22	EPA081A	3/17/03	A	0.033	0.050
	23	EPA081B	3/17/03	A	0.034	0.050
	24	EPA083A	3/20/03	A	0.032	0.048
	25	EPA084B	3/21/03	A	0.034	0.051
	26	EPA095B	4/15/03	A	0.015	0.025
	27	EPA096A	4/16/03	A	0.064	0.109
	28	EPA096B	4/16/03	A	0.064	0.111
	29	EPA108B	5/7/03	A	0.049	0.076
	30	EPA110B	5/9/03	A	0.020	0.031
	31	EPA113A	5/13/03	A	0.044	0.069
	32	EPA114A	5/14/03	A	0.020	0.031
	33	EPA123A	6/5/03	A	0.014	0.022
	34	EPA124B	6/6/03	A	0.014	0.023
	35	EPA126A	6/10/03	A	0.015	0.023
	36	EPA127B	6/11/03	A	0.019	0.029
	37	EPA128A	6/16/03	A	0.031	0.048
	38	EPA137A	7/11/03	A	0.018	0.029
	39	EPA138A	7/14/03	A	0.014	0.022
	40	EPA139A	7/15/03	A	0.013	0.020
	41	EPA143A	7/22/03	A	0.018	0.029
	42	EPA143B	7/22/03	A	0.019	0.029
	43	EPA150A	8/5/03	A	0.015	0.023
	44	EPA151B	8/6/03	A	0.018	0.030
	45	EPA152A	8/7/03	A	0.015	0.024
	46	EPA153B	8/8/03	A	0.014	0.024
	47	EPA163B	8/22/03	A	0.015	0.024
	48	EPA167A	8/28/03	A	0.018	0.029
	49	EPA168B	8/29/03	A	0.018	0.029
	50	EPA180A	9/20/03	A	0.032	0.052
	51	EPA180B	9/20/03	A	0.032	0.052
	52	EPA181A	9/21/03	A	0.065	0.108
	53	EPA181B	9/21/03	A	0.013	0.024
	54	EPA182A	9/22/03	A	0.070	0.111
	55	EPA182B	9/22/03	A	0.030	0.053
	56	EPA187A	9/28/03	A	0.035	0.056
	57	EPA187B	9/28/03	A	0.016	0.025
	58	EPA188A	9/29/03	A	0.016	0.027
	59	EPA188B	9/29/03	A	0.008	0.014

Surrogate type ^a	No.	Experiment ID	Date (mm/dd/yy)	Light ^b	Initial NO (ppm)	Initial NOx (ppm)
	60	EPA189A	9/30/03	A	0.017	0.021
	61	EPA189B	9/30/03	A	0.008	0.013
	62	EPA190A	10/1/03	A	0.034	0.054
	63	EPA190B	10/1/03	A	0.063	0.097
	64	EPA191A	10/2/03	A	0.008	0.013
	65	EPA191B	10/2/03	A	0.008	0.013
	66	EPA192A	10/3/03	A	0.009	0.014
	67	EPA193A	10/4/03	A	0.017	0.028
	68	EPA193B	10/4/03	A	0.032	0.048
	69	EPA197A	10/9/03	A	0.119	0.193
	70	EPA197B	10/9/03	A	0.064	0.104
	71	EPA198A	10/10/03	A	0.027	0.043
	72	EPA198B	10/10/03	A	0.045	0.072
	73	EPA201A	10/13/03	A	0.019	0.031
	74	EPA201B	10/13/03	A	0.038	0.069
	75	EPA206A	10/19/03	A	0.067	0.107
	76	EPA207A	10/20/03	A	0.038	0.062
	77	EPA209B	10/22/03	A	0.008	0.013
	78	EPA212A	10/25/03	A	0.050	0.081
	79	EPA212B	10/25/03	A	0.076	0.136
	80	EPA258A	3/12/04	A	0.020	0.032
	81	EPA555A	4/18/06	A	0.007	0.011
	82	TVA026	4/8/94	Bs	0.047	0.052
	83	TVA028	4/21/94	Bs	0.023	0.025
	84	TVA029	4/24/94	Bs	0.051	0.056
	85	TVA033	5/4/94	Bs	0.048	0.052
	86	TVA037	5/16/94	Bs	0.023	0.025

^aFor explanation of surrogate types, refer to Table 4-3.

^bA = arc; Bl = blacklights; S = natural sunlight; Bs = combination of blacklights and sunlight-simulators.